

In presenting the dissertation as a partial fulfillment of the requirements for an advanced degree from the Georgia Institute of Technology, I agree that the Library of the Institute shall make it available for inspection and circulation in accordance with its regulations governing materials of this type. I agree that permission to copy from, or to publish from, this dissertation may be granted by the professor under whose direction it was written, or, in his absence, by the Dean of the Graduate Division when such copying or publication is solely for scholarly purposes and does not involve potential financial gain. It is understood that any copying from, or publication of, this dissertation which involves potential financial gain will not be allowed without written permission.

0000
0000

7/25/68

INTERACTION OF NON-SPHERICAL MOLECULES WITH
HOMOGENEOUS SURFACES - ADSORPTION OF CCl_4
ON GRAPHITE AND BORON NITRIDE

A THESIS

Presented to

The Faculty of the Division of Graduate
Studies and Research

By

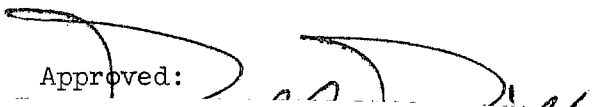
Joe Don DeLay


In Partial Fulfillment
of the Requirements for the Degree
Doctor of Philosophy
in the School of Chemistry

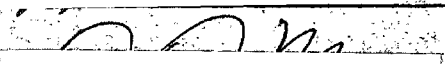
Georgia Institute of Technology

June, 1972

INTERACTION OF NON-SPHERICAL MOLECULES WITH
HOMOGENEOUS SURFACES - ADSORPTION OF CCl_4
ON GRAPHITE AND BORON NITRIDE

Approved: 


Chairman

Date approved by Chairman: 

June 1972

ACKNOWLEDGEMENTS

The author wishes to express appreciation to Dr. Robert A. Pierotti, to Mrs. Harriet Stobaugh and to his wife, Kay, for their invaluable contributions.

TABLE OF CONTENTS

	Page
ACKNOWLEDGEMENTS	ii
LIST OF TABLES	v
LIST OF ILLUSTRATIONS	vi
LIST OF SYMBOLS AND ABBREVIATIONS	viii
SUMMARY	xiii
Chapter	
I. INTRODUCTION	1
Physical Adsorption-General Theory	
Adsorbents and Heterogeneity	
Adsorption Techniques	
Statement of the Problem	
II. CONCEPTS AND EQUATIONS	11
Introduction	
Two-Dimensional Condensation	
Isosteric Heat	
Point B	
Henry's Law Region	
Gas-Solid Virial Coefficients	
Frenkel-Halsey-Hill Equation	
Significant Structures Theory	
III. EXPERIMENTAL	41
Introduction	
Microbalance Calibration	
Microbalance Experimental Difficulties	
Construction of Adsorbent Containers	
Temperature Measurement	
Capacitance Manometer and Pressure Measurements	
Temperature Regulating Devices	
Adsorbates and Adsorbents	
A Typical Run	

TABLE OF CONTENTS (Concluded)

Chapter	Page
IV. RESULTS AND PROCEDURES	63
Introduction	
Comparison of the Effects of Heterogeneity and Molecular Symmetry Upon Isotherm Shape	
Frenkel-Halsey-Hill Equation	
Two-Dimensional Critical Behavior	
Second Gas-Solid Virial Coefficients	
Experimental Isothermic Heats for the Graphite and Boron Nitride Systems	
Significant Structures Theory	
V. CONCLUSION AND RECOMMENDATIONS	109
Conclusion	
Recommendations	
APPENDIX	113
BIBLIOGRAPHY	182
VITA	188

LIST OF TABLES

Table	Page
1. Constants for the Clausius-Clapeyron Equations	60
2. Adsorbate Physical Constants	65
3. Experimental CCl_4 Point B Parameters for the Graphite and Boron Nitride Adsorbents	67
4. Relative Pressures at Point B for the Second Layer in the CCl_4 -Graphite System	68
5. Data Extracted from Frenkel-Halsey-Hill Plots for the CCl_4 -Boron Nitride System	77
6. Harmonic Potential Parameters Obtained from Fit of B_{2s} Values for the Graphite Adsorbent	84
7. Henry's Law Region B_{2s} Data and Zero Coverage Isothermic Heats for the Graphite Adsorbent	88
8. Significant Structures Parameters Obtained from the CCl_4 -Graphite System	103
9. Comparison of Significant Structures Theory Calculated Henry's Law Constants with Experimental Data from the CCl_4 -Graphite System	106

LIST OF ILLUSTRATIONS

Figure	Page
1. Photograph of Experimental Apparatus	42
2. Schematic of Experimental Apparatus	43
3. Variation of Electrobalance as a Function of the Pressure of a Non-Adsorbed Gas	47
4. Electrobalance and Containing Pyrex Bottle	50
5. Thermocouple Calibration Curve	52
6. Pressure Comparison of the Capacitance Manometer's 0.1 and 1.0 Ranges	54
7. Ice Point Isotherms for CCl_4 , CHCl_3 , and CH_2Cl_2 Adsorbed upon P-33 Graphite ³	70
8. Ice Point Isotherms for CCl_4 , CHCl_3 , CH_2Cl_2 and CH_3Cl Adsorbed upon P-33 Graphite ²	71
9. Ice Point Isotherms for CCl_4 , CHCl_3 , and CH_2Cl_2 Adsorbed upon Boron Nitride ³	72
10. Frenkel-Halsey-Hill Equation Plots for CCl_4 Adsorbed upon Graphite and Boron Nitride at the Ice Point	75
11. Two-Dimensional Critical Region Isotherms for the CCl_4 -Graphite Systems	78
12. Two-Dimensional Critical Region Isotherms for the CCl_4 -Boron Nitride System	80
13. Plots Demonstrating the Intercept Method for Determining Second Gas-Solid Virial Coefficient for the CCl_4 -Graphite System	82
14. Plots Demonstrating the Slope Method for Determining the Second Gas-Solid Virial Coefficient for the CCl_4 -Graphite System	83

LIST OF ILLUSTRATIONS (Concluded)

Figure	Page
15. Isoteric Heats as a Function of Coverage for the CCl_4 -Graphite and CCl_4 -Boron Nitride System	91
16. Multilayer Adsorption Region Isotherms for the CCl_4 -Graphite System	92
17. Adsorption Isotherms for the CCl_4 -Boron Nitride System	93
18. Comparison of the CCl_4 -Graphite Isosteric Heat Curve with a Literature Curve	94
19. Significant Structures Plot to Determine v and ϵ_{1s}^*/k	101
20. Fit of Significant Structures Equation to Experimental Isotherms at Three Temperatures	107

LIST OF SYMBOLS AND ABBREVIATIONS

A	surface area
A	Clausius Clapeyron constant
A_s	molar area of adsorbed surface phase at a monolayer coverage
a	average distance between nearest neighbor cells
a_f	free area
a_m^o	area occupied by a molecule at monolayer coverage
B	Clausius Clapeyron constant
B	mathematical assemblage as defined by equation (69)
B_{2s}	second gas-solid virial coefficient
B_{3s}	third gas-solid virial coefficient
B_{4s}	fourth gas-solid virial coefficient
B_{2g}^o	second gas-gas virial coefficient in the absence of an external field
C'	mathematical assemblage as defined by equation (68)
c	lattice coordination number, taken to be six
E	internal energy
F	Helmholtz free energy
f	fugacity
G	Gibbs free energy
g	Frenkel-Halsey-Hill equation parameter measuring the compatibility of the adsorbed gas film with the bulk adsorbate
g	acceleration of gravity in equation (54)

LIST OF SYMBOLS AND ABBREVIATIONS (Continued)

g	grams
$g(\theta)$	mathematical assemblage as defined by equation (67).
H	enthalpy
\bar{H}_{ads}	molar enthalpy of adsorbed gas
\bar{H}_{g}	molar enthalpy of unadsorbed gas
ΔH_{VAP}	enthalpy of vaporization
h	Planck's constant
I_x, I_y, I_z	moments of inertia about principal axes
j	degrees of rotational freedom lost upon adsorption
K_h	Henry's law constant, W/P
K_{SS}	Henry's law constant calculated from Significant Structures Theory
k	Boltzmann's constant
k_z	force constant for vibration perpendicular to surface
M	gram molecular weight
m	weight of one molecule in grams
N	number of molecules
N_{ads}	number of adsorbed molecules
N_m	number of molecules necessary to cover a monolayer
N_s	average number of molecules in a system
n_A	number of moles of adsorbent
n_{ads}	number of moles of adsorbed species per gram of adsorbent
n_g	number of moles of unadsorbed gas
P	pressure of gas in torr unless otherwise stated

LIST OF SYMBOLS AND ABBREVIATIONS (Continued)

P_o	equilibrium saturation vapor pressure in torr
p	pressure of gas in torr unless otherwise stated
Q	canonical ensemble partition function
Q_{ads}	canonical ensemble partition function for an adsorbed gas
Q_{N_s}	canonical ensemble partition function for a system containing N_s molecules
q_{2g}	molecular partition function of adsorbed non-spherical molecule
q_{3g}	molecular partition function of non-spherical molecule in bulk gas
q_{2s}	solid and configurationally degenerate solid partition function
q_{rg}	rotational partition function for bulk gas molecule
q_{rs}	rotational partition function for adsorbed molecule
q_{st}	isosteric adsorption heat
q_{st}^o	zero coverage isosteric adsorption heat
R	universal gas constant
R	distance of a molecule from the center of a cell
\tilde{r}	generalized coordinate
S	entropy
\bar{s}_{ads}	$(\partial S / \partial n_{ads})_{n_A, T, P}$
s_g	molar entropy of unadsorbed gas
T	temperature in degrees Kelvin
T_{2c}	two-dimensional gas critical temperature in degrees Kelvin

LIST OF SYMBOLS AND ABBREVIATIONS (Continued)

T_{3c}	three-dimensional gas critical temperature in degrees Kelvin
t	temperature in degrees centigrade
$u_s(\tilde{r})$	pair interaction potential
V	volume of unadsorbed gas
V_g	volume of unadsorbed gas
V_s	volume of a system
v_g	molar volume of unadsorbed gas
\bar{v}_{ads}	$(\partial V / \partial n_{ads})_{n_A, T, P}$
W	weight of adsorbed gas per gram of adsorbent
w	Frenkel-Halsey-Hill lateral interaction parameter
\bar{w}	mean interaction potential obtained by lattice summation
y	reduced distance from the center of the cell
Z	configuration integral
z^*	equilibrium separation of molecule from surface
z_0	distance of closest approach where the potential interaction between adsorbate and adsorbent is zero
δ	f/RT or λ/Λ^3
$\Gamma()$	gamma function
Γ	surface concentration
ϵ_{1s}^*	gas-solid potential well depth at equilibrium separation distance
ϵ_{12}^*	adsorbed gas-gas potential well depth at equilibrium separation distance

LIST OF SYMBOLS AND ABBREVIATIONS (Concluded)

ϵ_{12}^*	gas phase bulk gas-gas potential well depth at equilibrium separation distance
$\Delta\epsilon_1^*$	excess energy of adsorption due to the first adsorbed layer
θ	fraction of a monolayer coverage
Λ	$h/(2\pi mkT)^{\frac{1}{2}}$
λ	activity
μ_{ads}	chemical potential of adsorbed species
μ_g^0	standard chemical potential for an ideal gas
ν_x, ν_y	frequency of rocking vibration along x and y axes
ν_i	frequency of vibration of internal modes
Ξ	grand partition function for a field free ensemble
Ξ^e	grand partition function for an ensemble in an external field
Ξ_s	grand partition function for a system
σ	bulk gas symmetry number
σ_s	adsorbed gas symmetry number
Π	product
π	3.1416
ρ	density, g/ml

SUMMARY

The research reported here constitutes studies of the adsorption of several organic substances, CCl_4 , CHCl_3 , CH_2Cl_2 and CH_3Cl onto the solid adsorbents, P-33(2700) graphite and boron nitride. These studies include determining adsorption isotherms over a broad range of temperatures, -82°C to 72°C , and coverages, submonolayer through multilayer. BN and graphite have similar crystal structures and interatomic distances. The BN was found to have 6.2 ± 2 per cent of its $5.0 \text{ m}^2/\text{g}$ surface covered with high energy sites as compared to less than 0.1 per cent of the graphites' $11.5 \text{ m}^2/\text{g}$ surface. Carbon tetrachloride adsorbed on graphite showed a discernable second step in an isotherm at 273.15°K . None of the other adsorbate-adsorbent combinations examined at this temperature showed such a step. Carbon tetrachloride had a vertical discontinuity in the isotherm measured on graphite below the two-dimensional critical point, but had non-vertical isotherms in the same region when BN was used. Arguments were made that molecular symmetry exerts an influence similar to heterogeneity on isotherm step sharpness and second step formation. These arguments were carried into a comparison of CCl_4 -graphite and CCl_4 -BN Frenkel-Halsey-Hill plots. A $\Delta\epsilon^*_1$ of 710 calories was obtained by utilizing the initial linear portion of the Frenkel-Halsey-Hill plot for BN.

Zero coverage isosteric heats for graphite, determined via a second gas-solid virial coefficient treatment of data taken in the

SUMMARY (Concluded)

Henry's law region were CCl_4 (8350 ± 70 calories), CHCl_3 (8100 ± 100 calories), CH_2Cl_2 (8400 ± 350 calories) and CH_3Cl (6400 ± 60 calories). Fitting the virial equation results to a (3-9) potential approximated by a harmonic potential gave a gas-solid potential well depth, ϵ^*_{1s}/k , of 4040°K for CCl_4 and a distance of closest approach, z_0 , of 1.2 \AA compared to an expected z_0 of 3.1 \AA . The first maximum in the classical isosteric heat versus coverage plot was $10,000 \pm 300$ calories for CCl_4 -BN and $10,800 \pm 300$ calories for CCl_4 -graphite. The two-dimensional critical temperature for CCl_4 -graphite was $-38.4 \pm 0.3^\circ\text{C}$, while a value for CCl_4 -BN was above -35°C . The Significant Structures Theory provided an excellent prediction of experimental Henry's law constants and a reasonable fit of higher coverage isotherms over the temperature range studied for the CCl_4 -graphite system. Other than varying ϵ^*_{1s}/k within the limits of experimental error, there were no adjustable parameters used in the Significant Structures Theory. Utilizing the experimental data and molecular parameters in the Significant Structures Theory, values for ϵ^*_{1s}/k of $4160 \pm 65^\circ\text{K}$, ϵ^*_{12}/k of $391 \pm 0.5^\circ\text{K}$, ϵ^*_{12} gas phase/ k of $420 \pm 20^\circ\text{K}$ and a vibrational frequency for CCl_4 vibrating perpendicular to the graphite surface of $0.61 \pm 0.04 \times 10^{12} \text{ sec}^{-1}$ were determined.

CHAPTER I

INTRODUCTION

Physical Adsorption - General Theory

Adsorption occurs when a gas or vapor is allowed to come to equilibrium with a solid surface, and it is well established that this equilibrium results in having the concentration of gas molecules almost always greater in the vicinity of the surface [1]. This concentration excess is an experimentally measurable quantity. Adsorption processes fall into two categories, physical and chemical, with chemisorption involving the formation of a chemical bond with the surface and commanding bond energies on the order of those of chemical bonds [1]; whereas, physical adsorption involves heats which are of the magnitude of the heats of liquifaction of the adsorbates. Van der Waals forces are the predominant driving forces in physical adsorption, resulting in adsorbed gases forming layers which can on occasion reach thicknesses of many molecular diameters. Physically adsorbed gases or vapors may under suitable conditions behave as two-dimensional solids, liquids or gases [2]. Physical adsorption is an almost instantaneous process whose rate is limited by the rate of diffusion of the gas [3]. Adsorption is a surface phenomena, whereas absorption involves penetration of the gas into the structure of the solid [4]; consequently adsorption is distinguished from absorption by the location at which it occurs.

This study will concern itself with physical adsorption at the gas-solid interface. The basic terminology of physical adsorption is not complicated. The gas or vapor adsorbed is termed the adsorbate and the solid the adsorbent. The term monolayer is frequently employed in adsorption problems and may be defined as the amount of material necessary to make an adsorbed layer one molecule thick [5]. At surface coverages of only a few per cent of a monolayer where the adsorbate can act as a two-dimensional ideal gas the Henry's law region of adsorption is present. Any surface coverage less than a monolayer is referred to by the term sub-monolayer. Coverages involving enough material adsorbed to correspond to two or more monolayers fit the description of multilayer adsorption.

A physically adsorbed gas molecule can be either mobile or localized [6]. In localized adsorption the gas molecules are adsorbed onto definite points of attachment on the adsorbent in such a way that each point of attachment can accommodate only one adsorbed molecule [7]. In mobile adsorption the mutual adsorbate-adsorbent potential confines the adsorbate to a certain equilibrium distance from the surface, yet the adsorbate possesses unrestricted translation parallel to the surface. Molecules can, on occasion, be either localized or mobile. Hill has shown that the transition from localized adsorption to mobile adsorption can occur when the translation energy available to the adsorbate is as low as one-tenth of the potential energy separating one site from another [6]. A typical site potential barrier would be 500 calories [8]. Liquid air temperatures are

required before localized adsorption becomes an important consideration. The work reported here is in the -80°C to $+80^{\circ}\text{C}$ range; therefore, the adsorption observed should be mobile.

The adsorption isotherm is the starting point for physical adsorption studies. These isotherms are plots of the number of moles of vapor adsorbed per gram of adsorbent as a function of pressure at a constant temperature. They are essentially plots of the surface coverage as a function of free energy change [1]. Isotherms can not be expressed in terms of absolute quantities because of the adsorbent. While properties of liquid surfaces, such as surface tension, can be completely determined by temperature and the concentration of the components, the same is not generally true of solids [9]. Solid surfaces possess a measurable number of defects which contribute to non-reproducibility.

Adsorbents and Adsorbent Heterogeneity

The concept of a heterogeneous surface is an extremely important facet in the interpretation of adsorption measurements. The ideal, or perhaps better termed "homogeneous" surface, is usually far from a reality because all surfaces contain some imperfections and impurities. Grain boundaries, emergent points of screw and edge dislocations, vacancies and cracks are interspersed among the normal periodic variations found upon the surface [10]. The presence of different crystal faces with different indices can be considered heterogeneity. Discussions of non-uniform surfaces usually contain references to sites and site distributions [11]. For homogeneous surfaces, sites

are defined so that as the adsorbate travels parallel to and across the surface, the adsorption potential can be expressed as a continuous series of repeating units of potential maxima. Heterogeneous surfaces can sometimes be thought of as being composed of a desultory distribution of patches, each patch containing sites having a similar adsorption energy [11]. On other occasions, when the discontinuities in site energies are random, the difficulty in analyzing the surface is greatly multiplied. Halsey was among the first to recognize the place of heterogeneity in adsorption studies. Ross was an early advocate of treating a heterogeneous surface as a gaussian distribution of small homogeneous patches [12]. Recently Pierotti and Thomas have weighed the utility of using the exponential, gaussian and log-normal site distribution descriptions of heterogeneous surfaces [11].

The carbon black used in the present studies is known as P-33(2700) graphite. P-33 is a highly homogeneous thermal black with heterogeneity in the range of one-tenth of one per cent of the total surface area [13].

The second surface to be examined is that of boron nitride, which has a heterogeneous surface consisting of approximately 6 per cent of the total surface area [14]. The similarity of the structures of boron nitride and graphite makes for an interesting comparison. In the graphite crystal the carbon atoms are arranged in sheets of regular hexagons, the carbon to carbon bond distance being 1.42 \AA [15]. The distance between layers is 3.40 \AA . This large distance is indicative of van der Waals bonding between the

graphite sheets. In terms of a graphite hexagonal unit cell, "a" is 2.456 Å and "c" is 6.696 with the carbon atoms of alternate layers falling vertically one above the other [15,16]. The bulk graphite crystals are doubly truncated hexagonal and octagonal bipyramids [12]. In boron nitride the boron to nitrogen bond distance is 1.45 Å. The boron nitride unit cell is a hexagonal unit of alternating boron and nitrogen atoms, the constants of which are "a" equals 2.504 Å and "c" equals 6.660 Å [17]. These hexagonal rings are packed directly on top of each other, with boron nitrogen atoms being interchanged in alternate layers. The bulk boron nitride crystals are tabular [14].

Crystalline boron nitride appears to be less chemically reactive than graphite. Boron nitride is inert, even at elevated temperatures when exposed to oxygen, hydrogen and iodine [18]. At red heat it is hydrolyzed by water vapor to ammonia and boric oxide. Aqueous acids and alkalies cause no decomposition, but fusion of boron nitride with alkali metal hydroxides or carbonates forms borates. Boron nitride and graphite are isoelectronic. The density of graphite is near 2.25 grams per cubic centimeter; whereas, the density of boron nitride is near 2.20 grams per cubic centimeter [19].

Adsorption Techniques

There are many different techniques available for use in the study of surfaces. Some possible choices are: volumetric adsorption, gravimetric adsorption, calorimetric heats of adsorption of powders, infrared adsorption of surface bonded species, x-ray diffraction, electron microscopic surface area determinations, nuclear magnetic

resonance absorption by absorbed species, low energy electron diffraction, dielectric effects by absorbed species, chromatographic flow adsorption and reflection of light from thin films [1,10,11,12]. Only gravimetric methods involving microbalances will be discussed in detail here. The interested reader is referred to the reviews of Young and Crowell [1], Ross and Oliver [12], Pierotti and Thomas [11], and the works edited by Flood [10] for further discussions. Although this series of experiments must be classified gravimetric, volumetric methods are of such importance as to merit some discussion.

Preliminary to the measurement of an adsorption isotherm is the preparation of the surface [20]. All solid surfaces which have been exposed to a gas or vapor are covered by physically adsorbed film, which must be removed by outgassing. A combination of heating and pumping is usually sufficient to remove all van der Waals adsorbed gas. The time of heating to give reproducible surface areas may be estimated from an empirical formula according to Orr and Dalla Valle [21]. The formula is:

$$\text{time} = 14.4 \times 10^4 t^{-1.77} \quad (1)$$

where "time" is in hours and t is temperature of heating in degrees centigrade. This equation applies to temperatures between 100° and 400°C and vacua better than 5×10^{-6} torr.

The principle underlying the subsequent volumetric methods after degassing is as follows. The pressure, volume and temperature of

a quantity of adsorbate is measured and the number of moles of adsorbate calculated. This material is brought into contact with the adsorbent and, when constant pressure, volume and temperature are attained, the system is assumed to be at equilibrium. The number of moles of gas is recalculated and the difference between the original and final numbers of moles of gas represents the amount of gas adsorbed at this temperature. By holding the temperature constant and adding doses of adsorbate gas via a calibrated system of pipettes, a series of measurements of the number of moles adsorbed as a function of pressure is taken.

The pressures must be corrected for non-ideality of the adsorbate, for thermal transpiration and for the dead-space volume of the system, which must be accurately known [20]. The dead-space volume of the system is evaluated by expanding known volumes of helium into the system and noting the resulting temperatures and pressures. Helium is used because it is not appreciably adsorbed above 77°K [22].

A microbalance was used in this set of experiments to determine the amount of material adsorbed. A simple microbalance consisting of a calibrated quartz spring was described by McBain and Bakr in 1926 [23]. The spring extension was directly proportional to the amount adsorbed: however, bouyancy corrections became significant at higher pressures. With the proper corrections, quartz spirals have been used at pressures up to 60 atmospheres [24]. Studies over long periods of time, of the order of years, have been run using the quartz microbalance [25]. The sensitivity of quartz microbalances is

impressive. Darcy [26] used a quartz spring carrying a maximum load of 100 milligrams with a sensitivity of seven millimeters elongation per milligram. Other materials used in spring construction are Pyrex, beryllium-copper alloy and molybdenum. Beam type microbalances consisting of a quartz beam cemented at right angles to a supporting tungsten torsion fiber have sensitivities of 2×10^{-8} g with a load of one-tenth gram [27]. The advantages of this torsion type balance is that a tare may be used to eliminate the bothersome bouyancy corrections necessary with the quartz springs.

Automation in microbalances was achieved as early as 1934 when Lancke and Hoffmann [28] devised a photographic plate method for recording elongations in a quartz spring. The microbalance used here to measure adsorption is an automated form of the torsion balance. The Cahn R-G electromicrobalance [29] used to determine the amounts adsorbed in this work has a theoretical sensitivity of 10^{-8} g, but vibrations limited the experimental sensitivity to 10^{-6} g with a load of one gram. The upper limit of the measurable weight change was one-tenth gram. The principle of operation of this highly versatile balance is best explained by this condensed exerpt from the Cahn instruction manual [29]. See Figure 4,

The electrobalance is based upon the null-balance principle, which is generally accepted as being the most accurate and reliable method of measurement. The sample is suspended from the balance beam, and is counterbalanced by a tare. When the sample weight changes, the beam tends to deflect, momentarily. A flag attached to the beam moves with it, changing the light to a phototube and the phototube current. This current is amplified in a two-stage servo amplifier and the amplified current is applied to a coil attached to the beam, which is in a magnetic field. The current in the coil acts like a direct current motor, exerting a force

on the beam to restore it to the original balance position. Thus the change in electromagnetic force is equal to the change in sample weight. The beam is always in dynamic equilibrium, with the sum of the moments on it equal to zero.

By Ampere's Law, the electromagnetic restoring force is exactly proportional to the current that caused it. This current and the voltage it develops across the coil in its series circuit is extremely accurate. No recorder made is accurate enough to display it to its full limits. It is necessary to subtract, and measure, a part of the weight voltage with circuits inside the balance and only apply the excess to the recorder. Thus a known, accurately calibrated voltage, is subtracted from the voltage across the coil by means of an accurate potentiometer. A dial on the potentiometer reads directly in milligrams, corresponding to the amount of voltage being subtracted in the circuit. The excess of the coil voltage over reference voltage is then available for the recorder.

The remainder of the instrumentation is discussed in somewhat less detail in the chapter on experimentation.

Statement of the Problem

A reasonably complete study of carbon tetrachloride adsorption upon P-33(2700) graphite will be made. The submonolayer and multilayer regions of the adsorption isotherms will be emphasized, but not to the exclusion of the monolayer regions. The gas-solid virial equation and the Significant Structures Theory approximation for non-spherical molecules will be used to extract gas-solid and gas-gas interaction parameters. The two-dimensional critical temperature for carbon tetrachloride will be examined with the purpose of fixing an otherwise adjustable gas-gas interaction parameter in the Significant Structures Theory. Classical treatments such as monolayer coverages, isotheric heats as a function of adsorbate coverage and treatment of multilayer data by means of the Frenkel-Halsey-Hill

equation will be included. Further work of a less complete nature will be carried out in order to have a basis for comparison for the carbon tetrachloride-graphite adsorption data. Boron nitride will be used as a second adsorbent because it provides a surface which in terms of distance parameters and type of unit cell is almost identical to graphite. The adsorbate comparisons will be made with molecules of lower symmetry, but which are also members of the chlorine substituted methane series. These molecules are chloroform, dichloromethane and chloromethane.

CHAPTER II

CONCEPTS AND EQUATIONS

Introduction

The second chapter is continued much in the vein of the first chapter, but in somewhat more specific terms. It is the purpose of this chapter to discuss, from a historical viewpoint, the concepts and equations pertinent to a better understanding of the presentations in the chapter entitled RESULTS AND PROCEDURES. Sections in this second chapter are:

- (a) Two-dimensional condensation
- (b) Isosteric heat
- (c) Point B
- (d) Henry's law region
- (e) Gas-solid virial equation
- (f) Frenkel-Halsey-Hill equation
- (g) Significant Structures Approximation III.

Two-Dimensional Condensation

Theoretically, two-dimensional problems are more easily solvable than three-dimensional problems. The assumption is frequently made that the gas-solid adsorption potential allows adsorbed molecules translations parallel to the adsorbent surface, but confines these molecules to a certain equilibrium distance perpendicular to the

adsorbent surface [2]. The treatment of a surface film as a two-dimensional phase possesses validity provided there is negligible variation in the adsorption potential parallel to the adsorbent surface. Sodium halides [30], certain transition metal halides [31], graphitized carbon black [32], and graphite single crystals [33] appear to meet this criterion of surface uniformity in that the phenomenon of two-dimensional condensation has been observed in isotherms taken on these surfaces. Halsey has shown that two-dimensional condensation will occur on heterogeneous surfaces provided there are patches containing sites of equal energy [34]. This condensation, however, will occur over a range of temperatures and pressures and thus may not be experimentally observable. Some adsorbates showing two-dimensional condensation on graphitized carbon black [32] include CCl_4 , CHCl_3 and CFCl_3 . Krypton condenses two-dimensionally upon sodium bromide [35]. Xenon, methane and ethane show condensation of sodium chloride [30]. Krypton and methane condense in a two-dimensional manner upon graphite single crystals [33]. This is by no means a complete listing.

Several theories predict the existence of a two-dimensional critical temperature. Four of these theories will now be discussed briefly. The two-dimensional van der Waals theory assumes a hard sphere repulsive potential, a Lennard-Jones type attractive potential [36], and assumes that each molecule moves in a region with a uniform molecular distribution, as long as it is not contacting another molecule. This uniform distribution is the result of a random distribution of the molecules comprising the fluid. The Lennard-

Jones Devonshire, LJD, two-dimensional fluid maintains a cell formed by its neighboring molecules while each molecule moves across the adsorbent surface [37,38]. The encircling molecules form cells and are uniformly distributed in each element of area at a specified distance from the cell center. The LJD potential is also functionally dependent upon the displacement of the molecular center from the cell center. Lattice geometry and cell size determine the number of molecules per unit area of surface in the LJD theory. The Significant Structures Theory [38], SST, is a cell theory, but differs from the LJD theory in that the lattice of cells is disordered by allowing lattice vacancies. Certain degrees of freedom of these disordered SST cells are chosen as the most significant contributors to the surface phase partition function. All other arrangements are discarded and these most significant structures are used to compute thermodynamic parameters. The Scaled Particle Theory [38], SPT, recognizes the importance of the radial distribution of molecules about a central molecule. The short range influence of this chosen central molecule in the fluid results in a certain amount of short range order expressible as a fractional coverage exceeding the average fraction of a monolayer coverage. The chemical potential of this scaled particle model consists of an ideal gas term and a term dependent upon the intermolecular potential. The ideal gas term is dependent upon the fractional coverage and temperature only. The intermolecular potential term is obtained by computing the work necessary to add an isolated molecule to a system of $N-1$ molecules fully

coupled by their intermolecular potentials. The SPT molecule chosen as the central molecule is coupled to its already coupled neighbors by a scale factor which takes this molecule from effective isolation, e.g. zero coupling, to a full potential interaction, e.g. a coupling of one [39].

Predictions by these models of the two-dimensional critical temperature are given in terms of the ratio of the two-dimensional critical temperature to the three-dimensional critical temperature [40]. These ratios are: two-dimensional van der Waals (0.50); Lennard-Jones, Devonshire (0.53); Significant Structures (0.45); Scaled Particle (0.46). Experimental values for the ratio of the two-dimensional critical temperature to the three-dimensional critical temperature range from 0.36 to 0.47 [41]. These predictions assume that the gas phase potential well and the potential well of the adsorbed molecule are the same depth. This assumption is discussed further in the Significant Structures Theory section.

Isosteric Heat

Isosteric heat is a differential heat of adsorption which is a function of coverage. This heat will be defined thermodynamically, but it is of conceptual benefit to first consider this heat of adsorption in a qualitative manner. A useful approximation in dealing with the isosteric heat is that of pairwise interactions. The variation of isosteric heat as a function of surface coverage may be thought of as proceeding smoothly as monolayer coverage is approached and exceeded. At coverages of a few tenths of a per cent

of a monolayer only the adsorbate-adsorbent interactions are contributing factors. On a heterogeneous surface high energy patches of adsorption sites tend to be covered first, causing the isosteric heat to be affected by progressively lower adsorbate-adsorbent interaction energies as more molecules become adsorbed. Thus in this low coverage region a heterogeneous surface usually exhibits a decrease in isosteric heat of adsorption as adsorption progresses [42]; however, the opposite effect is observed when the surface is homogeneous. The zero coverage isosteric heat starts with a lesser magnitude upon a homogeneous surface, but this low coverage heat increases monotonically from its limiting value [42]. At approximately 5 per cent coverage the attractive part of the adsorbate-adsorbate pair interaction potential begins to make a noticeable contribution. One finds that increasing coverage beyond one-half monolayer [42] produces increasing isosteric heats as an adsorbate molecule interacts with an increasing number of adsorbed neighbors in addition to its adsorbent interaction. Nearing a monolayer, crowding occurs and the repulsive part of the interaction potential begins to contribute to the isosteric heat, slowing its rate of increase. Past the monolayer these interactions and the expected inverse cubic decrease in the van der Waals forces, due to the suddenly greater adsorbate distances from the surface, precipitate a rapid decline in isosteric heat [42,43]. As sufficient numbers of layers of adsorbate are deposited, the isosteric heat approaches either the heat of liquefaction or the heat of sublimation of the bulk adsorbate, depending upon the temperature of the experiment.

In actual calculations other factors, such as adsorbate-adsorbent structural compatibility [44], adsorbate packing and adsorbent perturbations [45] of the adsorbate, must also be considered.

In the thermodynamic derivation of the isosteric heat, according to Hill [46], it is assumed that the thermodynamic formalisms describing solutions may be extended to adsorption systems. Consider a two component system containing an inert, non-volatile, finely divided adsorbent, "A", and an adsorbed gas, "ads", in equilibrium with an unadsorbed gas, "g" so that the condensed phase has energy E , entropy S and contains n_A moles of adsorbent and n_{ads} moles of adsorbate and includes only those cases in which E is completely determined by n_A , n_{ads} , S and the volume, V , as the starting point. The change, dn_A refers to the addition of pure A in the same state of subdivision, etc. as the original sample. Using standard "textbook" solution thermodynamic methods, these equations may be written as

$$dE = TdS - PdV + \mu_{ads} dn_{ads} + \mu_A dn_A \quad (2)$$

$$dG = -SdT + VdP + \mu_{ads} dn_{ads} + \mu_A dn_A \quad (3)$$

$$d\mu_{ads} = -\bar{s}_{ads} dT + \bar{v}_{ads} dP + \left(\frac{\partial \mu_{ads}}{\partial \Gamma} \right)_{T,P} d\Gamma \quad (4)$$

Here

$$\Gamma = \frac{n_{\text{ads}}}{n_A} \quad (5)$$

$$\bar{s}_{\text{ads}} = \left(\frac{\partial S}{\partial n_{\text{ads}}} \right)_{n_A, T, P} \quad (6)$$

$$\bar{v}_{\text{ads}} = \left(\frac{\partial V}{\partial n_{\text{ads}}} \right)_{n_A, T, P} \quad (7)$$

G is the Gibbs free energy, P is pressure exerted by the non-adsorbed gas and the μ 's are chemical potentials. For the gas, the equation is:

$$d\mu_{\text{gas}} = -s_g dT + v_g dP; \quad (8)$$

where

$$s_g = \frac{S_g}{n_g}, \quad v_g = \frac{V_g}{n_g}, \quad (9)$$

and n_g is the moles of unadsorbed gas. At equilibrium between the gas and the adsorbed phase, $d\mu_{\text{ads}} = d\mu_g$ so that

$$-\bar{s}_{\text{ads}} dT + \bar{v}_{\text{ads}} dP + \left(\frac{\partial \mu_{\text{ads}}}{\partial \Gamma} \right)_{T,P} d\Gamma = -s_g dT + v_g dP. \quad (10)$$

Making the usual assumption of an ideal gas and that $v_g \gg \bar{v}_{\text{ads}}$, one may write at constant Γ that

$$\left(\frac{\partial \ln P}{\partial T} \right)_{\Gamma} = \left(\frac{s_g - \bar{s}_{\text{ads}}}{RT} \right) \quad (11)$$

$$\left(\frac{\partial \ln P}{\partial T} \right)_{\Gamma} = \left(\frac{\bar{H}_g - \bar{H}_{\text{ads}}}{RT^2} \right); \quad (12)$$

$$\left(\frac{\partial \ln P}{\partial T} \right)_{\Gamma} = \frac{q_{\text{st}}}{RT^2} \quad (13)$$

Thus the isotheric heat, q_{st} , is the difference between \bar{H}_g , the molar heat content of the unadsorbed gas and \bar{H}_{ads} , the molar heat content of the adsorbed gas. Recalling that the adsorbent, A, was assumed inert, the further approximation is made that constant Γ implies a constant number of moles adsorbed. The isosteric heat equation may then be written in its final form as:

$$\left(\frac{\partial \ln P}{\partial T} \right)_{n_{\text{ads}}} = \frac{q_{\text{st}}}{RT^2}. \quad (14)$$

Point B

Brunauer and Emmett [47] defined five points on adsorption isotherms and labeled these points A, B, C, D, and E. The significance and location of one of these points, point B, is the subject of this section. The point B is frequently taken to be the point at which the first physically adsorbed monolayer is completed [47]. Point B is located at the beginning of the linear portion of the isotherm after the first isotherm step. The point B of the isotherms studied in this series of experiments was taken directly from the isotherms and is used to determine surface areas of the adsorbents. Plots according to the B.E.T. equation may be used in some instances to analytically determine the point B; however, the B.E.T. equation is not linear when applied to CCl_4 data [48].

The selection of point B as the point designating the completion of a monolayer is largely due to Brunauer and Emmett [47]. Brunauer and Emmett [47] considered isotherms resulting from adsorption measurements on ten iron catalysts using N_2 , CO , Ar , O_2 and n-butane. These isotherms were run at temperatures near the adsorbate gases' boiling points, the monolayer volumes calculated, and the mean deviations for each point compared. Point B monolayer volumes exhibited the smallest mean deviation from the average point B monolayer volume. Analyzing Clausius-Clapeyron equation calculated heat of adsorption curves for two systems, Emmett and Brunauer [47] noted heats at monolayer volumes 25 per cent greater than point B and 25 per cent less than point B. The heat at 25 per cent of a monolayer greater than point B was 250 calories in excess of the heat of liquefaction and the heat

at 25 per cent of a monolayer less than point B was 1000 calories in excess of the heat of liquefaction. According to Halsey [49], since point B occurs where the affinity of the gas for the surface is changing most rapidly, this is the most logical point to set as the completion of a monolayer. The locations of the nitrogen point B compare favorably with shallow minimums in the adsorption entropy versus coverage calculations of Harkins and Jura [50]. Harkins and Jura say that these entropy minimums indicate maximum order in the adsorbate layer.

B.E.T. area determinations are routinely made using nitrogen [51]. If nitrogen is used near its boiling point in conjunction with the accepted 16.2 \AA^2 per molecule nitrogen area, then a self-consistent body of surface area data can be compiled. It must be noted that when other gases are used there are many cases where widely differing B.E.T. areas are obtained [52]; however, at the present time there is no theory that results in identical surface areas for a variety of gases.

Henry's Law Region

A large portion of the data examined in this present work is taken in the Henry's law region. The term, Henry's law, is obtained by an analogy to the well known law dealing with the solubility of gases in liquids. The amount adsorbed varies directly with the equilibrium gas pressure in this the simplest region of the adsorption isotherm [53]. This law may be stated:

$$n_{\text{ads}} = K_h p, \quad (15)$$

where p is the equilibrium pressure; K_h is the Henry's law constant and n_{ads} is the number of moles adsorbed per gram of adsorbent. This law is the expected limit of every isotherm at sufficiently low pressures [46]. The transition to Henry's law is of fundamental interest. Once the Henry's law region has been achieved at a given temperature, measurements at lower pressures will yield no further information [54]. It is also clear that isotherms in this linear region must extrapolate to a zero intercept.

In making experimental measurements current instrumentation is not a limitation as pressures of 10^{-16} torr are detectable; however, Henry's law data are reported in the literature to no less than 10^{-9} torr [55]. The prohibitive factors at these pressures are the equilibration times which may take 50 hours [54]. Heterogeneity in the surface must be considered even at very low coverages, since high energy sites may be close enough together for adsorbate-adsorbate interactions to occur [54]. This problem of lateral interactions at very low coverages can be overcome to some degree by taking the experiment to higher temperatures. Finally, the pressure range and experimental scatter of the data must be considered, because data taken over a small pressure range may have enough experimental scatter to obscure any slight curvature in the isotherm [53].

Gas-Solid Virial Coefficients

In 1901 Kammerlingh-Onnes suggested that gas phase equation of state data could be fitted to a power series in the number density of the gas molecules [56],

$$PV = NkT \left[1 + \left(\frac{N}{V}\right) B_2(T) + \left(\frac{N}{V}\right)^2 B_3(T) + \dots \right] \quad (16)$$

$B_2(T)$ is called the second virial coefficient and is a function of temperature only. $B_3(T)$ is called the third gas virial coefficient and $B_4(T)$ is called the fourth virial coefficient, etc.. In 1954 Steele and Halsey [57] applied the formalisms of this gas phase treatment to the gas-solid interface. This is a powerful approach to the interpretation of physical isotherm data. In the Henry's law region and at slightly higher coverages, where lateral interactions cause the first deviations from isotherm linearity, we have the region in which the virial approach to gas-gas and gas-solid interactions is most fruitful [58]. At high densities of adsorbate gas, the virial expansion does not converge and more model dependent approaches, such as the Significant Structures Theory, must be used [59]. However, in the initial experimental regions examined here, the virial formalism builds a mathematically exact bridge from experimental data via statistical mechanics to adsorbate-adsorbent interaction energies [58].

The derivation of the second gas-solid virial coefficient,

B_{2s} and the subsequent relating of B_{2s} to a mean gas-solid interaction potential, ϵ_{1s}^* , adsorbent surface area, A , and to the distance of closest approach of the adsorbate to the surface, z_0 , is given in detail by Pierotti and Thomas [59,60]. Only the main points of the derivation will be outlined here. Two concurrent derivations, identical, except that one deals with field free space and the other deals with space experiencing an external field, such as that exerted by an adsorbent surface, are presented. Also, it should be noted that the adsorbate gas is treated as a sphere. This is equivalent to saying that a spherical potential is used to describe the gas. CCl_4 , CHCl_3 , CH_2Cl_2 , and CH_3Cl are non-spherical and thus would most aptly be treated by a non-spherical potential; however, in the absence of such a potential the spherical potential is to be used. Sams [58] uses a very similar attack in his treatment of methane data.

The partition function best suited to an adsorption system in which the molecules adsorbed are in equilibrium with those in the gas phase is the grand canonical partition function, $\Xi(V,T,\mu)$ [60]. This partition function is a function of the Gibbsian chemical potential, μ , the system volume, V_s and the absolute temperature, T . The grand partition function in field free space [60],

$$\Xi = \sum_{N_s} Q_{N_s}(V_s, T) \lambda^{N_s}, \quad (17)$$

is expressed in terms of the canonical partition function, Q_{N_s} and an activity term, λ . N_s is the average number of particles in a system in the canonical ensemble of systems. The activity is expressed as:

$$\lambda = e^{\frac{\mu}{kT}} \quad (18)$$

The canonical partition function is

$$Q_{N_s} = \left[\frac{1}{(N_s! \Lambda^{3N_s})} \right] Z_{N_s}(V_s, T); \quad (19)$$

where Λ may be recognized as the one dimensional linear momentum partition function,

$$\left(\frac{2\pi mkT}{h^2} \right)^{-\frac{1}{2}}.$$

$Z_{N_s}(V_s, T)$ is a configuration integral dealing with the positions of the particles which compose a system. It is possible to evaluate the configuration integrals, Z_0 , Z_1 , and Z_2 analytically by means of pair potentials, but higher terms must be approximated. For a system containing no particles, there is only one configuration and $Z_0(V_s, T) = 1$. For a system containing one molecule the case is that

of an independent particle and $Z_1(V,T) = V_s$. The partition function describing two particle systems corresponds to the case where pair interactions are present. The configuration integral for a system where pair interactions are possible is expressed as

$$Z_{2s} = V_s \int_{\text{system volume}} e^{-u_s(\tilde{r})/kT} d\tilde{r} \quad (20)$$

where \tilde{r} is a generalized coordinate with its origin at the center of one of the particles and $u_s(\tilde{r})$ is the pair interaction potential.

The characteristic equation for the grand partition function is

$$PV_s = kT \ln \Xi_s. \quad (21)$$

The average number of molecules in an ensemble system is given by

$$N_s = \lambda \left(\frac{\partial \ln \Xi_s}{\partial \lambda} \right)_{V_s, T}. \quad (22)$$

These equations form a basis for relating the pressure of a system and its density to the intermolecular potential. Taking all the systems, forming an ensemble, and using standard methods of imperfect gas theory one can write [58]

$$\ln \Xi = \sum_{i \geq 1} V b_i \zeta^i, \quad (23)$$

where

$$\zeta = \frac{f}{RT} = \frac{\lambda}{\Lambda^3} \quad (24)$$

and

$$1! V b_1 = Z_1 ; \quad (25)$$

$$2! V b_2 = Z_2 - Z_1^2 . \quad (26)$$

Here f is the gas fugacity and V the total volume of the ensemble.

The same system in an external field yields

$$\ln \Xi^e = \sum_{i \geq 1} V^e b_i^e \zeta^i \quad (27)$$

with

$$1! V^e b_1^e = Z_1^e ; \quad (28)$$

$$2!V^e b_2^e = Z_2^e - (Z_1^e)^2 \quad (29)$$

The average number of particles adsorbed as a result of the external field is given by

$$\bar{N}_{\text{ads}} = \bar{N}_e - \bar{N} = \lambda \left(\frac{\partial \ln Z^e / \Xi}{\partial \lambda} \right)_{T,V} = \sum_{i \geq 1} V_i (b_i^e - b_i) \delta^i \quad (30)$$

The superscript e signifies the presence of the external field.

Rewritten using equation (24) and defining $B_{i+1,s}$ as $V_i (b_i^e - b_i)$,

the formula above reads as follows [59]:

$$\bar{N}_{\text{ads}} = \sum_{i \geq 1} B_{i+1,s} \left(\frac{f}{RT} \right)^i \quad (31)$$

Here the gas-solid virial coefficients, $B_{i+1,s}$, appear. Inverting this last series one has

$$f = \frac{\bar{N}_{\text{ads}} RT}{B_{2s}} \left[1 - \frac{B_{3s}}{B_{2s}^2} \bar{N}_{\text{ads}} - \left(\frac{B_{2s} B_{4s} - 2B_{3s}^2}{B_{4s}} \right) \bar{N}_{\text{ads}}^2 + \dots \right] \quad (32)$$

Equation (32) may be related to the isosteric heat at zero coverage

by the definition of isotheric heat, q_{st} , where [59]

$$q_{st} = RT^2 \left(\frac{\partial \ln f}{\partial T} \right)_{\bar{N}_{ads}} \quad (33)$$

Thus

$$q_{st} = RT - RT^2 \left(\frac{d \ln B_{2s}}{dT} \right) - RT^2 \left(\frac{d(B_{3s}/B_{2s}^2)}{dT} \right) \bar{N}_{ads} + \dots \quad (34)$$

The gas-solid virial coefficients may be experimentally evaluated by substituting the gas phase expression for fugacity into the expression for the gas-solid virial coefficients yielding

$$n_{ads} = \frac{\bar{N}_{ads}}{N_{Avagadro}} = B_{2s} \left(\frac{P}{RT} \right) + (B_{3s} + B_{2s} B_{2g}^o) \left(\frac{P}{RT} \right)^2 + \dots \quad (35)$$

where p is the equilibrium gas pressure above the adsorbent and B_{2g}^o is the gas phase second virial coefficient in the field free space. Here n_{ads} is the number of moles of vapor adsorbed per gram of adsorbent. B_{2s} and B_{3s} can be obtained from

$$\lim_{p \rightarrow 0} \left(\frac{n_{ads} RT}{P} \right) = B_{2s} \quad (36)$$

A plot of $n_{\text{ads}} RT/P$ versus P yields B_{2s} as an intercept at zero pressure [59]. Information about B_{3s} can be obtained from the slope of the line used to obtain B_{2s} . This furnishes one method for obtaining B_{2s} . An alternate method for obtaining B_{2s} is derived from the Henry's law constant. Written in terms of Henry's law [59],

$$\frac{W}{P} = K_h = \frac{MB_{2s}}{RT}, \quad (37)$$

where W is the weight adsorbed in grams per gram of adsorbent and M is the gram molecular weight. K_h is the limiting slope of a plot of W versus p . This extrapolation involving Henry's law should have zero W intercept at zero pressure.

Now we will examine theoretical values for B_{2s} subject to various adsorbate-adsorbent interactions. The expression for B_{2s} is defined by our statistical mechanical discussions and equations (20), (25), (28) and (30) as:

$$B_{2s} = \int_{V^e}^V \frac{1}{V} \{ \exp(-u_s(\tilde{r})/kT) - 1 \} d\tilde{r}. \quad (38)$$

Here \tilde{r} signifies a generalized coordinate [59], whose origin is at the center of an adsorbent molecule. Starting with a (6,12) potential, integration of B_{2s} over a semi-infinite solid adsorbent

yields a (3,9) potential law [61]. Integration over a single infinite plane of adsorbent yields a (4,10) potential. Integrating only the attractive part of the potential over a semi-infinite solid adsorbent yields a (3,12) potential law. Comparing the end results of these integrations to experiment, one finds little difference to choose between them. However, a (3, ∞) potential does give a significantly poorer fit of experimental data. Starting with a hard sphere molecule with an attractive potential, a (3, ∞) potential law results after integration over the solid's surface and volume.

The (3,9) law is frequently used to treat experimental adsorption data. This law, the end result of using an integration to sum the (6,12) potential interaction of each adsorbate molecule with each adsorbent molecule, is given via equation (38) as:

$$B_{2s} = Az_0 \sum_{i=0}^{\infty} \frac{1}{9i!} \left[\left(\frac{3}{2}\right)^{3\frac{1}{2}} \left(\frac{\epsilon_{1s}^*}{kT}\right)^{(7i)/9} \right] \Gamma\left(\frac{(3i-1)}{9}\right) \quad (39)$$

Here $\Gamma((3i-1)/9)$ is the gamma function; A is the adsorbent surface area; z_0 the distance of closest approach of the adsorbate to the surface; ϵ_{1s}^* is the potential minimum of the gas-solid interaction potential. This equation for B_{2s} involving the gamma function may be solved numerically utilizing computer scanning techniques [58].

The equation may also be approximated analytically [62]. Hansen [62] has obtained approximate analytic equations based upon a harmonic potential. At low reduced temperature, kT/ϵ_{1s}^* , where molecular

vibrations do not cause excessive excursions from the adsorbed molecule's equilibrium position, the harmonic approximation can be a good approximation. Using this harmonic approximation and expanding the potential law about its potential minimum yields an expression, $u_s(z) = \epsilon_{1s}^* + \frac{1}{2} k_z (z - z^*)^2$, provided there is no angle dependence in the molecule's surface interaction. In this equation z is the perpendicular distance of the molecule's center from the plane surface, k_z is the force constant for the molecular vibrations perpendicular to the surface and z^* is the distance from the surface at which the potential minimum, ϵ_{1s}^* , occurs. At low reduced temperature, if a harmonic potential approximation of a (3,9) potential is inserted into equation (38), the following simple expression for B_{2s} is obtained [59]:

$$\frac{B_{2s}}{Az_0} = \left(\frac{2\pi}{27}\right)^{\frac{1}{2}} 3^{1/3} \left(\frac{kT}{\epsilon_{1s}^*}\right)^{\frac{1}{2}} \exp\left(-\frac{\epsilon_{1s}^*}{kT}\right). \quad (40)$$

This is the expression used to extract parameters from the experimental data listed in this work. See Chapter IV.

Frenkel-Halsey-Hill Equation

A successful model in describing multilayer adsorption is the Frenkel-Halsey-Hill model [44]. In one derivation of this equation, Hill [63] extends Lennard-Jones and Corner's treatment of surface tension via the free volume model of liquid state. Hill [63] places the liquid molecules in cells at position, x , y , and z with the

cell center at x' , y' , and z' . Both sets of coordinates have the same origin. Then the liquid at $z < 0$ is removed and replaced by a solid. The liquid at $z > h$ is also removed, leaving a slab of liquid of thickness, h , upon the solid adsorbent. Hill [63] takes a potential of the form

$$u(r) = \infty, \quad r \leq r^*; \quad (41)$$

$$u(r) = - \epsilon (r^*/r)^6, \quad r > r^*. \quad (42)$$

The neighbor distribution is uniform outside of $r = r^*$. Hill's integration reduces the sixth power potential dependence to a cubic. Hill notes that the introduction of a repulsive term would reduce the cubic power slightly.

Singleton and Halsey [44] modified Hill's equations and introduced the possibility of perturbation of the adsorbate by either incompatibility with the adsorbent or by changing the pair interaction. They proposed the equation:

$$\ln \left(\frac{P}{P_0} \right) = - \left(\frac{\Delta \epsilon_1^*}{\theta^i kT} \right) + \frac{w(1-g)}{kT}. \quad (43)$$

For theoretical reasons i is frequently set equal to three. Recalling that Hill expected repulsion to reduce the third power dependence, it

is noted that experimentally i averages to about 2.6 [64]. The Δe_1^* is the excess energy of adsorption of the first adsorbed layer. Steele [64] gives the rough approximation that for the first layer $\Delta e_1^* = q_{st}^0 - \Delta H_{vap}$. The w is a lateral interaction parameter approximately equal to one half the energy of sublimation of the bulk crystalline adsorbate. This value for w is due to the coordination number in the adsorbate layer being approximately six as opposed to twelve in the bulk crystal. The g is a factor close to unity which measures the compatibility of the adsorbed film with the bulk adsorbate when the film is perturbed by the adsorbent.

As was implied in the opening paragraph of this section, the Frenkel-Halsey-Hill equation has been widely applied. Two examples of methods of attack using this theory are furnished by Singleton and Halsey [44] and by Pierotti and Halsey [65]. Singleton and Halsey analyzed the limiting thickness of layers of adsorbed inert gases. Pierotti and Halsey made comparisons between values of Δe_1^* obtained experimentally and those obtained from different expressions for the London dispersion constant.

Significant Structures Theory

The Significant Structures Theory of Liquids was developed by Eyring, Ree and Hirai [66]. Eyring and Walter [67] had first suggested a method of disordering a liquid by introducing lattice vacancies. This theory has been applied to a number of systems including, rare gases, methane, nitrogen, chlorine, hydrogen and fused salts [68]. McAlpin and Pierotti [68] have modified this theory

to describe physical adsorption. The Significant Structures Theory bases its description of a liquid upon the assumption that a liquid can be considered to possess simultaneously, but to varying degrees, properties derived from three types of structural arrangements of molecules. The first structure is solid-like, where each molecule is restrained to a given equilibrium position by its neighbors. Secondly, a structure consisting of a configurationally degenerate solid is used. Molecules in this degenerate solid possess some freedom of movement due to nearest neighbor lattice vacancies. The third contributing structure is gas-like, in that molecules may translate freely throughout the liquid's volume.

McAlpin and Pierotti [63] adapted the two-dimensional counterpart of the Lennard-Jones Devonshire Theory of Liquids to the gas-solid interface. The Lennard-Jones Devonshire Theory was used to formulate the solid-like and degenerate solid partition functions. Standard types of partition functions were used to describe both the two and three-dimensional gas phases. The degree of contribution of the two-dimensional solid-like and degenerate solid structures was obtained as $N(A_s/A)$ by analogy to Eyring, Ree and Hirai's three-dimensional term. N is the number of molecules in the surface phase at a given coverage, θ . A_s is the molar area of the surface phase at a monolayer coverage. A is the molar area of the two-dimensional surface phase at a given coverage, θ . This term, $N(A_s/A)$ approaches zero at low coverages and is N at a monolayer coverage. The degree of contribution of the gas-like phase, $N(A-A_s)/A$, is obtained similarly and possesses the correct limiting behavior. These terms

are transformed by McAlpin and Pierotti [68] into experimentally measurable quantities, θ and N_m . N_m is the number of molecules necessary to cover a monolayer. This yields $\theta^2 N_m$ for the solid-like and degenerate solid and $\theta(1 - \theta)N_m$ for the gas-like degrees of freedom. The partition function for the adsorbed phase Q_{ads} is [38,68]:

$$Q_{ads} = q_{2s}^{\theta^2 N_m} q_{2g}^{\theta N_m (1 - \theta)} \quad (44)$$

Here q_{2s} is the two dimensional solid-like and degenerate solid partition function. The q_{2g} is the two-dimensional gas partition function [36,38].

Once the partition functions for the gas phase and adsorbed phase are established, the characteristic equation for a canonical ensemble can be obtained as [68]

$$F_{ads} = - kT \ln Q_{ads} \quad (45)$$

and

$$F_{gas} = - kT \ln Q_{gas} \quad (46)$$

Here Q_{ads} is the canonical ensemble partition function for the adsorbed

gas; Q_{gas} is its gas phase counterpart and F is the Helmholtz free energy. The chemical potentials may then be obtained as

$$\mu_{\text{gas}} = \left(\frac{\partial F}{\partial N_{\text{gas}}} \right)_{T, V, N_{\text{ads}}} \quad (47)$$

and

$$\mu_{\text{ads}} = \frac{1}{N_m} \left(\frac{\partial F}{\partial \theta} \right)_{T, A, N_{\text{gas}}} \quad (48)$$

Here N_{gas} is the number of gas phase molecules and N_{ads} the number of adsorbed molecules. At equilibrium the chemical potentials may be equated. The isotherm equation is then extracted by recognizing that [68]

$$\frac{\mu_{\text{gas}}}{kT} = \frac{\mu_{\text{gas}}^0}{kT} + \ln p. \quad (49)$$

where p is the equilibrium gas phase pressure.

Now that the general procedure for obtaining the isotherm equation has been outlined, some specifics of the partition functions will be discussed. The gas phase partition function, q_{3g} , for a non-spherical molecules is [69,70]

$$q_{3g} = \left((\pi^{\frac{1}{2}} (8\pi^2 kT)^{3/2} (I_x I_y I_z)^{\frac{1}{2}} / \sigma h^3) \left(\prod_{i=1}^{n_v} (1 - e^{-h\nu_i/kT})^{-1} \right) \right) \quad (50)$$

$$\times (2\pi mkT/h^2)^{3/2} V_g.$$

V_g is the volume accessible to the gas phase molecule; σ is the symmetry number for the gas phase molecule; n_v is the number of internal vibrations characterized by frequencies, ν_i ; I_x , I_y and I_z are the moments of inertia of the molecule about its principal axes; π , k , T , h , and m have their usual meanings. The partition function of the adsorbed molecule, q_{2g} , is the expected combination of rotational, vibrational and translational partition functions and is given by [68,69,70]

$$q_{2g} = \left((\pi^{\frac{1}{2}} (8\pi^2 I_z kT)^{\frac{1}{2}} / \sigma_s h) \left(\prod_{i=1}^{n_v} (1 - e^{-h\nu_i/kT})^{-1} \right) \right) \quad (51)$$

$$\times (1 - e^{-h\nu_x/kT})^{-1} (1 - e^{-h\nu_y/kT})^{-1}$$

New parameters are, σ_s , the symmetry number of the adsorbed molecule, ν_x and ν_y . It was decided that the degrees of freedom corresponding to rotation about the x and y axes would be modified to appear as

rocking vibrations of frequency ν_x and ν_y . This involves the assumption that the adsorbed molecule, while free to rotate about an axis normal to the surface, would be prevented by a 3200 calorie rotational barrier [80] from flipping over.

The implications that a liquid has some of the characteristics of the solid lattice comes mainly from x-ray radial distribution function studies [39,71]. These radial distribution function studies show that liquids possess short range order. Molecules in a liquid command coordination numbers similar to the numbers of nearest neighbors in a solid. This order in liquids quickly degenerates into randomness, with the second coordination sphere nearing liquid densities. The partition function, q_{2s} , is obtained from the Lennard-Jones Devonshire cell theory of liquids. In the Lennard-Jones Devonshire, (LJD), theory we imagine the area divided up into a lattice of cells [37,38]. Each cell encircles one molecule. The pair interaction potential between a given molecule and all other molecules is not constant. The potential minimum is located at the center of the cell. The cell is circular with the nearest neighbors "smeared" around its circumference. The probability of observing the molecule displaced from the center of the cell is governed by the Boltzmann factor. As a result the area, a_f , an adsorbed molecule is free to move around in, is less than the geometrical area. The LJD model is not suitable for surface coverages significantly lower than the critical coverage of 0.70 of a monolayer [38], because at lower coverages the possibility of multiple occupancy of cells arises.

The LJD partition function used by McAlpin and Pierotti [38,69,70] was

$$q_{2s} = \left(\frac{2\pi mkT}{h^2} \right) a_f \exp \left(\frac{\bar{w}}{kT} \right) \left(1 + \frac{c(1-\theta)}{\theta} \right) . \quad (52)$$

The factor $1 + c(1 - \theta)/\theta$ accounts for the configurational degeneracy of the two dimensional solid. Here c is the lattice coordination number and was taken to be six; \bar{w} is a mean potential obtained by lattice summation using a Lennard-Jones (6,12) potential. \bar{w} is given by [69]

$$\bar{w} = -6.720 \epsilon_{12}^*/k . \quad (53)$$

Here ϵ_{12}^* is the Lennard-Jones parameter for the interaction of two adsorbed molecules with one another. The equation for obtaining a_f is given in Chapter IV as is the final form of the isotherm equation.

Two-dimensional critical properties can be calculated from the isotherm equation by the usual methods. The disappearance of the first and second derivations with respect to coverage yields the required Significant Structures parameters [38,68],

$$\frac{kT}{\epsilon_{12}^*} 2c = \frac{3}{5} ; \quad (54)$$

$$\frac{T_{2c}}{T_{3c}} = 0.45 . \quad (55)$$

Here T_{2c} is the two-dimensional critical temperature and T_{3c} is obtained from the three-dimensional counterpart. The relationship of T_{2c} to ϵ^*_{12} is a valuable one in that it eliminates an adjustable parameter by affording a simple means for obtaining ϵ^*_{12} from the experimental T_{2c} .

Sinanoglu and Pitzer [45] have shown that the perturbing effect of the solid adsorbent upon the adsorbed gas molecules results in an effective reduction of the ϵ^*_{12} of 20 to 40 per cent as compared to the value of the gas phase potential well depth. This means that the $(\epsilon^*_{12}/\epsilon^*_{12 \text{ gas phase}})$ is not unity and that equation (53) could to a second approximation be rewritten as:

$$\frac{T_{2c}}{T_{3c}} = 0.45 (\epsilon^*_{12}/\epsilon^*_{12 \text{ gas phase}}). \quad (56)$$

Once the ratio of T_{2c}/T_{3c} is known, an estimate of the reduction in ϵ^*_{12} is possible and through the use of equation (56) an estimate of the $\epsilon^*_{12 \text{ gas phase}}$ may be made. It has been shown in an earlier section that the value of T_{2c}/T_{3c} depends upon the model selected and this should be considered when such estimates are quoted.

CHAPTER III

EXPERIMENTAL

Introduction

The purpose of this chapter is to describe the experimental manipulations, equipment and chemicals that are used in this series of experiments. The principle measuring device is the Cahn R-G Automatic Electromicrobalance (Cahn Instrument Company, Paramount, California). Using this microbalance, weight measurements are made in the Henry's law region, e.g. 0 to 8 per cent of a monolayer, the monolayer region and the multilayer region. These weight measurements are made to precisions of 0.001 mg in the submonolayer region, 0.003 mg in the monolayer region and 0.01 mg in the multilayer regions. Other notable features of the adsorption system are: (1) capacitance manometer to allow isolation of the adsorption system and to measure pressures in the lower ranges, (2) metal bellows valves to handle organic vapors, (3) capacitance activated relay to allow a continuous variation of the cryostat's temperature via a vapor pressure thermometer. The apparatus is shown pictorially and schematically in Figures 1 and 2. Sections in this chapter are:

- (a) Microbalance calibration
- (b) Microbalance experimental difficulties
- (c) Construction of adsorbent containers
- (d) Temperature measurements

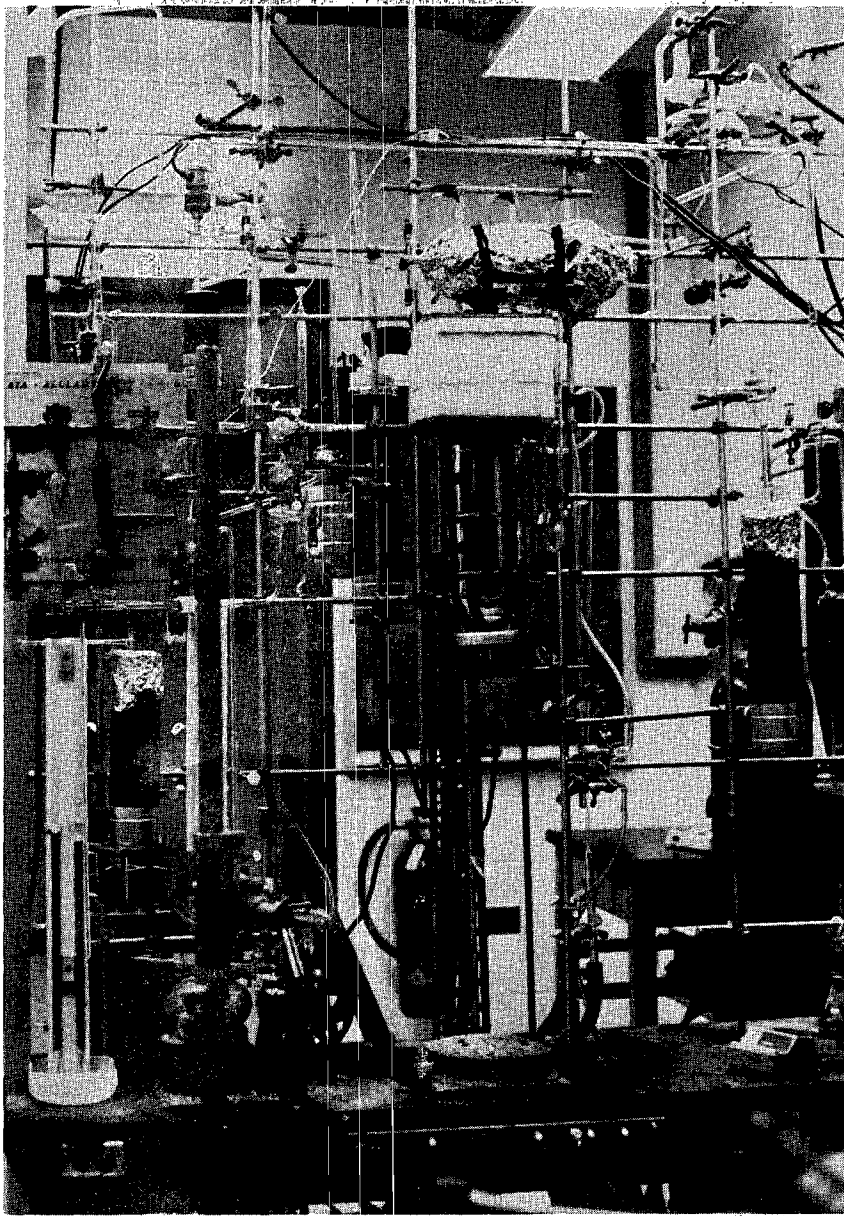


Figure 1. Photograph of Experimental Apparatus.

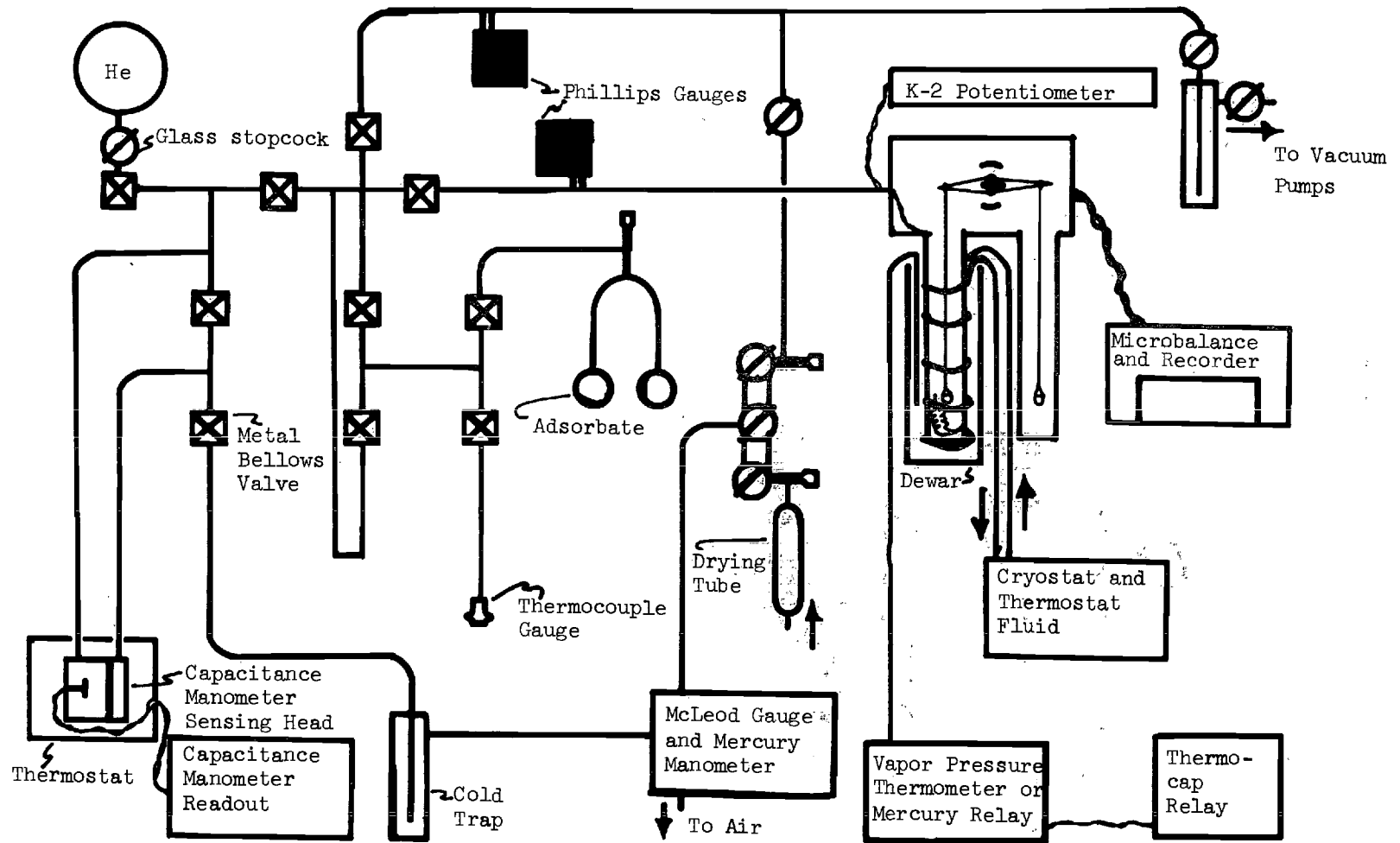


Figure 2. Schematic of Experimental Apparatus.

- (e) Capacitance manometer and pressure measurements
- (f) Temperature regulating devices
- (g) Adsorbates and adsorbents
- (h) A typical run.

Microbalance Calibration

The microbalance is calibrated using essentially the procedures and techniques described in the Cahn instruction manual [29]. Calibration is accomplished by varying a resistance so that the voltage difference from the microbalance motor across the microbalance potentiometer corresponds to five units when a change of 5 mg is dialed on the potentiometer. The voltage sent to the recorder is also adjusted to assure a known correspondence between the recorder readout and the weight change. Before the calibration procedure is begun, the adsorbent-containing bucket and the tare bucket must be nearly identical in weight.

The balance is calibrated [29] on the 10 mg Mass Dial Range, 1 mg Recorder Range with a 5 mg class M weight. The Mass Dial is read in per cent of the Mass Dial Range to four digits and must be multiplied by the Mass Dial Range setting to obtain the weight change in milligrams. The Mass Dial Range allows selection for weight changes of 1, 10, 100, or 200 milligrams and is marked accordingly. A full scale reading on the recorder may be adjusted to be 0.02, 0.04, 0.1, 0.2, 0.4, 1, 2, 4, 10 or 20 milligrams by means of the Recorder Range Dial. The Z Recorder Range Dial setting isolates the recorder from the microbalance and is used to obtain the recorder

zero.

The calibration procedure is as follows. First determine the weight of the tare bucket by means of a Mettler Balance and then adjust the weight of the sample containing bucket to as nearly an identical weight as possible. This adjustment is made by adding bits of glass or glass wool to the sample bucket. Next the sample bucket and tare are suspended from the electromicrobalance and the recorder zero noted with the Mass Dial set to zero. The Recorder Range is turned to Z. Then the balance is set to five on the Mass Dial and the 5 mg class M weight is placed upon the sample containing bucket. The Recorder Range is moved back to 1 mg and the recorder zero noted. If the balance is properly calibrated, the recorder zero with the Mass Dial at zero is at the same position on the chart paper as when there was a 5 mg weight on the sample bucket and the Mass Dial was set to five. Adjustments accomplishing this end could be made if necessary by means of the Set-5 or Set-(0-10) dials. An observation that greatly simplified this last step is that a movement of one unit of the recorder trace by the Set-(0-10) dial affects a movement in the Set-5 adjustment of two units of the recorder trace, but in the opposite direction. This observation meant that all final adjustments could be made using only one dial. Using the Cahn's 0.4 mg and 1.0 mg Recorder Ranges, the 10 mg and 100 mg Mass Dial Ranges, and the 1x and 10x factors, weight changes of 0.001 mg to 50 mg were measured. These weight changes are recorded using the one millivolt recorder setting on a Model 7127A, Hewlett-Packard strip chart recorder. The

recorder noise is minimized by means of a Cahn filter setting of two, in conjunction with an additional filter constructed from a 50 mfd electrolytic capacitor and a 1000 ohm carbon resistor.

Microbalance Experimental Difficulties

Some problems encountered during the operation of the microbalance are zero shift upon physical shock, weight change with pressure, static electricity, and the continued pendulum of action of the buckets in vacuo. The problem of zero change with physical shock was never satisfactorily solved. The use of either soft foam rubber seal or a sheet of flexible plastic film between the dewar assembly and the hang-down tube containing the sample bucket offers some relief. It is noticed that with helium and neon a weight loss on the order of 0.2 mg/g occurs in the pressure range 0 to 0.05 torr. See Figure 3. Concurrently it is noticed the temperature of the sample varies with pressure in the range 0 to 0.02 torr. These two conditions are alleviated by inserting an atmosphere of 0.1 torr of helium when low pressure measurements are to be made. At the temperatures where the measurements are made, the adsorption of the helium is insignificant. Static electricity is merely a minor problem; therefore, the poor heat transfer incurred when the hang-down sample tube is gold plated much out-weighs any gains. Wetting the hang-down tube sometimes helps and if that fails, letting in a dose of adsorbate gas usually solves this static build-up. Oscillation of the buckets in a vacuum is easily remedied by about 0.2 torr helium which quickly damps the swings and is easily pumped out.

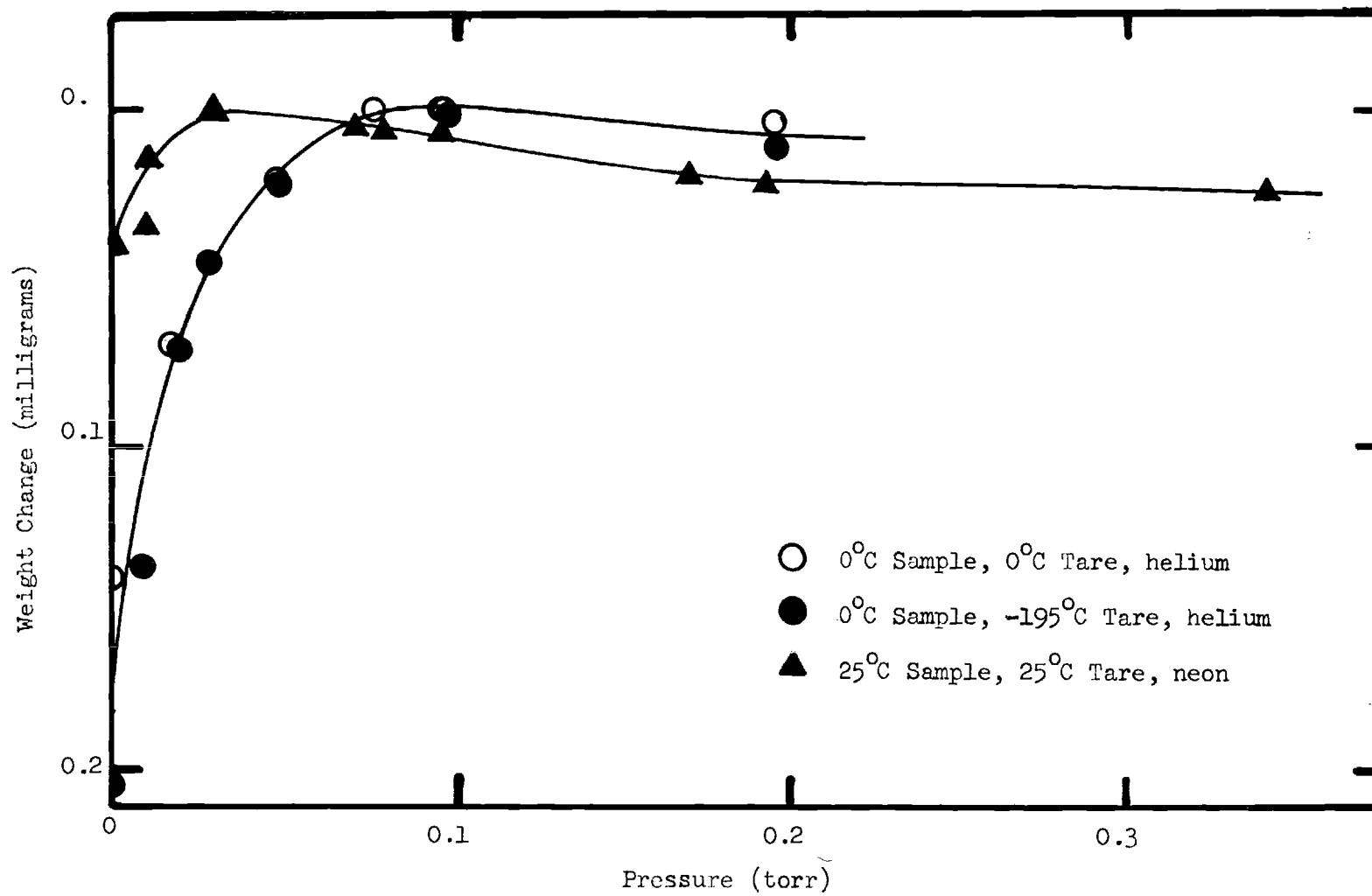


Figure 3. Variation of Electrobalance as a Function of Pressure of a Non-Adsorbed Gas.

The Pyrex bottle containing the microbalance is wrapped with aluminum foil to exclude light. The electromicrobalance operates upon the principle of measuring the current necessary to re-establish the equilibrium position of the balance arm after a weight change has occurred. The exclusion of light is necessary because a phototube-metal-flag-lamp assembly is used to determine when the equilibrium balance position is achieved.

Construction of Adsorbent Containers

Preliminary to the experiments, glass buckets are constructed. These glass buckets weighing approximately 0.3 g, are prepared by drawing out a 6 mm Pyrex glass tube and leaving a bulb of the original diameter on the tube's end. This bulb is heated to redness and inserted into a tube of asbestos paper, which is fabricated by wrapping wet asbestos paper around a glass tube of the desired diameter of the bucket and then drying the asbestos tube in an oven. The hot bulb is blown slowly larger inside of an end of the asbestos tube which has been re-wet. The bulb consequently takes the form of a cylinder the size of the inside diameter of the asbestos tube. The bulb's end opposite the drawn down portion is heated in a sharp flame to form and reinforce a rim. Drawn down glass rod is attached to this rim on its opposite sides, crossed and fused to make the tip of the handle. Now using the bucket handle to hold the bucket, the drawn down portion of the 6 mm glass tube is heated and pulled away, forming the bottom of the glass bucket. A trial and error method is used to obtain a bucket of the desired weight. Two buckets are made

and attached to the microbalance using 45 cm lengths of 0.004 cm diameter nichrome wire. Into one bucket is placed approximately 0.4 g adsorbent topped with 0.05 g of Pyrex glass wool. This Pyrex wool is cleaned by washing with concentrated nitric acid, rinsing with distilled water and drying in an oven. The total weight of the bucket and contents are counterbalanced by a tare bucket containing bits of glass and glass wool.

Temperature Measurement

The temperature measurement at the adsorbent requires finding a means of entry into the microbalance. The microbalance is contained inside of a vacuum tight Pyrex bottle. The Pyrex bottle is fused to upper portion of the hang-down tubes containing the tare bucket and the adsorbent bucket. See Figure 4. The 32mm outside diameter Pyrex tube housing the adsorbent bucket is removable. This removability is afforded by two Kovar to glass seals, one inch in diameter which are held together by means of a one inch stainless steel Swagelock fitting. Teflon ferules are used in this Swagelock fitting. Two one-eighth inch stainless steel Swagelock fittings allow entrance of the 0.011 inch diameter thermocouple wires into the microbalance bottle. A vacuum tight seal is obtained by redesigning the front Swagelock ferule. A solid front ferule is constructed of Teflon and center drilled with a #80 drill bit. The wires of the copper-constant thermocouple are threaded through these tiny holes and the Swagelock fittings tightened to make a vacuum tight seal. The thermocouple wires are led down the hang-down tube by 6 mm

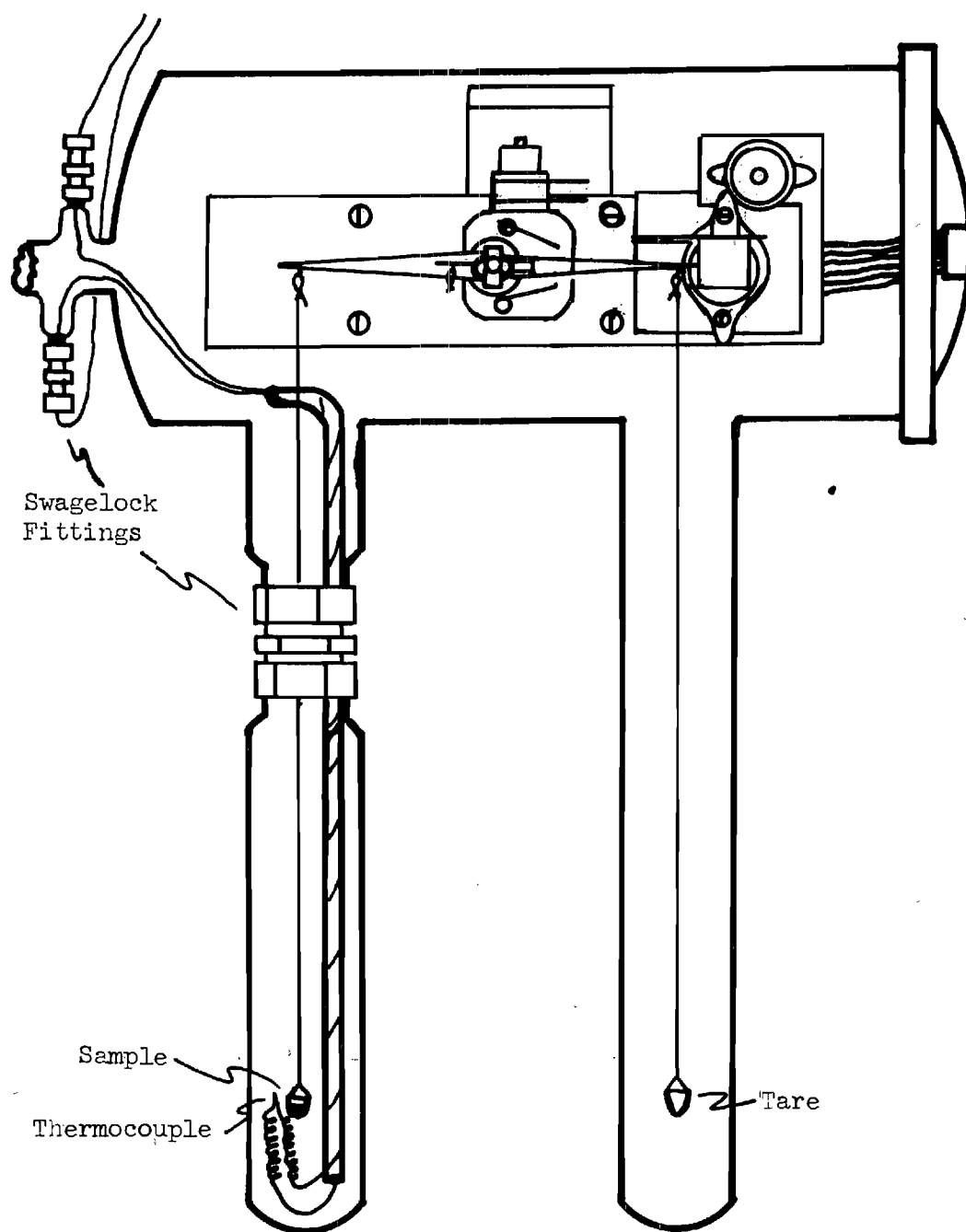


Figure 4. Electrobalance and Containing Pyrex Bottle.

glass tubing epoxied to the bottle. The last 10 cm of the thermocouple wires are coiled into short springs and the junction placed approximately 2 mm from the glass bucket containing the adsorbent. The purpose of coiling the wires is to minimize thermal conduction to the junction by the thermocouple wires. The temperatures are measured to within $\pm 0.05^{\circ}\text{C}$ using copper-constantan thermocouples in conjunction with a tabulation of emf temperature data (NBS Circular #561, Temp International Scale of 1927, emf in absolute units) furnished by the Leeds and Northrup Company. The thermocouple reference junction is placed in a dewar containing water and melting ice. A Leeds and Northrup K-3 potentiometer is used to measure the thermocouple emf. The recommended Leeds and Northrup galvanometer with a sensitivity of $0.005 \mu \text{ amp/mm}$ is used as the null instrument. The thermocouples were prepared by Dr. R. Ramsey. They were arc welded in a hydrogen atmosphere. The thermocouples are compared with a platinum resistance thermometer Leeds and Northrup no. 8163-c, serial no. 1547845. The constants used in the Callendar formula are $R_0 = 25.581$, $C = 0.00392568$, $\delta = 1.492$ and assuming the platinum resistance thermometer to be made of pure platinum $\beta = 0.111$. A graph of the difference between the platinum temperature and the thermocouple temperature versus the thermocouple temperature is used to make appropriate corrections in the measured thermocouple temperatures. See Figure 5.

Capacitance Manometer and Pressure Measurements

The capacitance manometer consists of a massive piece of

(Platinum Thermometer Temperature - Thermocouple Temperature)

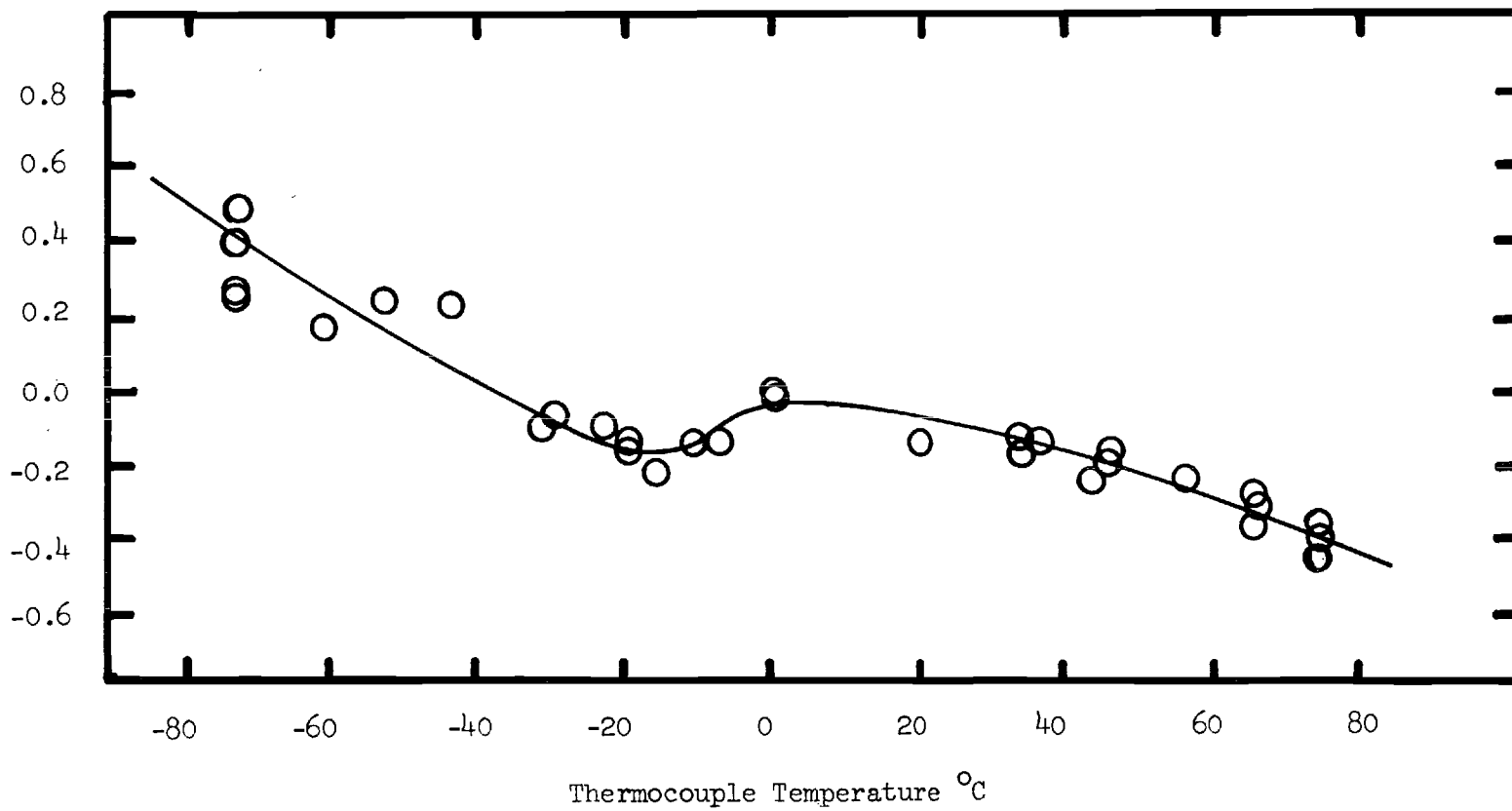


Figure 5. Copper-Constantan Thermocouple Calibration Curve.

stainless steel containing a stainless steel diaphragm. A pressure differential across this diaphragm causes it to deflect, thus changing a capacitance balance. This is displayed on the accompanying instrumentation. The response is claimed to be linear for small excursions of the membrane. See Figure 6. A variation of 0.05 torr per degree centigrade is quoted. A simple air thermostat was constructed, consisting of a box made from three-fourths inch plywood, a mercury relay inserted into a hole in a block of aluminum, and a 25 watt incandescent bulb. Contact between the relay and the aluminum block is improved by filling the hole with pump oil. The mercury relay activates an electronic relay which controls the incandescent bulb. This thermostat keeps the manometer's sensor head at a temperature which is constant over a period of weeks to better than 0.1°C . Thus the errors in pressure measurements due to fluctuations in ambient temperature are less than 0.005 torr.

Experimental work verifies the claims that the Granville-Phillips series 212, model B capacitance manometer's 0.1 and 1.0 range scales are linear with respect to pressure and related by a factor of ten. See Figure 6. This allows the more accurate calibration of the 1.0 scale to be used for the 0.1 scale. Pressures from 0.002 torr up to 2.0 torr are measured on this instrument. At higher pressures the capacitance manometer is used as a null indicator to signal when the pressure in the adsorbing system was the same as that in the McLeod Gauge or over the mercury manometer. Also the capacitance manometer is used to regulate the amount of adsorbate vapor admitted in each dose.

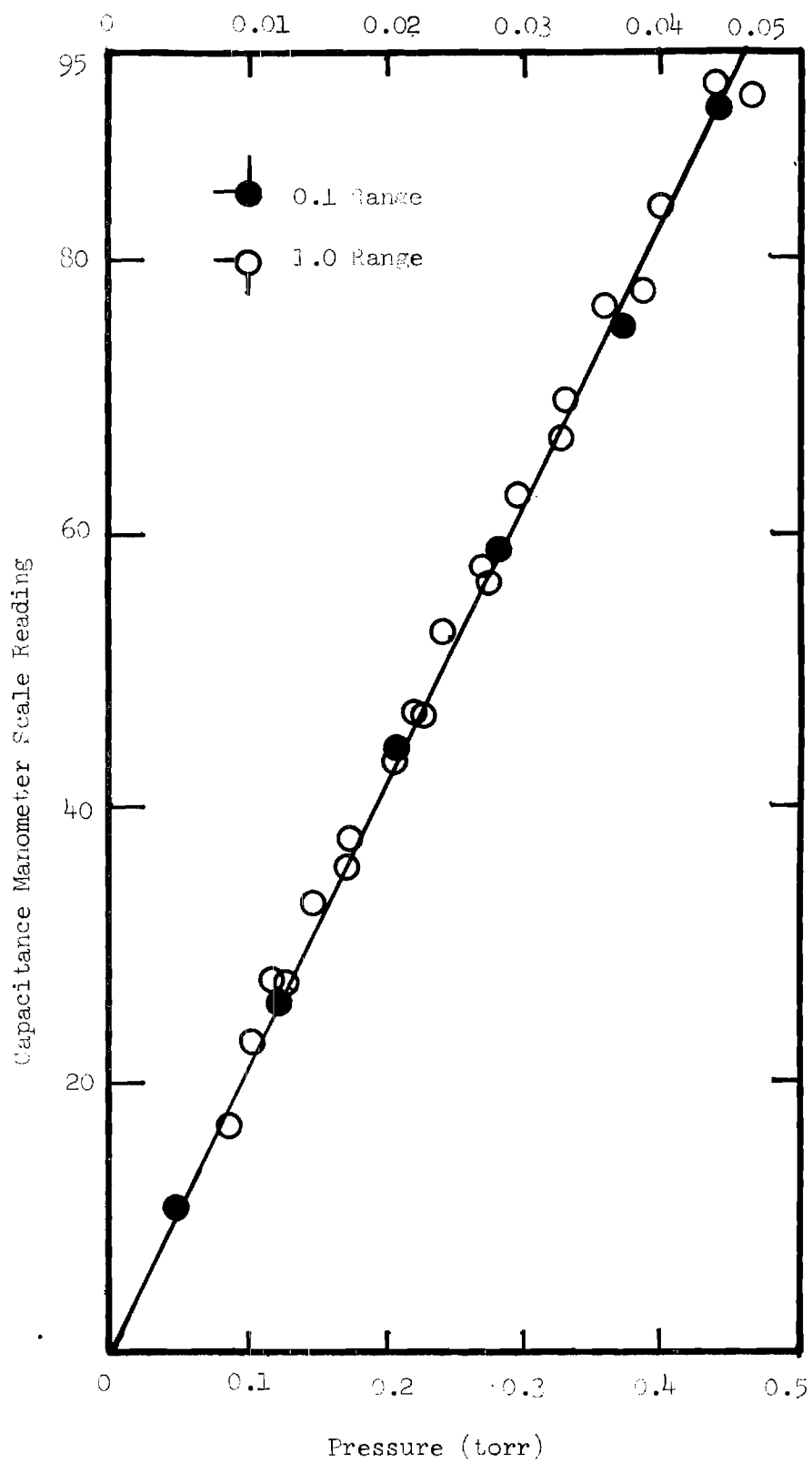


Figure 6. Pressure Comparison of Capacitance Manometer's 0.1 and 1.0 Ranges.

The mid-range pressures, e.g., 2.0 torr to 10.0 torr, are measured using a McLeod gauge. This gauge is also used to calibrate the capacitance manometer. The McLeod gauge is used in conjunction with a three liter ballast tank to minimize pressure variations due to a slightly varying rest position of the mercury below the McLeod cut-off point. McLeod pressures are doubly calculated to correct for the pressure above the column of mercury outside of the calibrated volumes. That is, a pressure is calculated and that pressure added to the height of the column open to the capacitance manometer. Using this new column height, the pressure is recalculated to give the final pressure. This correction amounts to approximately 2 per cent at high pressures and 0.2 per cent at the lower pressures measured. The McLeod gauge has three ranges, 0 to 0.3 ± 10^{-3} torr, 0 to $1.5 \pm 5 \times 10^{-3}$ torr and 0 to 9.6 ± 10^{-2} torr [72]. Adsorbate pressures greater than 10 torr are measured to ± 0.05 torr using a mercury manometer and a Gaertner M911 Cathetometer. The manometer is constructed from 16 mm Pyrex tubing. The heights of the mercury columns in both the McLeod gauge and the mercury manometer are corrected to zero degrees centigrade and sea level by the following formula:

$$h_{\text{corr}} = h_{\text{exp}} \left(\frac{\rho_{\text{TOC}}}{\rho_{\text{OOC}}} \right) \left(\frac{g_{\text{tech}}}{g_{\text{sea level}}} \right) = h_{\text{exp}} (0.998827 - 0.00018t) \quad (57)$$

Here ρ is the mercury density, g the acceleration of gravity and h_{exp}

the height of the mercury column. The t is the temperature of the column of mercury in centigrade degrees.

Pressure calculations using the gas second virial coefficients [73,74,75] of the vapors studied show pressure corrections to be less than 0.2 per cent. Since this correction is of the order of magnitude of the experimental errors, corrections are not made on the B_{2s} data treated in this work.

The vacuum system is evacuated by a Consolidated Vacuum Corporation GF-20 oil diffusion pump containing 130 ml of Dow Corning 702 silicone pump fluid. The back-up pump is a Precision Scientific model-25.

Nupro high vacuum bellows valves, 6 BG-SW, are used to alleviate the problem of organic vapors dissolving in the stopcock grease of the conventional high vacuum glass stopcocks.

Temperature Regulating Devices

Temperatures are maintained by three methods, depending upon the temperature desired. The simplest, most accurate method is to use a well stirred dewar full of water and melting ice. Temperatures below three degrees centigrade are controlled by means of a vapor pressure thermometer in combination with a capacitance relay. Temperatures above three degrees centigrade are regulated by a mercury relay.

For the low temperature control a series 200 Thermocap Relay (Niagara Electron Laboratories) is used in conjunction with a vapor pressure thermometer. The vapor pressure thermometer is also used

to select the temperature. The relay detects changes in the height of a mercury column which is a part of the vapor pressure thermometer. The relay sensor is a ring of copper foil placed around one arm of the mercury column. A change in the position of the mercury meniscus changes the capacitance that the foil experiences triggering the relay. The relay then activates a vacuum pump which pulls vapors from a liquid nitrogen reservoir through copper cooling coils placed in the cryostat. The copper coils are placed inside a large strip silvered dewar flask. See Figure 1. There is a polyethylene shield inside the coil so that the chilled bath fluid has to circulate up and then down through this shield to reach the part of the hang-down tube containing the adsorbent sample. A thin walled brass tube is connected to the gas thermometer and is positioned beside the sample to receive a similar circulation. The dewar contains four liters of absolute ethanol, m.p. -117°C . This ethanol is circulated by a football-shaped magnetic stirring bar. The gases used in the gas thermometer are methyl chloride in the -80°C to -40°C range and n-butane in the -40°C to 3°C range.

When a temperature greater than room temperature is desired a thermostated bath containing ethylene glycol at a temperature three to four degrees centigrade higher than the desired temperature is substituted for the liquid nitrogen reservoir. The heated glycol is circulated through the copper coils heating the four liter dewar, which now contains ethylene glycol and a small amount of water. The temperature is regulated by using a mercury relay to turn on and off

the pump circulating the heated ethylene glycol. The temperature control of the thermostat approaches the $\pm 0.01^{\circ}\text{C}$ claimed by the mercury relay specifications. Temperatures between zero degrees centigrade and room temperature are also controlled by this last method. However, the bath circulating the ethylene glycol is in this case cooled to a few degrees below the desired temperature.

Adsorbates and Adsorbents

The adsorbates are:

Baker Instra-analyzed

GC-spectrophotometric quality CCl_4

Baker Analyzed Reagent CHCl_3

Baker Analyzed Reagent CH_2Cl_2

Matheson High Purity 99.5 per cent minimum CH_3Cl .

One adsorbent is Sterling FT(2700), identical to the carbon black P-33(2700). The other adsorbent is designated high Purity Coarse Boron Nitride, 99.5 per cent pure by manufacture's assay and is obtained from the Carborundon Company, Refractories and Electronics Division, Latrobe, Pennsylvania.

The liquid adsorbates are distilled and the middle one-third fraction taken. The middle fractions distill over a 0.1°C range. The adsorbates are then placed into an inverted V-shaped sample container and degassed by repeated cycles of freezing in liquid nitrogen, pumping and then subliming to the other arm of the sample container. The methyl chloride is used directly from the Matheson lecture bottle container. The adsorbents, after being placed in the

sample buckets, are degassed by heating in a vacuum of 5×10^{-5} torr or better. The graphite is heated for 12 or more hours at 300°C and the boron nitride is heated for 12 or more hours at 400°C before a run was made [21].

A Typical Run

In a typical run, calculations of the saturation vapor pressure of the adsorbate and the pressures and weights adsorbed that would be at points of interest are made. The saturation vapor pressure of CCl_4 is calculated using [76]:

$$\log (P_{\text{torr}}) = (-0.05225/T^{\circ}\text{K})A + B. \quad (58)$$

The saturation vapor pressures of CHCl_3 , CH_2Cl_2 and CH_3Cl are calculated by [77]:

$$\log (P_{\text{torr}}) = (-0.2185/T^{\circ}\text{K})A + B. \quad (59)$$

See Table 1 for the constants for these equations. Next traps are filled with liquid nitrogen. The sample is degassed overnight and cooled to room temperature. The cryostat is precooled to near the desired temperature by dumping liquid nitrogen into the large dewar. The cryostat is assembled, and the temperature is controlled by means of the vapor pressure thermometer and Thermocap Relay. The swinging of the glass buckets is stopped by letting some helium into the

Table 1. Constants for Clausius-Clapeyron Equations [76,77].

Compound	Temperature Range ^o C	A	B
CCl ₄	-80 to -19	36,585	8.540
CCl ₄	-19 to +20	33,914	8.004
CHCl ₃	-58 to +254	7,500.5	7.735083
CH ₂ Cl ₂	-70 to +41	7,527.3	8.81330
CH ₃ Cl	-100 to +138	5,375.3	7.546207

system. Next the helium is pumped out and the zero of the microbalance established on the recorder's strip chart. The recorder range is set on 0.4 mg and the mass dial set to 10 mg. The capacitance manometer's sensitivity is dialed to a value that would give the monolayer pressure in about 10 excursions from 0 to 100 on the 1.0 range of the instrument. The capacitance manometer is zeroed at zero on its meter and the adsorbing system isolated by closing the proper valve. The capacitance manometer is set at the 0.1 range and a dose of vapor admitted. The weight change is recorded until the trace becomes linear. The pressure is read from capacitance manometer and recorded. More vapor is admitted and the new reading of pressure and weight noted. This is repeated until it was necessary that a scale change be made to the 1.0 range. Data is taken on the 1.0 range until the capacitance manometer read-out indicates 100. Dry air is then admitted to the side of the manometer diaphragm opposite the adsorbent and the capacitance manometer's meter is nulled on the 0.1 range setting. Previously the mercury has been set to near the cut off point of the McLeod gauge and now dried air is admitted to force the mercury into the McLeod gauge. The mercury is set on one of the three calibrated volume marks. Five minutes later the McLeod capillary is tapped and the columnar heights of the mercury read by means of the cathetometer. The room temperature is noted. This procedure is repeated until approximately 10 torr pressure of the admitted vapor is built up. At this time further readings of pressure are made after nulling the capacitance manometer, but these pressure measurements are made using

the mercury manometer. Sometime previously, the increasing weight of adsorbed vapor has moved the recorder pen across the width of the strip chart. The milligram weight on the 1.0 mg scale is calculated and the recorder pen set to that point by the recorder zero control. Pressure and weight readings are continually taken until the weight reaches approximately 10 mg. The weight is noted and either a 10 x factor change or the balance control being reset to the 100 mg mass dial range is afforded, according to the maximum weight expected. All along at periodic intervals, the emf of the thermocouple is taken. If all goes well, the run is taken to completion. However, on occasion at relative pressures exceeding 0.5, the system initiates condensation due to the wall of the hang-down tube being cooler than the sample bucket. The run has to be abandoned at this point and repeated using smaller doses of vapor at the high relative pressures. This condensation becomes a greater problem as the temperature of the cryostat is lowered due to an increasing thermal gradient inside the large diameter hang-down tube.

CHAPTER IV

RESULTS AND PROCEDURES

Introduction

Considered in this chapter are the results of this experimental investigation and the procedures used to extract parameters of interest from these results. These data are compared with similar data obtained by other investigators. In certain instances, such as obtaining second gas-solid virial coefficients, the graphs presented are meant only to give the reader cognizance of the magnitudes of the experimental numbers and the fluctuations of the experimental measurements. Complete results are presented in tabular form.

Evaluation of data is accomplished by techniques ranging from qualitative examination of isotherm shapes to virial methods possessing a high degree of mathematical rigor. Two series of isotherms taken at the ice point allow a comparison of the isotherm shapes of four chlorine substituted methanes adsorbed on two different adsorbents. Differences in Frenkel-Halsey-Hill plots for carbon tetrachloride adsorption are examined. The location of a two-dimensional critical temperature in carbon tetrachloride on graphite isotherms and the lack of subcritical isotherms for this same adsorbate on boron nitride is related to heterogeneity. The Henry's law region of carbon tetrachloride isotherms is treated using the virial expansion approach to extract gas-solid parameters. Isosteric

heats of adsorption are computed as a function of coverage to beyond two statistical monolayers with two adsorbents and carbon tetrachloride. Finally, by using measured isotherm data and other physical properties, isotherms are predicted to a fair degree of accuracy by means of the Significant Structures Theory. Some physical properties of the four substituted methane adsorbates are listed in Table 2 for future reference.

Comparison of the Effects of Heterogeneity and Molecular
Symmetry Upon the Shape of Adsorption Isotherms

Isotherms are carried out on graphite using several different adsorbate vapors. The graphite sample is Sterling FT(2700). This was from the same batch that Robert Smallwood used for his study [78]. This graphite is identical to that denoted P-33. This type of highly graphitized carbon black has a surface area of about $12 \text{ m}^2/\text{g}$ and presents a highly homogeneous basal plane to molecules being adsorbed [61]. It has a residual heterogeneity of less than 0.1 per cent [52]. The boron nitride sample is designated - High Purity Coarse - 99.5 per cent pure by manufacturer's assay, and is from the same batch as that studied by R. Ramsey [14]. Ramsey made an estimate of the heterogeneity of the boron nitride sample by computing the ratio of edge surface to basal plane surface. This estimate arises from measurements taken from electron microscope photographs. The result is that 5 to 10 per cent of the boron nitride surface is edge. Taking this as a basis for the heterogeneity, Ramsey is able to fit his experimental data. In this work the point B is used to determine

Table 2. Adsorbate Physical Constants [77]

Adsorbate	Molecular Weight	Melting Point °C	Dipole Moment Debyes	Saturation Vapor Pressure at °C, torr	Three Dim. Critical Temp °C
CCl_4	153.84	-23.0	0.00	32.96	283.2
CHCl_3	119.38	-63.5	1.01	54.36	262.0
CH_2Cl_2	84.93	-96.7	1.57	133.67	236.2
CH_3Cl	50.49	-97.7	1.87	1764.13	143.1

the relative amounts of heterogeneity. Point B is computed as an average of values read directly from individual isotherms. Carbon tetrachloride isotherms are measured at five temperatures on BN. The BN heterogeneity is then calculated to be 6.2 ± 2 per cent. See Table 3. The BN surface area is found to be $5 \text{ m}^2/\text{g}$. Levy examined a BN sample having a larger surface area and also found isotherms whose shape indicated heterogeneity [79]. Levy [79] used krypton as the adsorbate. McAlpin has estimated Levy's BN to have 20 per cent of its surface heterogeneous [70].

As for the adsorbates, CCl_4 is a spherical top molecule in the gas phase, but is probably only a symmetric top when adsorbed. There is expected to be only a minimal amount of tumbling of the CCl_4 molecule adsorbed on the surface [70,80]. The CHCl_3 molecule is less symmetrical than the CCl_4 in the gas phase, but would also be expected to be a symmetric top on the surface. When adsorbed, the CH_2Cl_2 could be considered a pseudo-triatomic molecule. The small size of the hydrogens on CH_3Cl make it possible to consider this symmetric top as a pseudo-diatomic molecule. The isosteric energy of adsorption at zero coverage is high for all these vapors. See Table 6. Carbon tetrachloride has the largest van der Waals radius of the adsorbates [80] and thus should experience the greatest decrease in adsorption energy when a second layer is formed.

Isotherms measurements were made on both graphite and boron nitride and are displayed as moles adsorbed per gram adsorbent versus relative pressure. This method of data display is chosen because it gives a good basis for comparing adsorbates which widely differed

Table 3. Experimental CCl_4 Point B Parameters* for the Graphite and Boron Nitride Adsorbents

Adsorbent	Point B Low Energy Surface mg/g	Point B High Energy Surface mg/g	Surface Area m^2/g	Per cent Total Surface Area
BN	$3.87 \pm .04$	-	4.7	94
BN	-	$.24 \pm .04$	0.3	6.2
C	$9.26 \pm .06$	-	11.5	100

* The point B was read directly from the isotherm. The area per molecule was calculated from liquid density data via equation (74).

Table 4. Relative Pressures at Point B for the Second Layer in the CCl_4 -Graphite System*

Temperature $^{\circ}\text{C}$	$\frac{P}{P_0}$	$\frac{P}{P_0}$
-11.9	12.2/16.51	0.74
-9.4	14.3/19.06	0.75
-5.0	18.85/24.82	0.78
-0.9	24.14/30.46	0.79
2.9	30.1/37.13	0.81

* Second layer point B was estimated by taking twice the monolayer point B. See Table 3.

in molecular weight, vapor pressure and critical temperature. The first series of isotherms under discussion here are all run at the ice point of water. Upon examining the adsorption isotherms of the CCl_4 , CHCl_3 , and CH_2Cl_2 and CH_3Cl , one finds several features of interest. See Figures 7, 8, and 9. The first observation is that CCl_4 forms a second step in its isotherm on graphite. No second step was found in the BN-CCl_4 isotherm. Also none of the adsorbates studied forms a second step at these temperatures on either graphite or boron nitride. The second step formed in the CCl_4 isotherm came at a high value of relative pressure, approximately 0.75. The high relative pressure seems to indicate that the second step is not formed easily. These observations point to the pseudo-spherical nature of CCl_4 allowing a second layer formation, but due to a lesser degree of symmetry, the other molecules, CHCl_3 , CH_2Cl_2 , CH_3Cl not being able to form a second step. Chloroform eventually does form a distinct second step at -52°C and Davis and Pierce [81] present evidence that this second step formation is related to the reduced temperature. Using the two-dimensional critical temperatures [32] to obtain a reduced CHCl_3 temperature comparable to that at which the CCl_4 isotherms were measured, predicts a second CHCl_3 isotherm step in the neighborhood of -37°C . A similar calculation using the three-dimensional critical temperature predicts a CHCl_3 second isotherm step at -19°C .

The BN-CCl_4 isotherm taken at the ice point did not exhibit a discernable second step, but this could easily be due to the 6 per cent heterogeneity of the BN surface. Singleton and Halsey [44] conclude that even a slight disturbance of the bulk crystal can

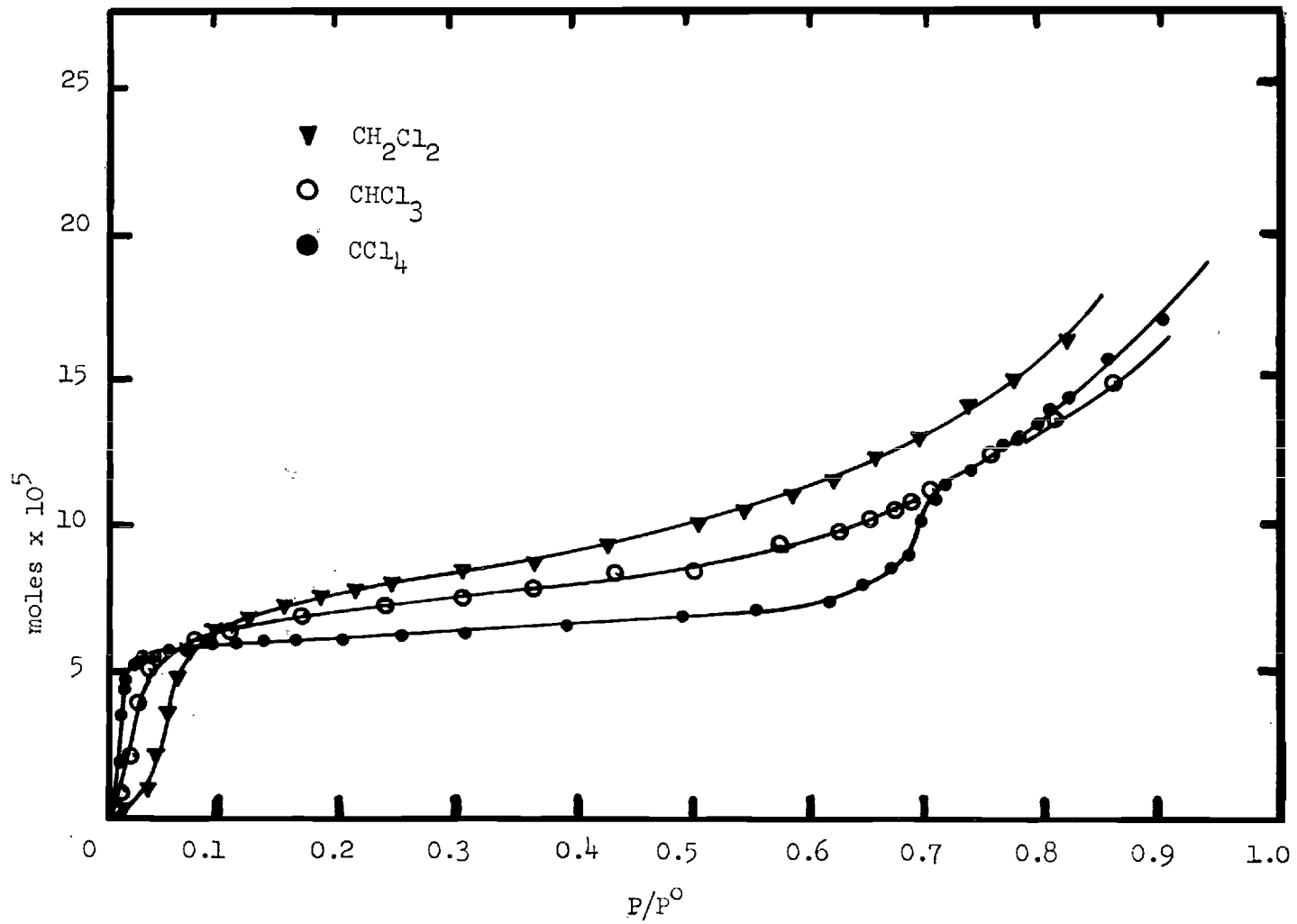


Figure 7. Ice Point Isotherms for CCl₄, CHCl₃ and CH₂Cl₂ Adsorbed Upon P-33 Graphite.

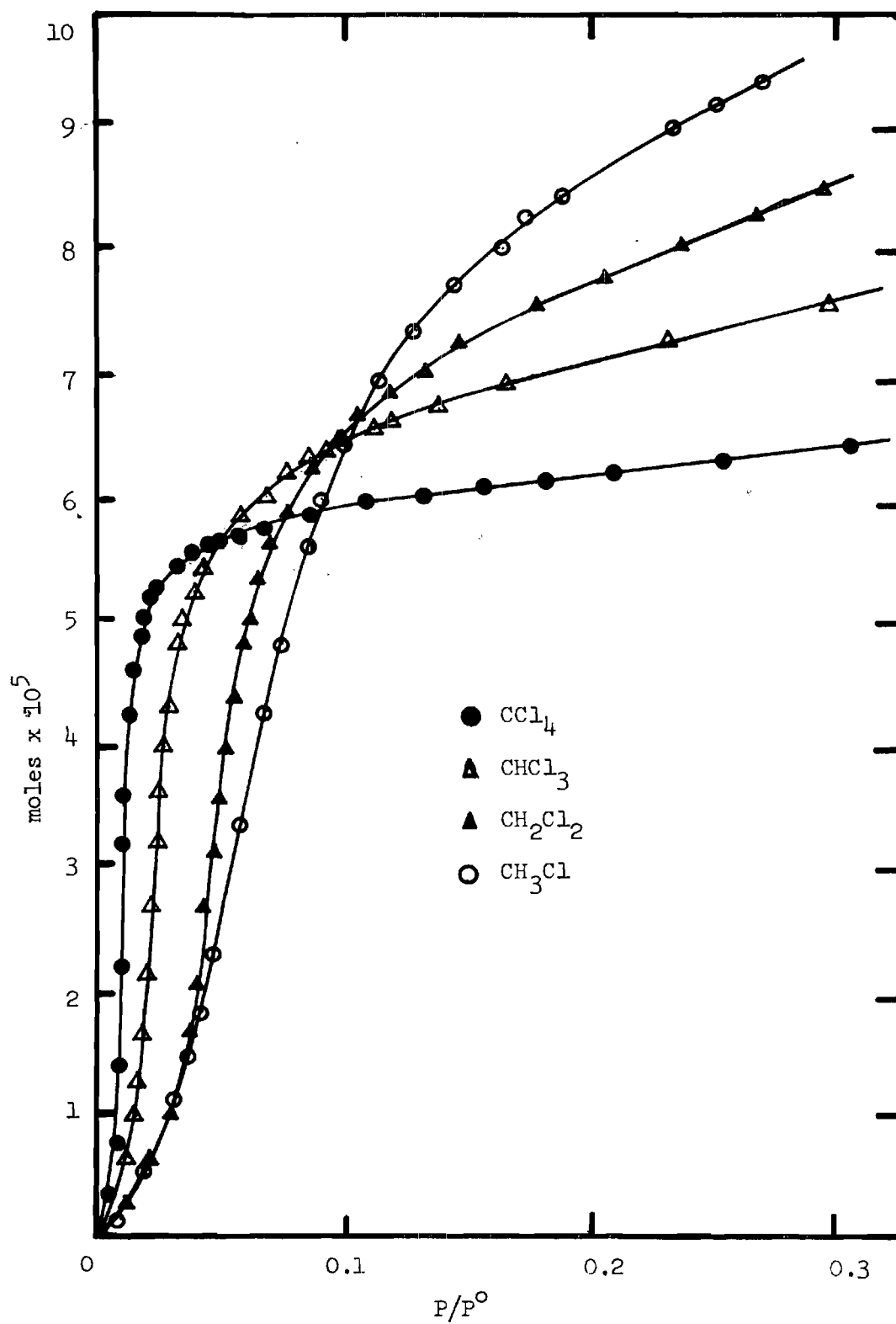


Figure 8. Ice Point Isotherms for CCl_4 , CHCl_3 , CH_2Cl_2 and CH_3Cl Adsorbed Upon P-33 Graphite.

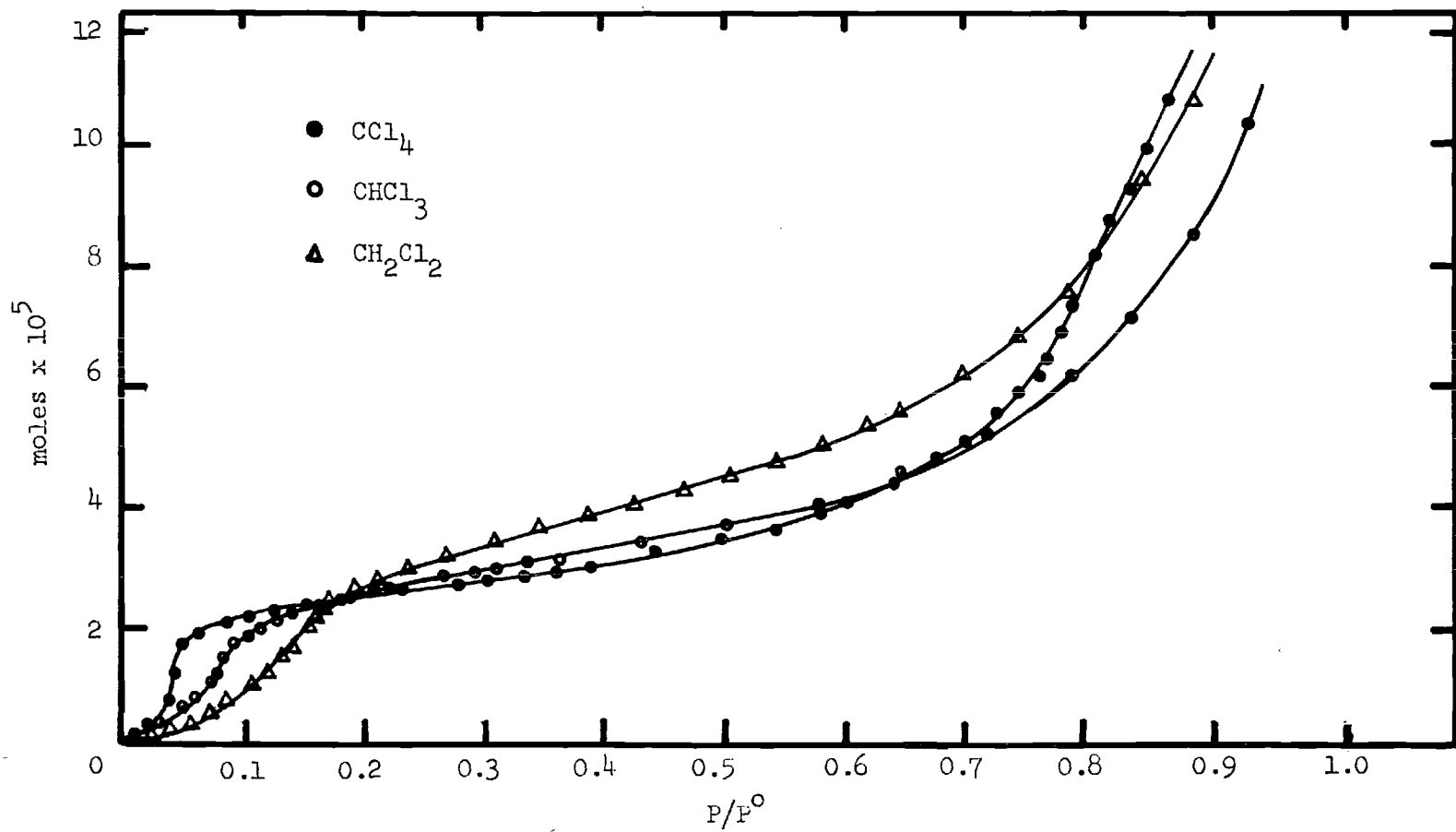


Figure 9. Ice Point Isotherms for CCl_4 , CHCl_3 and CH_2Cl_2 Adsorbed Upon Boron Nitride.

halt the development of distinct layers in the adsorbed phase.

The series of substituted methanes studied exhibits a decrease in the structure of the first isotherm step with a lowering of the molecular weight and symmetry of the adsorbates [82]. Of the vapors adsorbed upon graphite CCl_4 has the sharpest first step. In order of decreasing first step sharpness CHCl_3 is next; however, CH_2Cl_2 and CHCl_3 are approximately the same. See Figure 8. This may be explained in part by noting that CH_3Cl has a higher symmetry than does CH_2Cl_2 . Packing in the adsorbed layer should be easier for the CH_3Cl molecule than for the CH_2Cl_2 molecule as is demonstrated by the packing in the solid which results in the melting points of these two compounds differing by only one degree centigrade. This step sharpness order is repeated for CCl_4 , CHCl_3 and CH_2Cl_2 when adsorbed upon boron nitride, but there is a loss in sharpness in going from graphite to BN due to heterogeneity. The vertical riser of the graphite- CCl_4 isotherm occurs at a relative pressure of 0.01; whereas, the riser in the BN- CCl_4 system occurs at a relative pressure of 0.04. Similar comparisons may be made from the graphs displaying the isotherms of the other vapors. See Figures 7 and 9. The step heights vary in the expected manner, decreasing in height as the molecular volumes and weights increase.

Frenkel-Halsey Hill Equation

An examination of the Frenkel-Halsey-Hill equation may be of some utility in this discussion.

The Frenkel-Halsey-Hill equation may be written as [44]

$$\ln \left(\frac{P}{P^0} \right) = - \frac{\Delta \epsilon_1^*}{\theta^3 kT} + w(1-g)/kT \quad (60)$$

Here P is pressure; P_0 is saturation vapor pressure; $\Delta \epsilon_1^*$ is excess energy available to an adsorbed atom due to presence of adsorbate; θ is the fraction of a monolayer covered by adsorbate; k is Boltzman's constant; T is absolute temperature; w is the lateral interaction energy between the adsorbate molecules and g is a compatibility factor between the adsorbate and the surface.

A comparison between the $1/\theta^3$ versus $\ln(P/P^0)$ plots for CCl_4 adsorbed upon BN and upon graphite, reveals some interesting areas of agreement. See Figure 10. It is noted, however, that one finds much more curvature in the graphite plot than in the BN curve which is almost linear in the region of coverage between 0.9 monolayers and 2.7 monolayers. If this linear portion of the BN curve is extrapolated to infinite coverage, the resulting intercept corresponds to a relative pressure of 0.82. From the multilayer isotherm of CCl_4 adsorbed upon graphite at a comparable temperature we find the second step point B for this isotherm occurs at a relative pressure of 0.79. See Figure 16 and Table 4. While possibly fortuitous, this close correspondence in intercept relative pressure and point B relative pressure may have some significance. As was stated earlier it was thought the high relative pressure where the second CCl_4 on graphite step was formed was due to difficulty in forming a second layer. The extrapolated relative pressure, 0.82, is slightly higher than point B

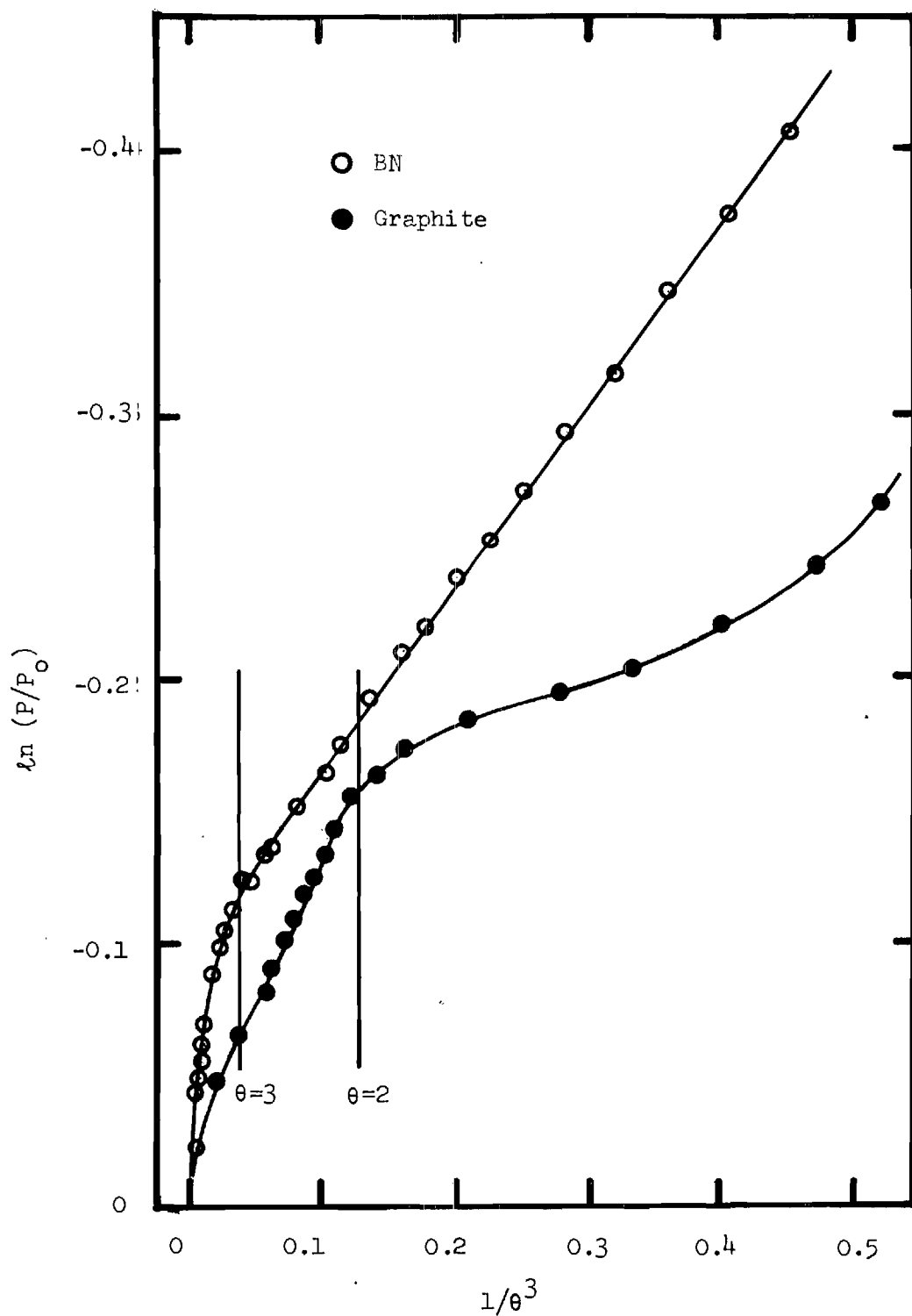


Figure 10. Frenkel-Halsey-Hill Equation Plots for CCl_4 Adsorbed Upon Graphite and Boron Nitride at the Ice Point.

relative pressure, 0.79. Noting that the linear portion of the Frenkel-Halsey-Hill equation, obtained at high surface coverages, is frequently taken to be due to adsorption onto a liquid-like surface, it is suggested that the cited correspondence in the BN and graphite isotherm relative pressures and the slope change in the Frenkel-Halsey-Hill plot near 2.7 statistical monolayers is due to a transition from an ordered layer to a disordered liquid-like layer at a point where the adsorbate is attempting to form an ordered second layer.

A value for $\Delta\epsilon_1^*$ may be extracted from the variation of the slope of the Frenkel-Halsey-Hill plot as a function of temperature [43,65]. See Table 5. The usual region for examining slopes is that of much higher coverages than those examined here. The slopes examined here are those between a coverage of 1.0 and 2.7 monolayers. The average value for $\Delta\epsilon_1^*$ obtained for this portion of the isotherm is 710 calories. These data are recorded for the benefit of future workers and their significance is not discussed here.

Two-Dimensional Critical Behavior

The effect of heterogeneity upon an isotherm is apparent in the region of two-dimensional critical behavior. The two-dimensional critical temperature for the P-33 graphite- CCl_4 system is estimated from the isotherms in Figure 11 to be $-38.4 \pm 0.3^\circ\text{C}$. A value for T_{2c} of -34°C is calculated by Machin and Ross [32] in this temperature range.

The rationale used to determine whether or not the BN- CCl_4 system exhibits two-dimensional condensation involves comparative

Table 5. Data Extracted from Frenkel-Halsey-Hill
Plots for the CCl_4 -BN System

Temperature °C	First Intercept	Slope	(RT) x (Slope) Calories
-11.8	-.2709	-1.4557	756
-8.4	-.2137	-1.2997	684
-3.7	-.2055	-1.3129	703
0.0	-.2065	-1.2509	679

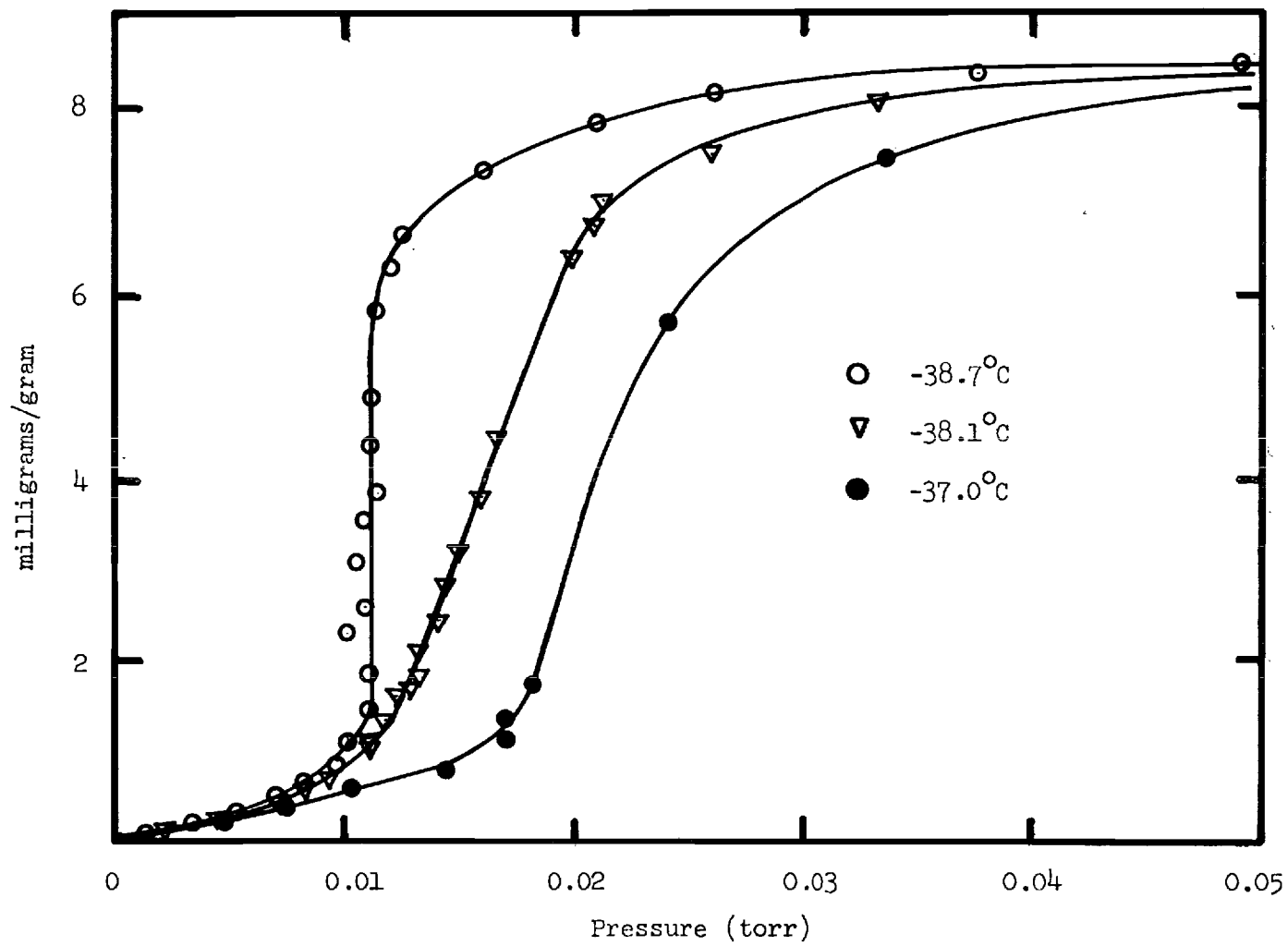


Figure 11. Two-Dimensional Critical Region Isotherms for the CCl_4 - Graphite System.

values of the isosteric heats. Since the isosteric heat for CCl_4 adsorption is lower on the BN than on graphite, the two-dimensional critical temperature for BN-CCl_4 should be slightly higher, e.g., closer to the three-dimensional critical temperature for CCl_4 . Therefore, measuring BN-CCl_4 isotherms at and below -38.4°C should be at a low enough temperature to see two-dimensional condensation. As can be seen in Figure 12, CCl_4 does not exhibit vertical risers at or slightly below -38.4°C in the BN-CCl_4 system studied. This failure to show easily recognizable two-dimensional condensation isotherms can be attributed to the BN heterogeneity obscuring the vertical risers which should be seen. Crawford and Tompkins [83] have pointed out that the pressure at which this two-dimensional first order phase change occurs is related to the heat of adsorption. Since a heterogeneous surface has a larger range of adsorption heats than a homogeneous surface, condensation should take place over a greater range of pressures.

Second Gas Solid Virial Coefficients

The second gas-solid virial coefficient, B_{2s} , is defined by [59]:

$$B_{2s} = \int_{\tilde{v}} e^{-u_s(\tilde{r})/kT} - 1 \, d\tilde{r} \quad (61)$$

where $u_s(\tilde{r})$ is the interaction potential between an adsorbed molecule and an adsorbent molecule. The \tilde{r} denotes a generalized coordinate

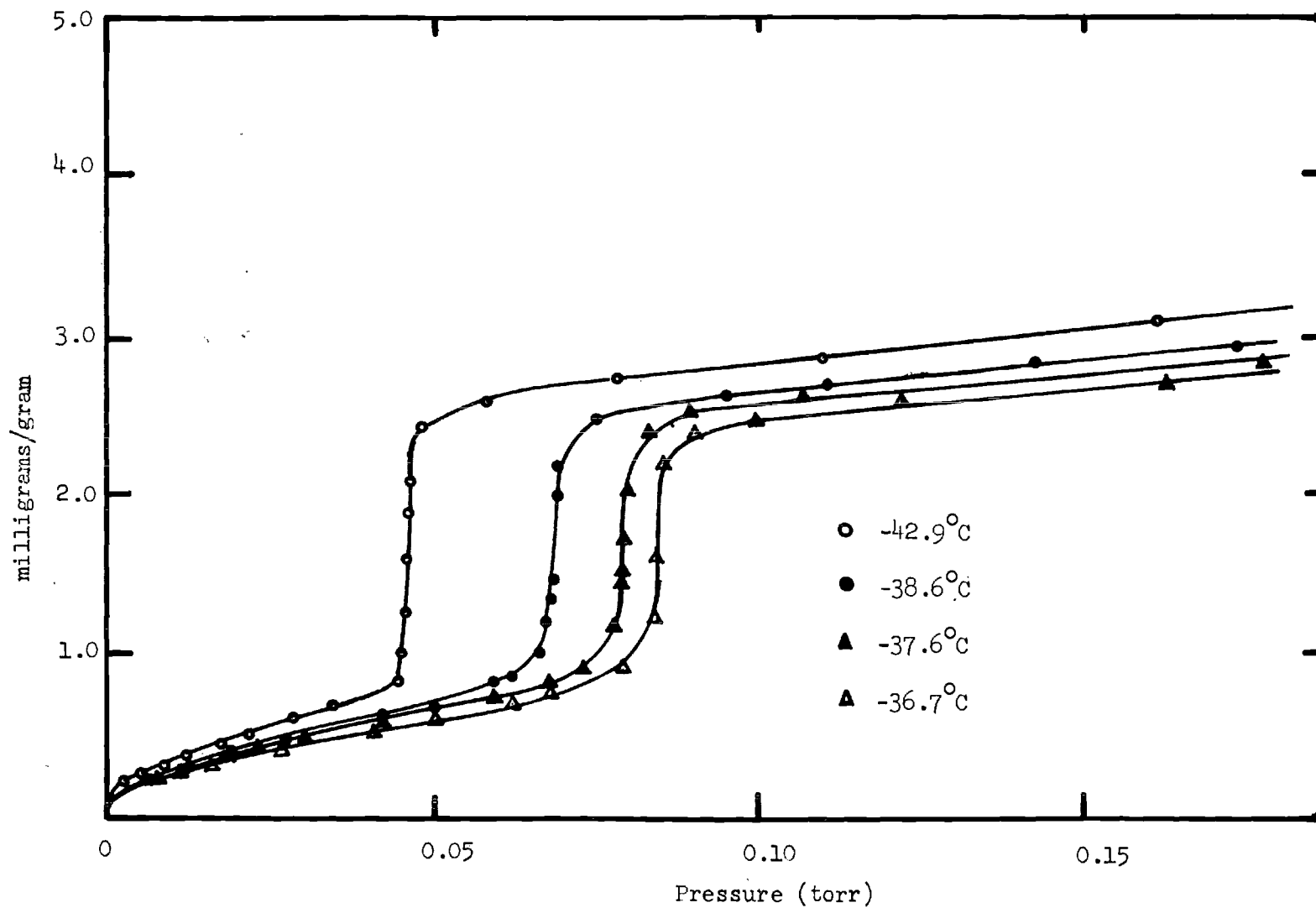


Figure 12. Two-Dimensional Critical Region Isotherms for the CCl_4 - Boron Nitride System.

extending over the volume of the adsorbent. Comparison between experimentally and theoretically derived B_{2s} allows extraction of parameters characterizing the adsorbate-adsorbent interactions and allows evaluation of theoretical models and potentials [84]. B_{2s} may be related to adsorption experiments in terms of a power series in pressure and temperature [59]. From this series, we can obtain B_{2s} via equation (36). A plot of equation (36) yields B_{2s} as an intercept at zero pressure [59]. See Figure 13. Information about B_{3s} , the third gas-solid virial coefficient, can be obtained from the slope of this linear extrapolation. Near zero pressure, a plot of W versus P obtained in the curve's linear region will allow a calculation of K_h from the slope of the plot. The B_{2s} may be calculated by:

$$W/P \quad K_h = B_{2s} M / RT. \quad (62)$$

Here W is the weight adsorbed in grams per gram of adsorbent and M is the gram molecular weight. See Figure 14. This extrapolation should have a zero intercept. This gives an alternate method for calculation of B_{2s} . Both types of plots are made and the results are listed in Table 6. This analysis was only made on the graphite adsorbent, because the high energy sites resulting from the BN heterogeneity make it impractical to attempt a similar study on BN.

As mentioned in the introduction, several potentials may be used in examining experimental B_{2s} data. The (3-9) potential is the one to be used in this work. This potential is included in equation

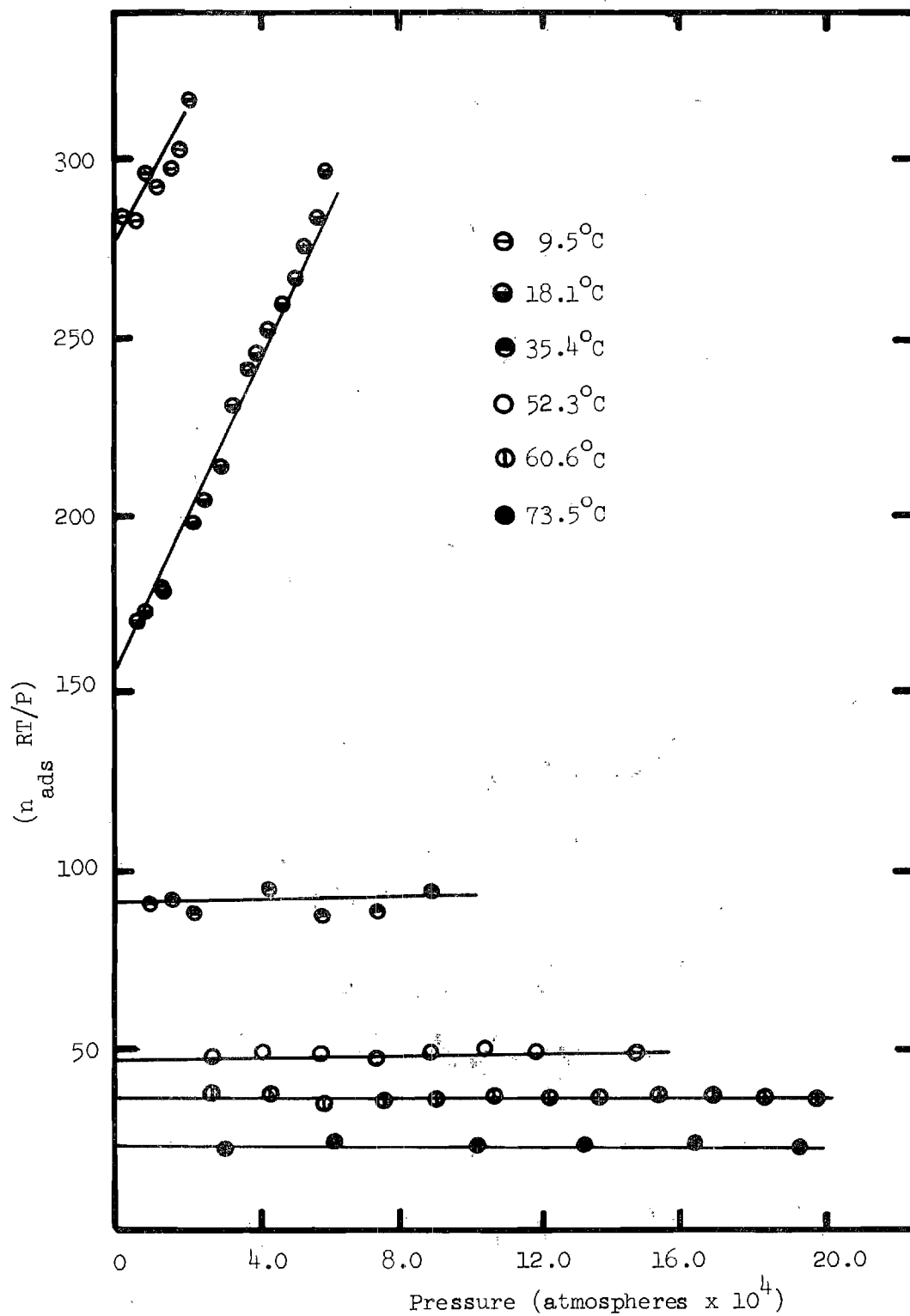


Figure 13. Plots Demonstrating the Intercept Method for Determining Second Gas-Solid Virial Coefficients for the CCl_4 - Graphite System.

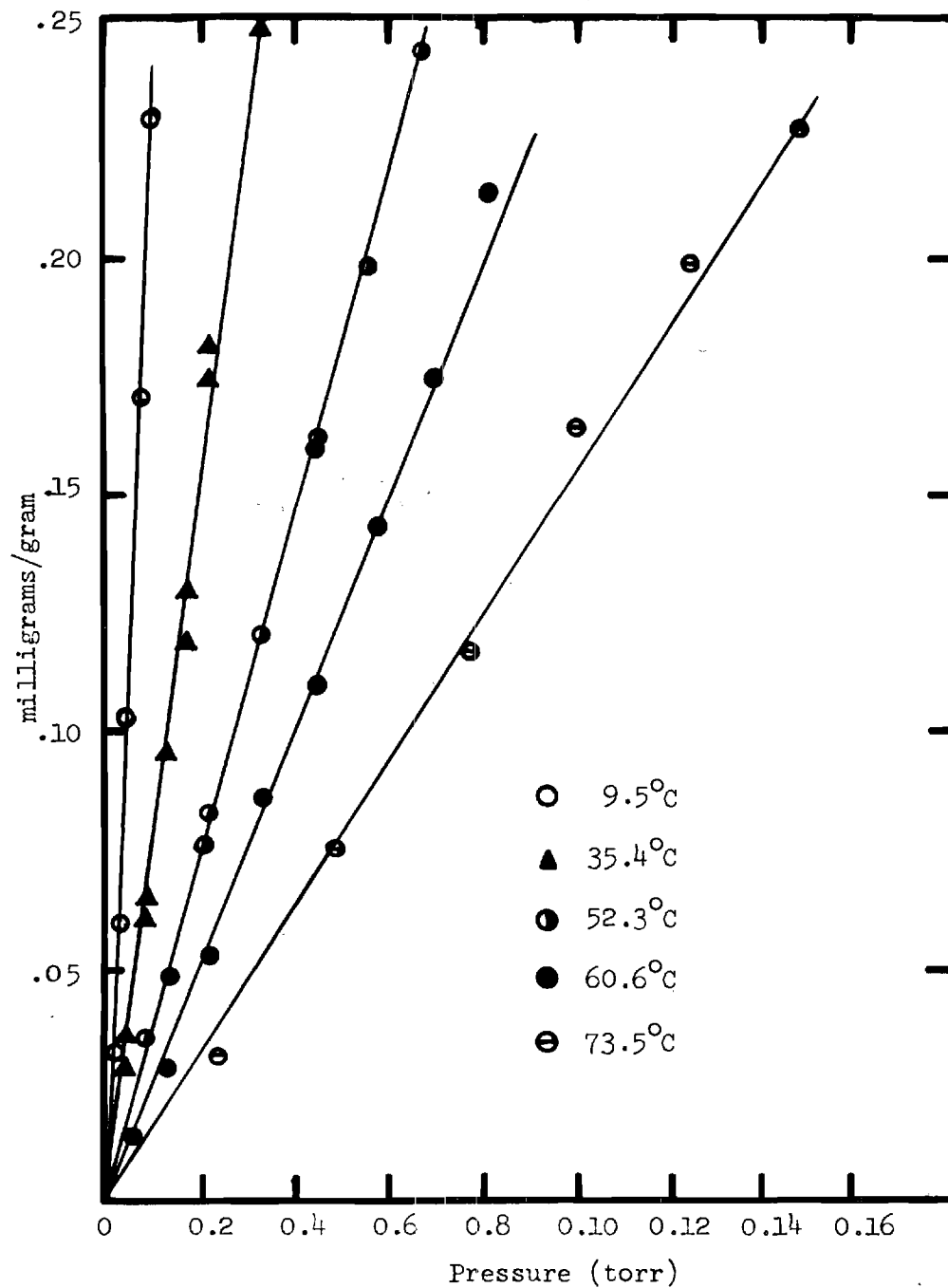


Figure 14. Plots Demonstrating the Slope Method for Determining the Second Gas-Solid Virial Coefficient for the CCl_4 Graphite System

Table 6. Henry's Law Region B_{2s} Data and Zero Coverage Isothermic Heats for the Graphite Adsorbent.

Temperature K	B_{2s}^* Intercept cm^3/g	B_{2s}^{**} Slope	$q_{st}^0 - RT^{***}$ Calories	Adsorbate
282.66	277	291	7730 ± 70	CCl_4
291.22	154	174		
308.41	90.2	90.9		
325.41	46.3	45.1		
333.76	33.9	36.1		
346.65	22.3	22.4		
268.14	196	207	7570 ± 100	CHCl_3
283.42	90.7	95.4		
296.12	51.4	53.5		
310.67	30.9	31.4		
324.39	16.2	17.8		
247.76	98.0	98.7	7900 ± 350	CH_2Cl_2
252.19	72.4	78.1		
256.70	50.0	58.0		
267.92	25.9	30.6		
273.33	21.7	24.2		
291.71	7.5	-		
190.0	163	185	6090 ± 60	CH_3Cl
191.8	143	165		
208.1	36	44.2		
216.0	23.1	28.8		
216.6	23.8	25.8		

* B_{2s} calculated from $\frac{n_{ads} RT}{P}$ versus p plot

** B_{2s} calculated from n_{ads} versus P plot

*** Errors calculated by comparison with slope isothermic heats or by standard deviation of plot, the larger error being quoted here.

(40). Rearranging equation (40), the desired expression is obtained as

$$AZ_0 = B_{2s} / ((2\pi/27)^{1/2} 3^{1/3} (kT/\epsilon_{1s}^*)^{1/2} \exp(\epsilon_{1s}^*/kT)). \quad (63)$$

Experimental data will be treated using this equation. Here A is the adsorbent surface area, ϵ_{1s}^* is the gas-solid interaction potential when the adsorbate molecule is at its equilibrium distance from the adsorbent, z_0 is the distance of closest approach of the adsorbate to the surface and k is the Boltzmann constant. The calculation of AZ_0 for a specified vapor and its experimental values of B_{2s} is made with the assumption that the value for Az_0 should be a constant. Using a trial value of ϵ_{1s}^* , a value for AZ_0 is computed for each experimental value of B_{2s} . Now other trial values of ϵ_{1s}^* are used and a series of values of AZ_0 computed for each value of ϵ_{1s}^* . The average deviation of each series is compared and the series of AZ_0 values with the smallest average deviation is selected, averaged and used as the calculated value of AZ_0 . The ϵ_{1s}^* used to calculate this series with the smallest average deviation is selected as the ϵ_{1s}^* for that vapor adsorbed on that adsorbent. Normally the Az_0 product is factored by assuming a value for z_0 . However, this AZ_0 value is factored by assuming a value for A. The calculated values for z_0 are variously arrived at by taking different methods to estimate molecular radii. For example one such formulation of z_0 involves the sum of the crystallographic carbon atom's radius and the non-

bonding radius obtained from the imperfect gas behavior. Using the experimental area of the adsorbent is subject to problems. This is illustrated by the data of Pace and Siebert [52]. For a particular graphitized carbon black these workers find a spectrum of areas from an "argon area" of $86.1 \text{ m}^2/\text{g}$ to a "helium area" of $266.6 \text{ m}^2/\text{g}$. The carbon black, P-33 used here, is better characterized. P-33 areas obtained from the B.E.T. measurements range from $11.8 \text{ m}^2/\text{g}$ to $13.3 \text{ m}^2/\text{g}$ [61,84,85]; whereas, areas calculated from the gas-solid virial expansion via model potentials fall between $8.0 \text{ m}^2/\text{g}$ and $14.6 \text{ m}^2/\text{g}$ [61,86]. It was decided to use the experimental value for the P-33 area determined in this work. That area is $11.5 \text{ m}^2/\text{g}$. With this area being set, values for z_0 are computed for the various vapors and the values for ϵ_{1s}^* extracted.

The calculation of a distance of closest approach, z_0 , from radii is still necessary in order to have grounds for comparison for the z_0 values calculated from the harmonic model. Assuming the CCl_4 to be positioned so that each of the three chlorines is over the center of a hexagon formed by the graphite carbons, and is a non-rotating, locally adsorbed molecule, the distance of closest approach would be approximately 1.85 \AA . For a locally adsorbed, rotating molecule or for CCl_4 undergoing mobile adsorption, the distance of closest approach would be approximately 3.1 \AA . The 3.1 \AA is obtained by using one-half the 1.42 \AA carbon to carbon bond distance in crystalline graphite and a 2.4 \AA van der Waal's radius [80]. The van der Waal's radius is for CCl_4 sitting in a tripod position upon a plane. The next possible molecular position, with a 2.8 \AA van der

Waal's radius, is separated by a 3200 calorie rotational barrier [80]. Since CCl_4 adsorption is expected to be mobile adsorption and considering the high rotational barrier the proper z_0 would be 3.1 \AA . The difference between the 1.85 \AA and the 3.1 \AA is due to a non-rotating, locally adsorbed CCl_4 being able to sit in the depressions corresponding to the centers of the hexagonal lattices; whereas, the closest the CCl_4 could come in mobile adsorption would be the sum of the graphite carbon's radius and the distance from the center of mass to the point of contact of the CCl_4 chlorines.

Distances of closest approach calculated from adsorption measurements by means of the harmonic potential B_{2s} equation are listed in Table 7. The more symmetrical molecules as "seen" by the adsorbent give the more realistic results. This trend agrees with the earlier qualitative observations deduced from the isotherms shapes. This demonstrates, and Myers and Prausnitz [84] concur, that results from a Henry's law, e.g. gas-solid virial coefficient treatment, provide a sensitive test of models for hindered rotation. Hindered rotation being omitted from the potential being used to describe these non-spherical molecules is one cause for the z_0 values not being more realistic. Pierotti [67] found that when a potential recognizing hindered rotation was used he could accurately reproduce the experimental values for B_{2s} for benzene adsorbed upon graphite.

Comparison of the values of q_{st}^0 and ϵ_{1s}^* for CCl_4 adsorbed upon graphite is informative. See Tables 6 and 7. The 8350 calories q_{st}^0 is about one-half RT larger than the 8,040 calorie ϵ_{1s}^* .

Everett [88] demonstrated that from the definition of isosteric heat

Table 7. Harmonic Potential Parameters Obtained from Fit
of B_{2s} Values for the Graphite Adsorbent

Adsorbent	$Az_o \times 10^4$ cm ³	$z_o \times 10^8$ cm	$e^* \lg/k$ K
CCl ₄	13.627	1.2	4040
CHCl ₃	7.062	0.6	3925
CH ₂ Cl ₂	0.969	0.1	3950
CH ₃ Cl	0.953	0.1	3150

that q_{st}^0 is one-half RT greater than ϵ_{1s}^* for mobile adsorption and one-half RT less than ϵ_{1s}^* for localized adsorption. The value found for ϵ_{1s}^* is consistent with our expectations, as the adsorption of CCl_4 on graphite was expected to be mobile.

Experimental Isothermic Heats for the Graphite
and Boron Nitride Systems

The isothermic heat for adsorption is a differential quantity which varies with the degree of surface coverage. The usual definition and the one used here is that the isothermic heat, q_{st} , is given by [89]:

$$q_{st} = - R \left(\frac{\partial \ln P}{\partial 1/T} \right)_{n_{ads}} \quad (64)$$

P is pressure in torrs; T is absolute temperature; n_{ads} is the number of moles of adsorbed molecules per gram of adsorbent; R is the gas constant. The CCl_4 -graphite system intercept at zero coverage for the plot in Figure 15 of q_{st} versus moles of CCl_4 adsorbed is obtained from the two-dimensional second virial coefficient data. At zero coverage [59]:

$$q_{st}^0 = RT + R \left(\frac{d \ln B_{2s}}{d(1/T)} \right) \quad (65)$$

The isothermic heats obtained by means of a least squares fit of

experimental data to equation (65) are found in Table 6. Plots according to equation (65) and the high coefficients of correlation obtained from the least squares program attest to equation (65) being linear over the temperature range of these measurements.

Figure 15 shows plots of isosteric heat of adsorption versus moles of CCl_4 adsorbed at coverages above the Henry's law region. The CCl_4 graphite isosteric heat plot is a composite of data from eight isotherms. These isotherms measured at temperatures of -11.9°C , -8.4°C , -7.4°C , -5.0°C , -2.5°C , -0.9°C , 0.0°C , and 23.0°C . See Figures 7 and 16. The CCl_4 on BN isosteric heat is a composite of data from four isotherms. These isotherms are measured at temperatures of -11.8°C , -8.4°C , -3.7°C , and 0.0°C . See Figure 17. The isosteric heat curves are computed point by point by a least squares fit to the logarithmic variation of the pressure of CCl_4 vapor as a function of reciprocal absolute temperature at selected values of constant weights of adsorbed CCl_4 . The expected error in the isosteric heat curves is computed point by point by dividing the change in reciprocal absolute temperature over the experimental range into the standard deviation of the fluctuations of the points of each least squared isostere. Because of the nature of the isotherms, the experimental accuracy of a point on both of the isosteric heat curves is on the order of plus or minus 300 calories.

Avgul, Kiselev and Lyginia [80] have published an isotherm for CCl_4 adsorbed on the thermal carbon black, T ℓ -(3000 $^\circ$). See Figure 18. Their isotherm shows an indication of second layer formation, but from the manner in which their curve is drawn it is evident

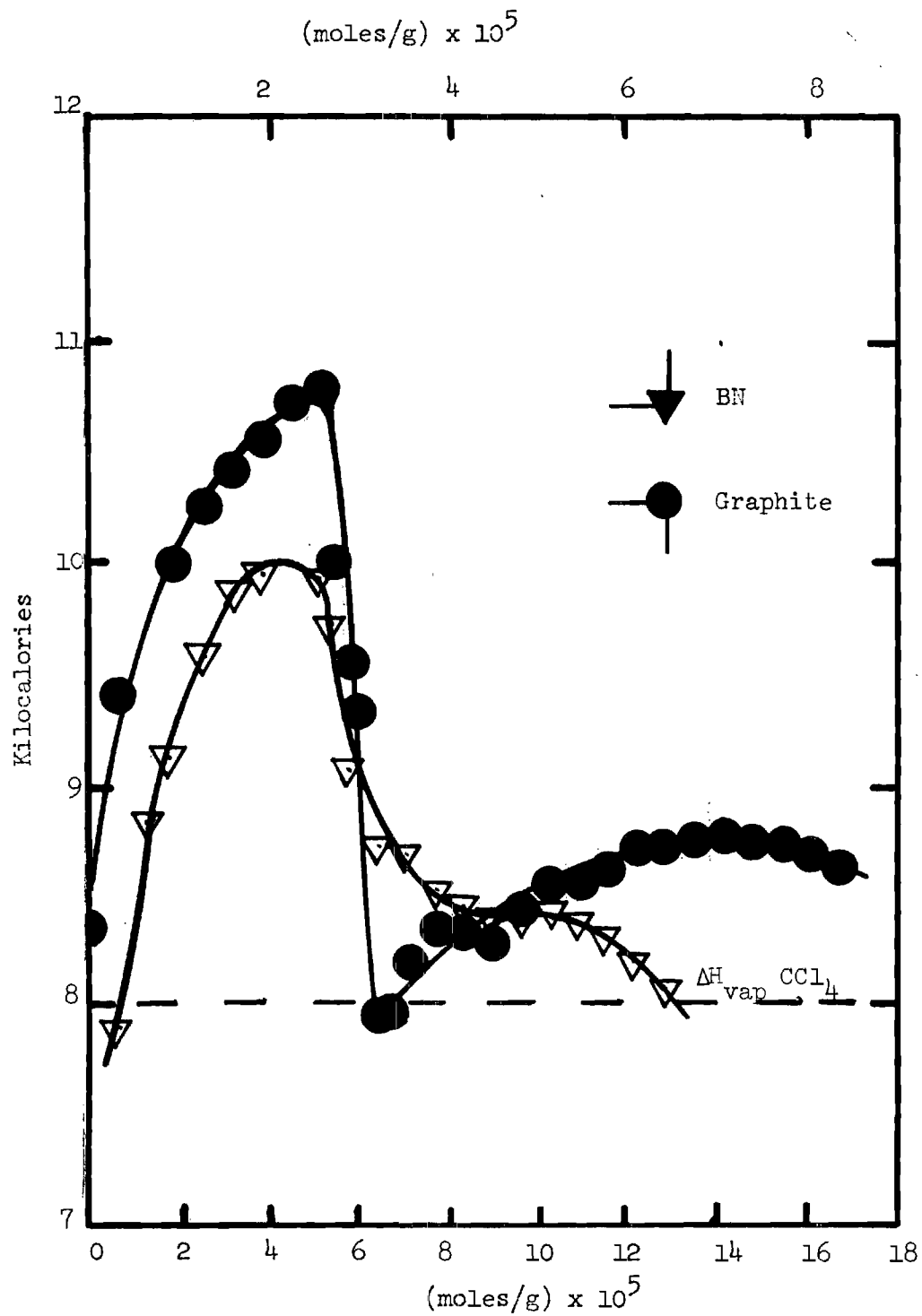


Figure 15. Isosteric Heats as a Function of Coverage for the CCl_4 -Graphite and CCl_4 Boron Nitride Systems.

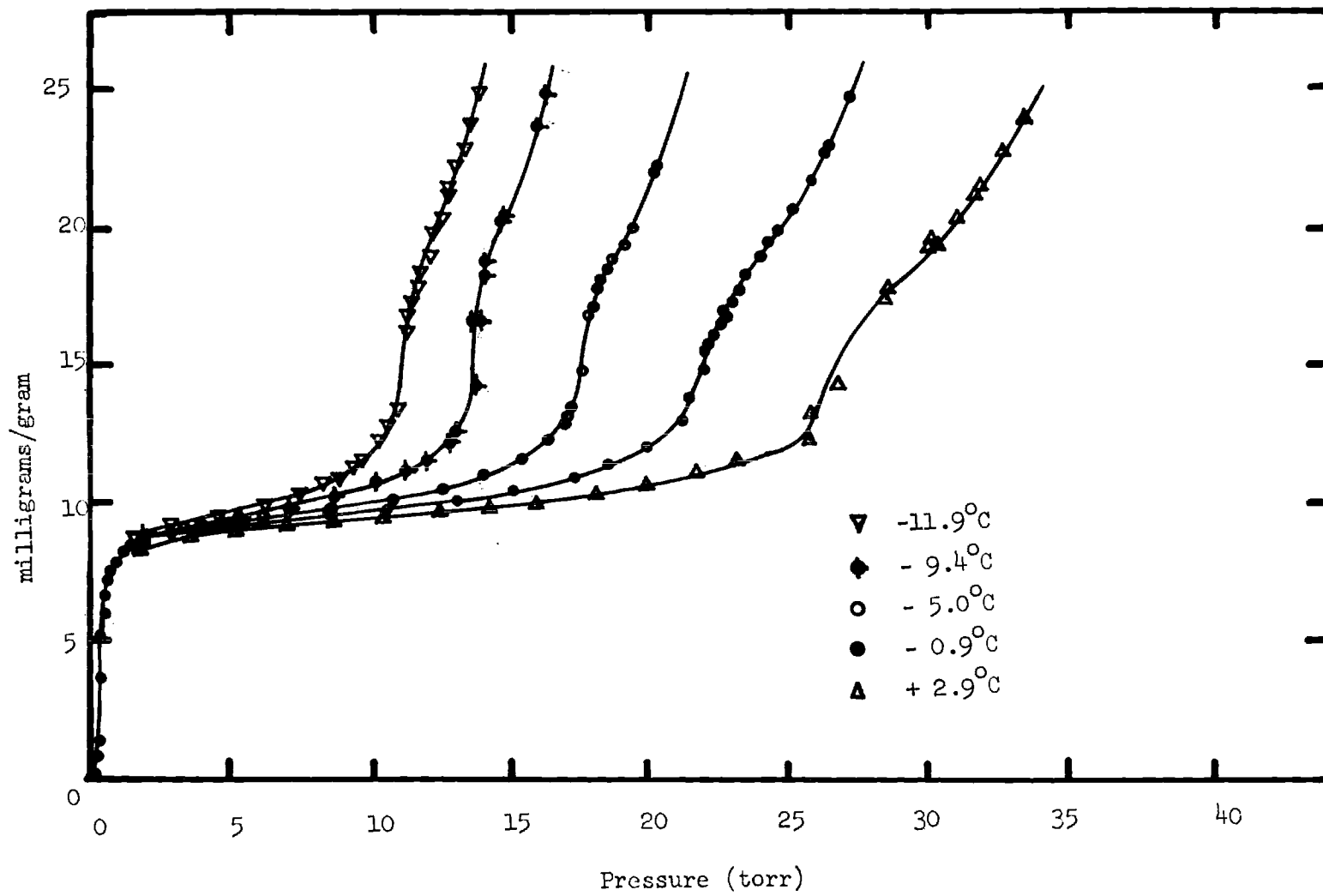


Figure 16. Multilayer Adsorption Region Isotherms for the CCl₄-Graphite System.

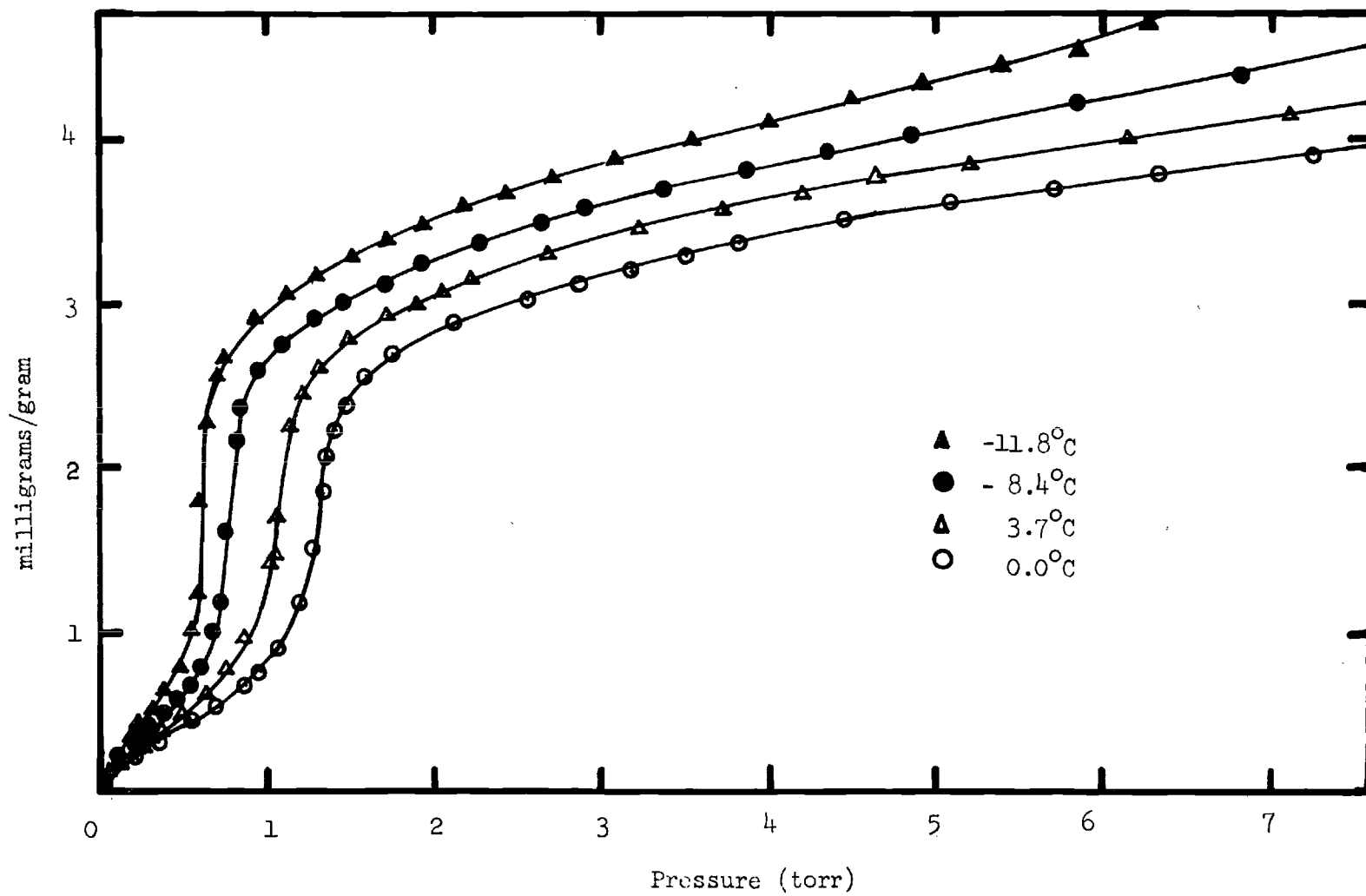


Figure 17. Adsorption Isotherms for the CCl_4 -Boron Nitride System.

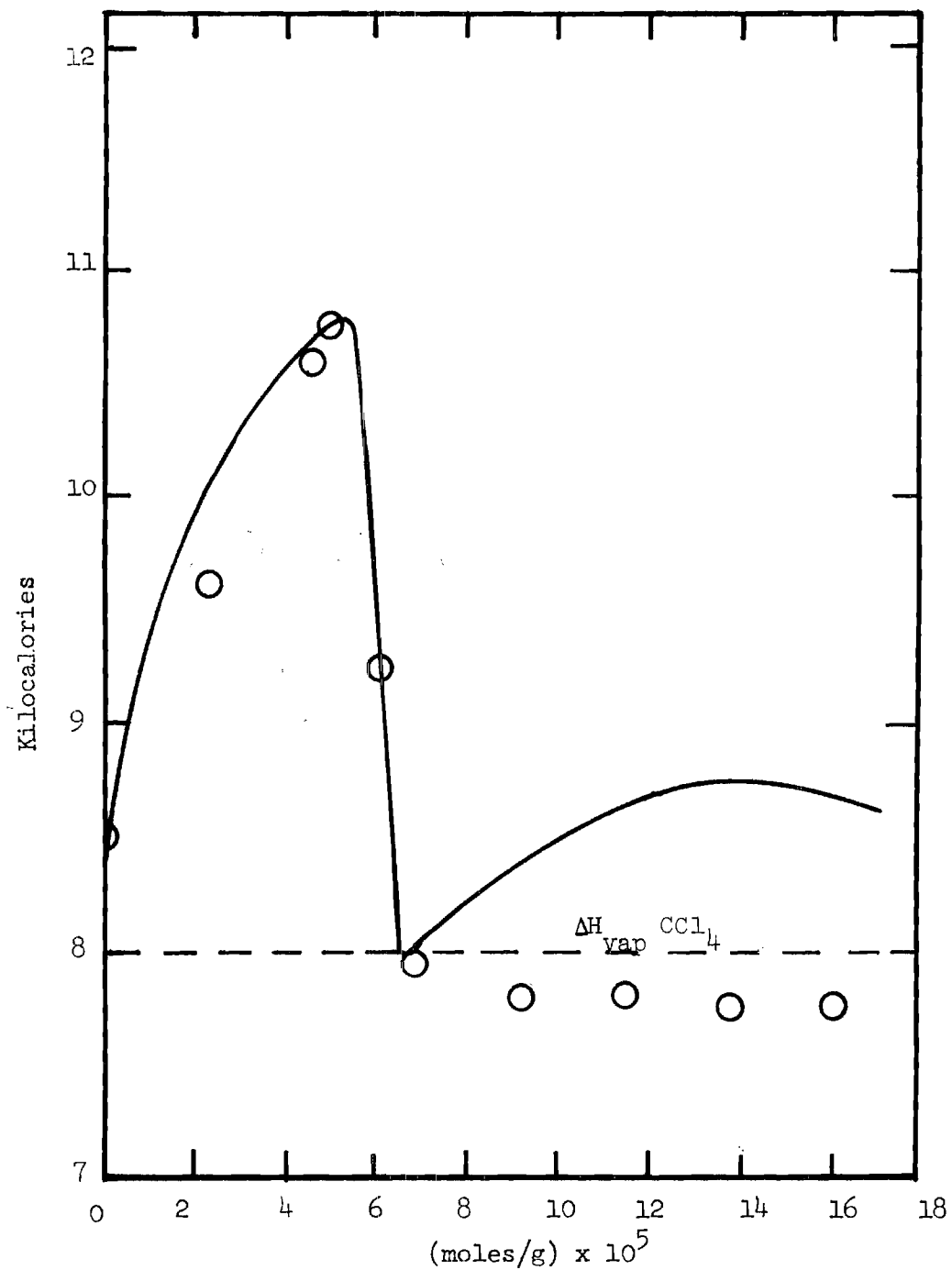


Figure 18. Comparison of the CCl_4 - Graphite Isosteric Heat Curve with a Literature Curve (Solid Line This Work, Points Due to Avgul et. al. [80]).

that they dismiss the possibility of a second step. Their heat curve is obtained calorimetrically and agrees at several points with the isosteric heat data obtained in this work. Their heat curve extrapolates to 8,500 calories at zero coverage while this present work yields a value of 8,350 calories, calculated from two-dimensional gas-solid virial coefficients. Their maximum heat comes at 5.1×10^{-5} moles/gram adsorbed CCl_4 , which is identical to this present work, Avgul [80], et. al., had a maximum isosteric heat of 10,800 calories which is also identical to the value obtained in this work. Their curve's inflection point after the first maximum comes at a point equivalent to the monolayer coverage of 6.02×10^{-5} moles/gram found in this work. A difference in the two isosteric heat curves comes near a coverage of two monolayers. Above one monolayer, the present work exhibits a second maximum of 8,800 calories after a minimum of 7,900 calories. Avgul, Kiselev and Lyginia's heat curve displays a minimum of 7,800 calories, but the second maximum is only 7,900 calories. Another comparison is furnished by Ross and Oliver's [90] chromatographically obtained isosteric heat of adsorption. Ross and Oliver find their limiting isosteric heat for CCl_4 , adsorbed upon graphite in the temperature range 372°K to 463°K , to be 8,350 calories. In this present work the isosteric heat is measured between 283°K and 347°K and has a value of 8,350 calories. Ross and Oliver also list a limiting isosteric heat of 8,100 calories for CHCl_3 , which agrees with the 8,100 calorie value found in this work.

Figure 15 consists of two plots, one for graphite and one for BN with the usual CCl_4 adsorbate. Observation of the curves shows

monatonic decreases in heats as zero coverage is approached. Below 6 per cent of a CCl_4 monolayer, the BN adsorbent heat curve should show a slope reversal indicative of its surface heterogeneity. Data is not sufficient to fix either the slope reversal or the intercept for the BN curve in this low coverage region. The maximum isosteric heat for CCl_4 adsorbed upon BN is 10,000 calories. This is 800 calories less than the graphite maximum. The inflexion points of the curves coming after the isosteric heat maximum should closely coincide with the location of the monolayer. There is, of course, some leeway in drawing the curves. The CCl_4 adsorbed upon the graphite has a heat curve inflexion at 6.02×10^{-5} moles/gram, which is identically the monolayer volume calculated from point B measurements. The point B monolayer coverage of 2.52×10^{-5} moles/gram is smaller than the point of inflexion, 2.75×10^{-5} moles/gram for the BN- CCl_4 system. At the temperature of these isotherms CCl_4 has a heat of vaporization of approximately 8,000 calories. Isosteric heats at CCl_4 coverages beyond 2.5 statistical monolayers are 8,630 calories and 8,170 calories for graphite and BN respectively. Thus it appears that several additional layers of CCl_4 must be adsorbed upon the graphite before the interactions of the adsorbent surface become negligible and the heat of adsorption achieves the limiting heat of vaporization; however, the CCl_4 adsorbed upon BN has reached this limiting heat within experimental error.

Significant Structures Theory

Several models are available for treatment of coverages beyond

the Henry's law region. We have already mentioned the Frenkel-Halsey-Hill equation. A more basic approach is the Significant Structures model. The Significant Structures Theory is useful up to coverages approaching a monolayer. With modifications, the Significant Structures Theory has treated inert gases up to three statistical monolayers [91]. However, the complexity of the molecules studied here is such that only the lower coverage form is currently useful.

The results stemming from the Significant Structures Theory rest ultimately upon observed molecular properties. There are approximations, but these are made with experimental results in mind. With this type of qualification, it can be stated that within experimental error this data treatment by the Significant Structures theory involves no adjustable parameters [70]. The Significant Structures Theory is a mating of the straight forward partition function for an ideal gas and the intuition necessary to build a workable partition function for the adsorbed phase. Once the partition functions are formulated the theory is put into the form of an isotherm via the chemical potential route. See equation (49). The isotherm equation can be written for non-spherical CCl_4 as follows [38,69,70]:

$$\ln(P) + g(\theta) = - 2\theta \ln(B/C') - \mu_g^0/kT - \ln(C') \quad (66)$$

$$+ \ln(q_{rg}/q_{rs});$$

where

$$g(\theta) = -\ln(\theta) - (5\theta^2)/(6-5\theta) + 2\theta\ln(6-5\theta) - 1. \quad (67)$$

Here

$$\ln(C') = (2 + j)\ln(T) + (1 + j)\ln(k/h\nu) - \ln(\Lambda^2/ea_m^0) + \epsilon_{1s}^*/kT \quad (68)$$

and

$$B = ((e^{-h\nu/2kT})/(1 - e^{-h\nu/kT})) e^{\epsilon_{1s}^*/kT} \quad (69)$$

$$\times (2\pi mkT/h^2) a_F \bar{w}/RT ;$$

$$\mu_g^0/kT = \ln((2\pi mk/h^2)^{3/2} / k^{5/2}) + 5/2 \ln T; \quad (70)$$

$$q_{rg}/q_{rs} = (8\pi^2 kT) (I_x I_y)^{1/2} / 4h. \quad (71)$$

Here p is the adsorbate pressure in dynes/cm²;

θ is fraction of a monolayer covered by adsorbate;

j is number of rotational degrees of freedom lost upon adsorption;

T is absolute temperature;

ν is vibrational frequency of CCl_4 perpendicular to the adsorbent

surface;

a_m^0 is area occupied by a molecule in square centimeters;

k is Boltzmann's constant;

h is Planck's constant;

e is the base of natural logarithms;

R is universal gas constant;

m is molecular mass of CCl_4 ;

$I_x = I_y$ is moment of inertia of CCl_4 ;

a_f is the area within which an adsorbed molecule is free to move;

\bar{w} is a pair summation of the adsorbate's lateral interactions with other adsorbate molecules, numerically $-6.72 \epsilon_{12}^*/k$;

μ_g^0 is the standard chemical potential for an ideal gas;

ϵ_{1s}^* is the Significant Structures counterpart of the virial ϵ_{1s}^* ;

q_{rg} is the rotational partition function for bulk gas;

q_{rs} is the rotational partition function for adsorbed gas.

The first step in the evaluation of the parameters is to plot $\ln(P) - g(\theta)$ versus θ and obtain the intercepts at zero coverage [69,70].

Values of θ in the range zero to one-third are used because of curvature in these plots at higher coverages. This allows an experimental evaluation of $\ln C'$, since the intercept is the sum of this term and the readily calculatable μ_g^0/kT and $\ln(q_{rs}/q_{rg})$. A second linear plot involves $\ln C' - (2 + j) \ln T$ versus $1/T$ and yields a slope of ϵ_{1s}^*/k and an intercept from which ν is obtained. See

Figure 19. The free areas, a_f , are calculated using Newsome's [91] spherical molecule free area program. The equation evaluated by this program is [37,38]:

$$a_f = \pi a^2 \int_0^{a/2} \exp \{ (c\epsilon_{12}^*/kT)(\mathcal{L}_s(y) - 2M_s(y)) \} dy. \quad (72)$$

Here "a" is the average distance between nearest neighbor cells:

c is the coordination number of the lattice formed by the centers of the cells, taken to be six;

ϵ_{12}^* is a Lennard-Jones type gas-gas interaction parameter;

$\mathcal{L}_s(y)$ and $M_s(y)$ are polynomials in y [37];

y is the reduced distance from the center of the cell,

$$y = R^2/a^2;$$

R is the distance of a molecule from the center of the cell.

Kiselev's area for a freely rotating CCl_4 molecule is 40 \AA^2 [80].

From this we find a molecular radius of 3.568 \AA giving a value for "a" of 7.136 \AA .

The free area a_f , is evaluated as a function of ϵ_{12}^*/k at 260°K and 320°K . These results are plotted as ϵ_{12}^*/k versus a_f and an interpolation formula arrived at consisting of

$$a_f(\text{\AA}^2/\text{molecule}) \cong 0.8 + 0.00025 (T^\circ\text{K} - 260) \quad (73)$$

$$+ 0.0022(400 - \epsilon_{12}^*/k).$$

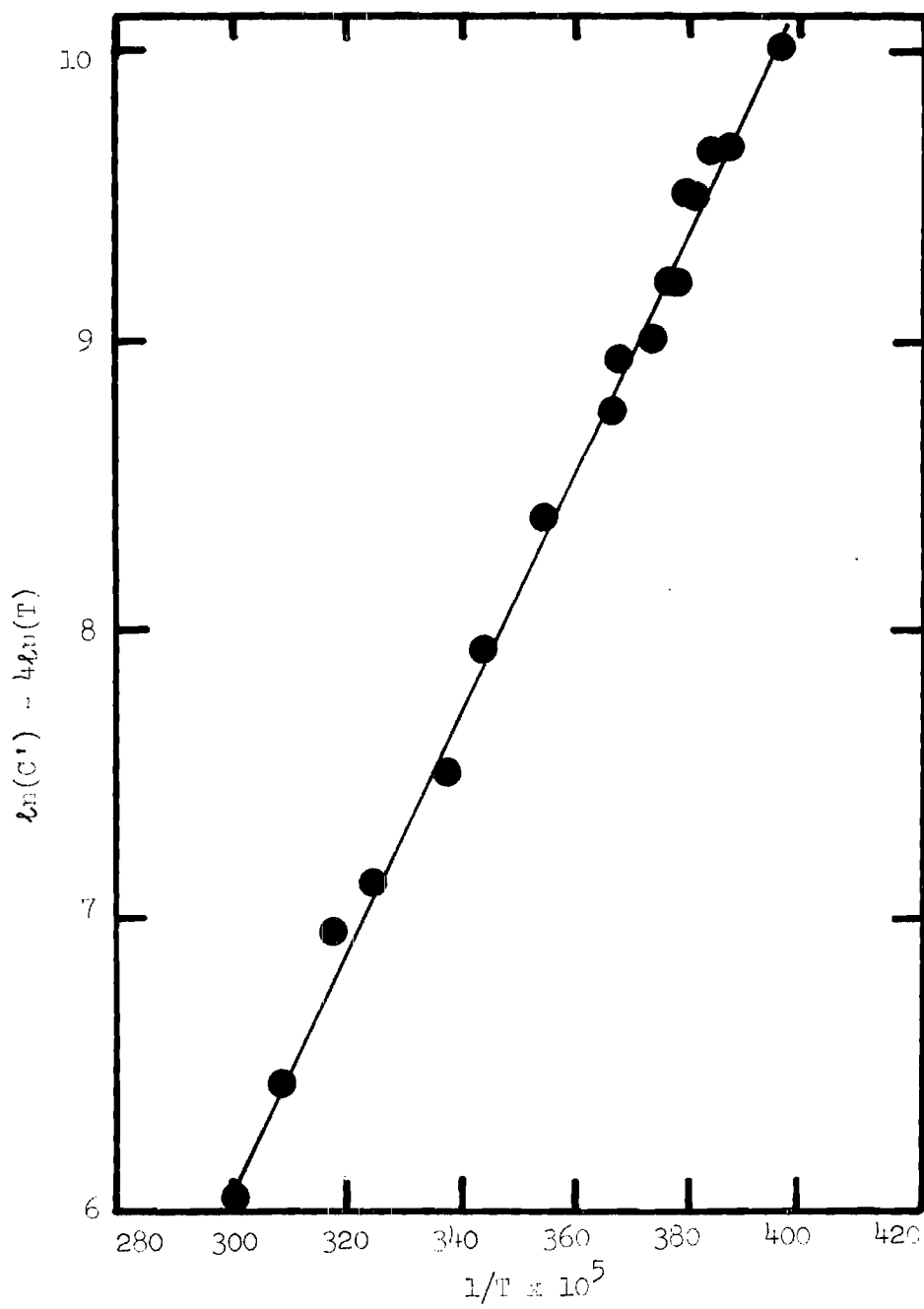


Figure 19. Significant Structures Plot to Determine ν and e^*_{1s}/k .

Equation (73) is used to compute the a_f values required by the Significant Structures Theory. The ϵ^*_{12}/k is calculated using the Significant Structures results that $\epsilon^*_{12}/k = 5/3 T_{2c}$. T_{2c} is the two-dimensional critical temperature of CCl_4 adsorbed upon graphite.

The area of a molecule at monolayer coverage, a_m^0 , is calculated using liquid density measurements [92] from

$$a_m^0 (\text{\AA}^2/\text{molecule}) = 3.464 ((M/4\sqrt{2} N\rho) \times 10^{23})^{3/2}. \quad (74)$$

Here M is molecular weight;

N is Avagadros number;

ρ is the solid or liquid density. The liquid density of CCl_4 was calculated from an interpolation formula arrived at from density data [93].

$$\rho_{\text{CCl}_4} (\text{g/ml}) = 1.60370 - (0.00195)(t^\circ\text{C} - 15). \quad 75)$$

The moment of inertia, $I_x = I_y = I_z$, is $48.76 \times 10^{-39} \text{ g-cm}^2$ for CCl_4 . With these parameters, I_z , a_m^0 , a_f , ϵ^*_{12} , ϵ^*_{1s} , ν , and assuming $j = 1$, the isotherms can be evaluated as a function of adsorbent coverage.

The parameters of most significance are ϵ^*_{1s} , ϵ^*_{12} and ν . These are presented in Table 8. The difference between the ϵ^*_{1s} values is largely due to the use of different symmetry numbers for the

Table 8. Significant Structures Parameters Obtained
from the CCl_4 -Graphite System

ϵ^*_{1s}/k $^{\circ}\text{K}$	$\nu \times 10^{12}$ sec^{-1}	ϵ^*_{12}/k $^{\circ}\text{K}$
$4160^a \pm 65$	$0.61^a \pm 0.04$	$391^a \pm 0.5$
4540^b	0.66^b	395^b

a results of this investigation

b according to McAlpin [70]

adsorbed CCl_4 . McAlpin uses a symmetry number of six; whereas, a symmetry number of three is used here. The parameters reported here are obtained as a result of the data taken in this present work; however, McAlpin and Pierotti [68] treat the data of Machin and Ross [32]. The new parameters also fit the data of Machin and Ross when the modified symmetry number is used. The value of ϵ^*_{12}/k extracted from the Significant Structures Theory is 391°K . As mentioned earlier this value for ϵ^*_{12}/k is dependent upon the model chosen. The only literature value found for comparison is the gas phase ϵ^*_{12} gas phase/ k value 327°K [94]. This literature value is the result of a Lennard-Jones (6-12) potential fit to CCl_4 viscosity data. Using a T_{2c}/T_{3c} of 0.42 determined by experiment, in conjunction with equations (54) and (56) and similar equations [38] for the LJD and SPT, approximate values of ϵ^*_{12} gas phase/ k are calculated and have values of 420, 425 and 400°K for the Significant Structures Theory, Lennard-Jones Devonshire and Scaled Particle Theory respectively [95].

In the present work the reduction in the adsorbed phase ϵ^*_{12}/k averages to 12 per cent and the ϵ^*_{12}/k is larger than the gas phase literature value of 327°K . Sinanoglu and Pitzer [45] have predicted that the ϵ^*_{12}/k could be 20 to 40 per cent smaller than the ϵ^*_{12} gas phase/ k . Sams, Constabaris and Halsey [61] find a reduction in the gas-gas interaction energy of 20 per cent for the adsorption of argon upon P-33 (2700); however, Johnson and Klein [96], treating the same data, find a reduction of only 8 per cent in the gas phase value. Sams [58] finds a 15 per cent reduction in the gas phase value

in his treatment of methane. Sherwood and Prausnitz [97] have analyzed the potential parameters obtained from the fit of bulk gas phase second virial coefficients to several different potentials. The potentials examined are the square well potential, the Lennard-Jones, Kihara, exponential-6 and Sutherland Potential. While CCl_4 is not examined, the spherically symmetric molecules, methane, tetrafluoromethane and neopentane are examined and considering the goodness of the fit of second virial coefficient and third virial coefficient data, the exponential-6 potential provides the best fit for these spherically symmetric molecules. Comparing the Lennard-Jones and exponential-6 ϵ^*_{12} gas phase/k values shows methane (LJ, 149°K ; exp-6, 226°K), neopentane (LJ, 233°K ; exp-6, 635°K) and tetrafluoromethane (LJ, 152°K ; exp-6, 404°K). From these results it is clear that a low value for the Lennard-Jones potential well depth for gas-gas interactions in the bulk phase is to be expected and that a reduction upon adsorption of 12 per cent in ϵ^*_{12} gas phase/k is a reasonable amount.

Since a considerable portion of this chapter has been devoted to the second gas-solid virial coefficient, it should be of interest to see how well the Significant Structure Theory reproduces these parameters. This comparison can be made through the Henry's law constants because they are functionally related to B_{2s} . See Table 9. As can be seen, the Significant Structure's K_{ss} are in good agreement with the K_n values, calculated from Henry's law. It is also of interest how well the quoted parameters predict isotherms at higher coverages. Figure 20 shows that limiting the variation of

Table 9. Comparison of Significant Structures Theory
 Calculated Henry's Law Constants with
 Experimental Data from the CCl_4 -Graphite
 System.*

Temperature $^{\circ}\text{C}$	Calc. $K_{ss} \times 10^{-3}$ g/g-torr	Exp $K_h \times 10^{-3}$ g/g-torr
18.1	1.613	1.474
35.4	0.745	0.734
42.2	0.563	0.568
52.3	0.380	0.353
60.6	0.266	0.268
73.5	0.180	0.164

* Calculated using equations (37) and (66).

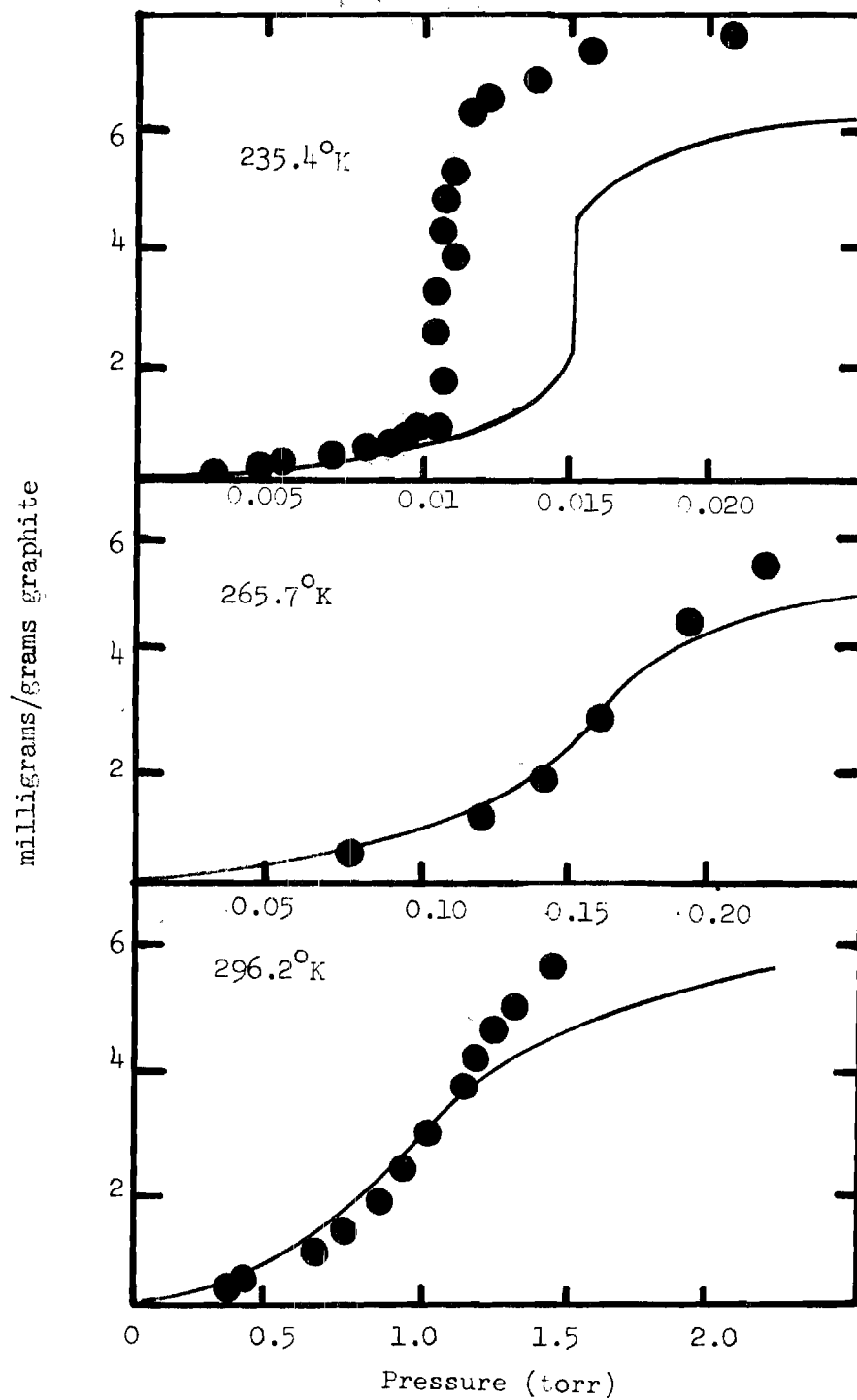


Figure 20. Fit of Significant Structures Theory to CCl_4 Experimental Isotherms (Points are experimental).

the e^*_{1s}/k to experimental errors is sufficient to allow prediction of reasonable values for isotherm pressures at coverages approaching a monolayer.

CHAPTER V

CONCLUSION AND RECOMMENDATIONS

Conclusion

A study of the physical adsorption of CCl_4 on P-33 graphite has been completed. One other adsorbent, BN and three other adsorbates were also studied, but in less detail. Measurements were made in the -83°C to $+73^\circ\text{C}$ temperature range.

From the high coverage regions of the isotherms it was concluded that the influence of molecular symmetry via layer packing, dipole moments and molecular motions of the adsorbates had a measurable effect on the ordering of the second layers of molecules. It was also noted that heterogeneity had an effect on the isotherms similar to that caused by decreasing the adsorbate symmetry. The heterogeneity of BN was measured by the point B method and calculated to be 6.2 ± 2 per cent of its $5 \text{ m}^2/\text{g}$ area. A comparison of the Frenkel-Halsey-Hill equation plots led to the conclusion that this equation might be in some cases more sensitive to attempts at the ordering of the adsorbate molecules in the multilayer regions than the isotherm itself. The excess energy of adsorption, $\Delta\epsilon^*_1$, obtained from the Frenkel-Halsey-Hill equation was 710 calories.

It was observed that CCl_4 adsorbed upon graphite exhibited a two-dimensional critical temperature of $-38.4 \pm 0.3^\circ\text{C}$. The absence of a vertical discontinuity in the CCl_4 -BN isotherms taken in what

should be an area of two-dimensional condensation made a definite statement about the two-dimensional critical temperature difficult. Heterogeneity on the BN was given as the reason for this difficulty, because of a comparison between these BN- CCl_4 isotherms and the extremely unambiguous critical isotherm measured upon the more homogeneous graphite. However, it was concluded that the possibility of a two-dimensional CCl_4 -BN critical temperature at or slightly above -35°C could not be completely dismissed.

The results of the B_{2s} investigation were expressed in terms of isosteric heats and as, ϵ^*_{1s}/k , a gas-solid interaction parameter. The zero coverage isosteric heats were: CCl_4 (8350 ± 70 calories), CHCl_3 (8100 ± 100 calories), CH_2Cl_2 (8400 ± 350 calories), CH_3Cl (6400 ± 60 calories). The high value for CH_2Cl_2 was not expected; however, due to its high heat of vaporization and high dipole moment it was expected that q°_{st} for CH_2Cl_2 would be as large or larger than the value for CHCl_3 . The ϵ^*_{1s}/k values were calculated via a harmonic potential model which did not have an angle dependence. A comparison of z_0 values calculated from this harmonic model to a z_0 calculated from van der Waal's and crystallographic radii revealed that the closest agreement between z_0 data obtained by means of these two methods was for the most symmetrical molecule, CCl_4 . The ϵ^*_{1s}/k for CCl_4 was 4040°K . The model calculated CCl_4 Az_0 was roughly one-third of the expected value.

The maximum isosteric heat for the CCl_4 -graphite system was some 800 calories in excess of the maximum isosteric heat of $10,000 \pm 300$ calories measured in the CCl_4 -BN system.

The Significant Structures Theory extracted the following parameters from the CCl_4 -graphite system: ϵ^*_{1s}/k being 4160 ± 65 $^\circ\text{K}$, ν being $0.61 \times 10^{12} \text{ sec}^{-1}$ and ϵ^*_{12}/k being 391 $^\circ\text{K}$. Using ν and ϵ^*_{12}/k as listed and adjusting ϵ^*_{1s}/k within the limits of experimental error to be 4200 $^\circ\text{K}$, reasonable isotherms were predicted. Henry's law constants predicted by the Significant Structures Theory differed from the experimental values by only a few per cent over the experimental temperature range. The ratio of the two-dimensional critical temperature to three dimensional critical temperature was experimentally 0.42 while the predicted ratio according to the Significant Structures Theory was 0.45 [68]. Utilizing these two ratios the Significant Structures predicted ϵ^*_{12} gas phase $/k$ to be 420 $^\circ\text{K}$.

Recommendations

The recommendations can be divided into experimental equipment and suggested areas of study. The microbalance has proven its ability to measure an isotherm from coverages of hundredths of a monolayer to the saturation vapor pressure, provided the fluctuations in temperature of the cryostat are sufficiently small. Fabricating the hang-down tube from metal tubing with only a small portion of glass left for observation purposes might be helpful. Improved stirring and circulation of the fluid in the cryostat dewar, coupled with an improved seal at the top of the dewar could be useful. It is also suggested that the thermocouple be replaced by a platinum resistance thermometer. Several studies are suggested by this work. A study

involving fluorinated methanes, methanol or formaldehyde in the submonolayer, monolayer and multilayer regions would be useful in examining the symmetry arguments advanced in this dissertation. The two-dimensional critical temperatures of these molecules adsorbed upon graphite could be compiled. A study of isotherms of these molecules at chosen fractions of their two-dimensional critical temperatures could be made, providing what could be an informative check on the law of corresponding states. Angle dependent potential functions for CCl_4 , CHCl_3 , CH_2Cl_2 and/or CH_3Cl could be tested using the B_{2s} values quoted in this work. The Significant Structures Theory could be applied to these or to other non-spherical molecules by including new values for: moments of inertia about the principal axes, symmetry numbers, numbers of degrees of freedom lost upon adsorption, T_{2c} , and the frequency of vibration of the adsorbed molecule perpendicular to the adsorbent. The results from this Significant Structures treatment could be of interest in testing the predicted adsorbent perturbations of the adsorbate-adsorbate interactions. Perhaps a modification of the Significant Structures Theory could be made to explain the presence or absence of multiple steps in non-spherical molecule isotherms.

APPENDIX

CCl₄ on Graphite, -38.76°C

mg/g	torr
.037	.0012
.179	.0032
.302	.0052
.467	.0069
.617	.0081
.865	.0095
1.096	.0101
1.427	.0110
1.754	.0110
2.233	.0098
2.552	.0107
2.948	.0104
3.488	.0107
3.807	.0113
4.340	.0110
4.854	.0110
5.829	.0113
6.286	.0119
6.630	.0124
6.934	.0139
7.335	.0159
7.870	.0208
8.170	.0260
8.371	.0376
8.524	.0491
8.760	.0740
8.900	.0994
8.995	.1272
9.150	.1908
9.250	.2371
9.315	.2891

CCl₄ on Graphite, -38.13° C

mg/g	torr
.147	.0027
.214	.0044
.300	.0052
.511	.0071
.590	.0082
.700	.0092
.987	.0109
1.115	.0109
1.314	.0117
1.572	.0122
1.646	.0128
1.769	.0133
2.051	.0133
2.415	.0141
2.788	.0144
3.193	.0150
3.748	.0158
4.429	.0166
6.416	.0198
6.789	.0207
7.025	.0212
7.521	.0258
8.106	.0332
8.644	.0612
8.855	.0884
9.047	.1373
9.148	.1781
9.199	.2036

CCl₄ on Graphite, -37.03°C

Weight Adsorbed mg/g	Pressure CCl ₄ torr
.172	.00456
.344	.00741
.540	.01111
.771	.01425
1.100	.01710
1.326	.01700
1.744	.0180
5.711	.0239
6.706	.0279
7.480	.0336
8.278	.0600
8.789	.1482
8.924	.2066
8.900	.2423
9.089	.3007

CCl_4 on Graphite, -19.99°C

mg/g	torr
0.044	0.0045
0.177	0.0115
0.297	0.0192
0.457	0.0275
0.705	0.0390
1.029	0.0435
1.995	0.0512
0.123	0.0083
0.273	0.0192
0.518	0.0301
0.614	0.0371
1.260	0.0410
1.604	0.0435
2.923	0.0570
1.719	0.0486
0.712	0.0352
0.570	0.0314
2.724	0.0582
5.770	0.0768
7.251	0.1408
7.585	0.1920
8.013	0.3840
8.143	0.5120
8.254	0.6336
8.362	0.7872
8.742	1.0560

CCl_4 on Graphite, -14.33°C

mg/g	torr
0.047	0.0083
0.108	0.0166
0.219	0.0262
0.373	0.0371
0.531	0.0477
0.617	0.0525
2.267	0.0960
5.036	0.1216
7.109	0.1926
7.494	0.2600
7.760	0.3328
7.400	0.4096
7.991	0.4672
8.067	0.5213
8.199	0.6387
8.681	1.5994
8.833	2.2107
9.003	2.9037
9.968	6.281
0.059	0.0122
0.076	0.0154
0.120	0.0205
0.174	0.0275
0.302	0.0371
0.609	0.0550
0.823	0.0646
1.339	0.0710
2.194	0.0774
3.402	0.0730
4.815	0.0986
6.264	0.1037
6.731	0.1664
7.416	0.2432
7.797	0.4032

CCl_4 on Graphite, -11.98°C

mg/g	torr
1.105	0.073
2.049	0.092
3.208	0.105
4.250	0.113
5.262	0.123
5.900	0.135
6.338	0.150
6.608	0.161
7.104	0.192
7.104	0.192
7.360	0.239
7.600	0.298
8.015	0.473
8.524	1.210
9.143	2.772
9.521	4.452
9.907	6.102
10.378	7.45
10.671	8.20
10.734	8.20
10.845	8.80
11.432	9.54
11.484	9.64
11.299	9.39
12.223	10.24
12.049	10.09
12.835	10.48
13.402	10.93
17.256	11.38
16.642	11.23
19.757	12.22
20.201	12.42
22.108	12.82
22.746	13.27
23.527	13.37
24.802	13.66
25.768	13.86
21.278	12.72
20.943	12.67

CCl_4 on Graphite, -11.98°C (Continued)

mg/g		torr
18.860	o	11.98
18.192		11.58
17.897		11.50
18.091		11.63
17.588		11.38
16.065		11.08
15.979		11.03
22.75		13.17

CCl_4 on Graphite, -9.39°C

mg/g	torr
0.190	0.024
0.127	0.016
0.087	0.010
0.109	0.015
0.153	0.019
0.188	0.025
0.242	0.034
0.459	0.055
1.48	0.102
3.30	0.139
5.32	0.162
6.31	0.189
6.90	0.222
7.26	0.2535
7.69	0.335
7.95	0.437
8.12	0.5330
8.28	0.663
8.39	0.788
8.55	1.044
8.67	1.299
8.77	1.554
8.85	1.8095
9.16	3.2206
9.50	5.1563
9.83	6.9756
10.17	8.504
10.67	10.10
12.23	12.63
12.62	12.93
12.23	12.68
14.19	13.63
16.51	13.43
16.59	13.82
18.67	13.92
18.12	13.92
20.13	14.47
20.26	14.57

CCl_4 on Graphite, -9.39°C (Continued)

mg/g	torr
23.47	15.77
24.7	16.06
25.3	16.61

CCl₄ on Graphite, -7.42°C

mg/g	torr
0.493	0.079
1.146	0.128
1.801	0.146
2.795	0.165
5.068	0.195
6.081	0.219
6.821	0.262
7.251	0.305
7.603	0.357
7.784	0.418
7.959	0.488
8.177	0.6097
8.424	0.872
8.522	1.026
6.932	0.262
7.312	0.305
7.985	0.488
8.179	0.610
8.624	1.283
8.755	1.498
8.860	1.7551
8.937	2.103
9.009	2.383
9.068	2.675
9.127	2.967
9.186	3.283
9.240	3.5513
9.507	5.326
9.592	5.9178
9.677	6.504
9.771	7.090
9.854	7.676
9.961	8.2623
10.061	8.82
10.172	9.38
10.299	9.93
10.437	10.492
10.590	11.09

CCl_4 on Graphite, -7.42°C (Continued)

mg/g	torr
10.771	11.73
10.978	12.18
11.207	12.73
11.528	13.38
11.878	13.87
12.271	14.22
12.729	14.57
13.096	14.82
13.472	15.07

CCl_4 on Graphite, -6.96°C

mg/g	torr
0.44	0.068
1.71	0.133
3.49	0.159
5.41	0.188
6.14	0.212
6.64	0.2413
7.23	0.299
7.55	0.357
7.90	0.483
8.01	0.5951
8.17	0.725
8.28	0.8544
8.40	1.101
8.52	1.347
8.62	1.595
8.71	1.841
8.78	2.088

CCl₄ on Graphite, -5.01°C

mg/g	torr
0.146	0.037
0.393	0.075
0.96	0.130
3.25	0.187
5.55	0.226
6.09	0.2455
6.65	0.280
7.04	0.318
7.49	0.390
7.87	0.5128
8.25	0.762
8.45	1.011
8.58	1.261
8.69	1.510
8.78	1.7592
9.20	3.838
9.52	6.118
9.84	8.36
10.19	10.64
10.55	12.38
10.99	13.78
11.62	15.27
12.31	16.21
12.90	16.76
13.16	16.86
13.47	17.01
14.80	17.36
16.03	17.61
16.86	17.66
17.16	17.81
17.79	17.96
18.12	18.10
18.43	18.30
18.78	18.45
19.30	18.90
19.96	19.20
22.01	20.09
22.18	20.14
27.3	21.74

CCl₄ on Graphite, -2.54°C

mg/g	torr
0.253	0.081
0.589	0.142
1.364	0.206
2.231	0.230
3.089	0.246
4.476	0.270
5.329	0.290
5.81	0.317
6.423	0.354
6.90	0.405
7.259	0.459
7.456	0.500
7.668	0.567
7.884	0.6751
8.043	0.801
8.187	0.952
8.288	1.081
8.375	1.218
8.456	1.3756
8.515	1.52
8.568	1.66
8.631	1.80
8.683	1.94
8.711	2.04
8.792	2.36
9.104	4.04
9.192	4.72
9.281	5.41
9.366	6.0887
9.415	6.74
9.519	7.40
9.591	8.05
9.679	8.7039
9.766	9.50
9.844	10.05
9.927	10.69
10.083	10.79
10.331	13.48

CCl₄ on Graphite, -2.54°C (Continued)

mg/g	torr
10.556	14.42
10.792	15.37
11.205	16.66
11.494	17.56
11.864	18.20
12.294	18.20
12.294	18.90
12.574	19.24
12.934	19.55
13.45	19.70
14.094	19.95
15.004	20.24

CCl_4 on Graphite, -0.86°C

mg/g	torr
0.033	0.002
0.090	0.017
0.133	0.023
0.183	0.040
0.249	0.054
0.323	0.070
0.426	0.090
0.629	0.120
0.795	0.164
1.50	0.188
3.65	0.2469
5.11	0.280
5.94	0.319
6.60	0.373
7.07	0.438
7.38	0.505
7.71	0.763
7.93	0.884
8.18	1.022
8.34	1.280
8.46	1.538
8.56	1.7965
8.82	2.7959
9.04	4.201
9.23	6.091
9.52	8.40
10.14	15.02
10.87	17.06
11.37	18.04
11.99	19.74
12.99	20.98
13.92	21.18
14.72	21.72
15.15	21.82
15.70	21.93
16.09	22.10
16.42	22.28
16.70	22.55

CCl_4 on Graphite, -0.86°C (Continued)

mg/g	torr
16.95	22.42
17.31	22.72
17.74	23.02
18.19	23.17
18.81	23.72
19.42	24.02
18.74	24.41
20.54	24.91
21.46	25.56
22.60	26.15
22.84	26.35
24.45	26.99

CCl₄ on Graphite, °C

mg/g	torr
0.046	0.011
0.069	0.019
0.061	0.024
0.113	0.034
0.147	0.043
0.186	0.054
0.228	0.063
0.343	0.093
0.557	0.132
0.827	0.171
1.168	0.200
1.708	0.228
2.172	0.243
3.370	0.275
4.042	0.289
4.927	0.307
5.537	0.332
6.125	0.360
6.522	0.393
6.900	0.432
7.094	0.460
7.339	0.507
7.590	0.567
7.777	0.635
7.952	0.7138
8.111	0.813
8.230	0.916
8.397	1.109
8.521	1.297
8.624	1.494
8.713	1.7017
8.797	1.949
8.872	2.208
8.958	2.566
9.042	2.9370
9.177	3.664
9.282	4.448
9.385	5.269

CCl₄ on Graphite, 0°C (Continued)

mg/g	torr
9.460	6.071
9.522	6.6677
9.638	7.51
9.722	8.45
9.803	9.28
9.908	10.192
10.043	11.40
10.200	12.84
10.400	14.369
19.553	15.36
10.723	16.41
10.934	17.30
11.193	18.35
11.506	19.34
11.921	20.29
12.518	21.28
13.343	22.03
14.199	22.52
15.677	22.87
17.042	23.27
17.895	23.82
18.581	24.26
19.191	24.76
19.800	25.21
20.416	25.71
21.055	26.10
21.738	26.60
22.518	27.05
23.486	27.60
24.582	28.09
27.882	29.04
34.59	30.03

CCl₄ on Graphite, +2.90°C

Weight Adsorbed mg/g	Pressure CCl ₄ torr
0.405	0.0586
0.437	0.0688
0.479	0.800
0.535	0.0949
0.555	0.1098
0.680	0.1247
0.744	0.1340
0.820	0.1461
0.921	0.1582
0.975	0.1731
1.088	0.1862
1.597	0.2567
2.169, 2.068	0.2880
2.899	0.3205
3.793	0.3389
4.372	0.3605
5.011	0.3878
5.520	0.4164
6.197	0.4685
6.728	0.5358
7.283	0.6861
7.632	0.8828
8.192	1.633
8.622	3.390
8.873	5.068
9.057	6.941
9.224	8.598
9.400	10.288
9.580	12.276
9.776	14.165
9.998	15.804
9.948	15.805
10.260	17.891
10.587	19.681
11.029	21.521
11.484	22.960
12.331	25.595
14.394	26.639

CCl₄ on Graphite, +2.90°C (Continued)

Weight Adsorbed mg/g	Pressure CCl ₄ torr
17.735	28.327
17.416	28.279
19.258	30.119
19.086	29.720
20.192	30.812
19.467	29.868
20.093	30.762
21.309	31.656
20.032	30.412
20.933	31.457
22.648	32.353
26.787	34.392
24.748	33.199
25.289	33.746
23.788	33.297

CCl₄ on Graphite, +9.51°C

mg/g	torr
.022	.008, .009
.031	.014, .017
.059	.028
.013	.046
.170	.070
.229	.094
.297	.118
.362	.141
.443	.167
.508	.187
.595	.207
.704	.2323
.794	.249

CCl_4 on Graphite, $+18.07^\circ\text{C}$

mg/g	torr
.015	.010
.030	.017
.044	.025
.070	.049
.109	.075
.163	.108
.229	.143
.297	.178
.338	.196
.421	.2337
.497	.255
.578	.285
.650	.313
.707	.334
.796	.364
.877	.391
.964	.414
1.036	.432
1.143	.456

CCl₄ on Graphite, +23.04°C

mg/g	torr
0.298	0.272
0.489	0.416
0.893	0.626
1.314	0.774
1.707	0.870
2.170	0.9561
2.784	1.048
3.083	1.088
3.583	1.154
4.057	1.213
4.552	1.285
4.980	1.351
5.251	1.410
5.557	1.483
6.013	1.6145
6.319	1.743
6.544	1.865
6.779	2.013
7.087	2.257
7.242	2.437
7.415	2.700
7.533	2.899
7.670	3.190
7.782	3.481
7.878	3.772
7.963	4.063
8.035	4.366
8.100	4.6455
9.002	15.91
9.40	24.96
10.01	39.87
10.40	47.93

CCl_4 on Graphite, $+35.36^\circ\text{C}$

mg/g	torr
.028	.0472
.059	.0847
.094	.1319
.129	.1716
.174	.2145
.033	.0418
.063	.0858
.094	.1287
.118	.1716
.249	.3317
.316	.4488
.397	.5660
.515	.6831
.646	.7943
.776	.9056
.883	1.017
1.043	1.128

CCl₄ on Graphite, +42.19°C

mg/g	torr
.028	.0510
.048	.0915
.072	.1391
.094	.1842
.122	.2318
.157	.2804
.185	.3471
.222	.4160
.249	.4687
.301	.5330
.338	.6026
.395	.6953
.467	.8111
.537	.9268
.624	1.043
.707	1.150
.781	1.251
.835	1.321
.894	1.3753
.953	1.461
1.047	1.553
1.119	1.622

CCl₄ on Graphite, +52.25°C

mg/g	torr
.0220	.0220
.0280	.0440
.033	.0682
.059	.1452
.070	.1804
.082	.2200
.013	.0401
.035	.0823
.048	.1393
.076	.2111
.161	.4448
.126	.3279
.159	.4448
.198	.5616
.244	.6784

CCl_4 on Graphite, 60.6°C

mg/g	torr
.013	.0675
.028	.1317
.052	.2177
.085	.3404
.109	.4630
.142	.5807
.174	.6983
.214	.8160
.244	.9337
.273	1.0513
.308	1.169
.345	1.276
.373	1.382
.410	1.489
.436	1.595
.469	1.700
.504	1.805
.541	1.805
.541	1.910
.574	2.015

CCl_4 on Graphite, $+73.50^\circ\text{C}$

mg/g	torr
.031	.2398
.074	.4796
.116	.7778
.164	.9992
.198	1.221
.225	1.442

CHCl_3 on Graphite, -5.01°C

mg/g	torr
.061	.041
.085	.058
.107	.072
.120	.084
.131	.094
.153	.106
.186	.128
.205	.142
.234	.157
.262	.174
.290	.193
.314	.207
.370	.232
.415	.1211
.461	.279
.524	.309
.574	.331
.651	.363
.699	.380
.771	.409
.873	.442
.967	.469
1.120	.5071

CHCL₃ on Graphite, 0°C

mg/g	torr
.022	.0068
.037	.0299
.049	.044
.059	.064
.076	.081
.136	.140
.183	.203
.237	.232
.431	.299
.448	.391
.577	.483
.787	.589
.998	.685
1.239	.772
1.519	.854
1.978	.9653
2.555	1.069
3.233	1.192
3.724	1.277
3.832	1.248
4.285	1.329
4.722	1.437
5.124	1.555
5.445	1.673
5.715	1.800
5.928	1.9087
6.239	2.119
6.487	2.365
6.678	2.584
6.835	2.8219
6.938	3.103
7.113	3.398
7.256	3.759
7.364	4.096
7.437	4.274
7.553	4.6956
7.652	5.16
7.750	5.65

CHCl_3 on Graphite, 0°C (Continued)

mg/g	torr
7.836	6.16
7.911	6.60
8.063	7.5573
8.276	9.10
8.672	12.73
9.034	16.26
9.390	19.89
9.800	23.57
10.275	27.10
10.923	30.68
11.328	32.42
11.775	33.91
12.334	35.60
12.704	36.44
13.100	37.34
13.540	38.23
13.999	39.18
14.477	40.12
14.957	41.02
15.443	41.96
15.953	41.96
16.454	43.90
16.954	44.84
17.482	45.79
18.025	46.68
20.696	50.11
22.998	51.95

CHCl₃ on Graphite, 10.27°C

mg/g	torr
.022	.048
.055	.103
.087	.158
.140	.226
.118	.198
.135	.226
.153	.2510
.190	.312
.229	.373
.260	.415
.321	.469
.343	.5283
.386	.587
.432	.641
.480	.706
.509	.740
.563	.793
.605	.842
.655	.896
.714	.955
.766	1.002
.825	1.058

CHCl_3 on Graphite, 22.97°C

mg/g	torr
.034	.109
.083	.259
.114	.350
.133	.425
.175	.5184
.201	.603
.229	.682
.266	.782
.306	.872
.334	.960
.373	1.046
.417	1.134
.448	1.209
.487	1.292
.539	1.410
.611	1.538
.670	1.653
.744	1.783
.814	1.904
.893	2.029
.969	2.150
1.066	2.275

CHCl₃ on Graphite, 37.52°C

mg/g	torr
.007	.109
.044	.296
.079	.482
.094	.5473
.127	.713
.159	.884
.199	1.098
.229	1.249
.260	1.426
.307	1.618
.345	1.777
.384	1.961
.421	2.138
.465	2.310
.513	2.492
.555	2.658
.600	2.845
.644	3.012
.690	3.178
.740	3.367
.788	3.534
.836	3.702
.886	3.870
.937	4.040
.996	4.226
1.058	4.404
1.120	4.572
1.177	4.750

CHCl₃ on Graphite, 51.24°C

mg/g	torr
.022	.289
.048	.550
.066	.814
.090	1.100
.122	1.351
.153	1.623
.179	1.894
.216	2.145
.240	2.388
.279	2.673
.308	2.959
.336	3.202
.376	3.202
.376	3.466
.389	3.730
.439	3.968
.476	4.258
.515	4.422
.550	4.786
.590	5.050
.627	5.315
.670	5.584
.703	5.843
.745	6.109
.788	6.371
.825	6.624
.869	6.899

CH₂Cl₂ on Graphite, +0.18°C

mg/g	torr
.003	.135
.014	.222
.025	.323
.035	.420
.046	.521
.057	.579
.064	.656
.077	.753
.087	.820
.105	.926
.109	.9649
.137	1.105
.166	1.298
.197	1.506
.220	1.680
.269	1.8922
.308	2.090
.348	2.274
.385	2.449
.391	2.633
.470	2.813

CH₂Cl₂ on Graphite, 0°C

mg/g	torr
.018	.307
.038	.396
.062	.575
.101	.793
.162	1.189
.248	1.625
.373	2.259
.513	2.853
.651	3.329
.866	3.9625
1.104	4.47
1.406	4.94
1.762	5.39
2.272	5.94
2.650	6.33
3.036	6.73
3.362	7.10
3.724	7.59
4.069	8.0373
4.323	8.46
4.533	8.92
4.754	9.51
5.011	10.43
5.329	12.0305
5.499	13.16
5.653	14.36
5.828	15.9587
6.006	18.00
6.166	20.0353
6.417	24.11
6.627	28.09
6.827	32.07
7.016	36.09
7.205	40.02
7.373	44.00
7.572	48.27
7.777	52.55

CH₂Cl₂ on Graphite, 0°C (Continued)

mg/g	torr
7.992	56.77
8.278	62.09
8.608	67.36
8.977	72.48
9.390	77.65
9.889	82.77
10.483	87.95
11.198	93.07
12.016	98.34
12.901	103.51
14.949	113.20

CH₂Cl₂ on Graphite, -5.23°C

mg/g	torr
.039	.258
.057	.389
.088	.560
.109	.708
.140	.930
.188	1.120
.232	1.312
.270	1.482
.319	1.653
.367	1.818
.415	1.988
.482	2.185
.542	2.366
.606	2.526
.693	2.718

CH₂Cl₂ on Graphite, -16.45°C

mg/g	torr
.017	.053
.017	.080
.034	.158
.052	.204
.072	.265
.096	.334
.109	.401
.142	.462
.169	.5306
.197	.604
.223	.667
.246	.729
.279	.803
.311	.879
.347	.958
.385	1.036
.406	1.0745
.450	

CH₂Cl₂ on Graphite, -20.96°C

mg/g	torr
.029	.053
.038	.074
.043	.102
.057	.140
.072	.173
.087	.204
.109	.255
.082	.207
.066	.171
.037	.102
.052	.130
.075	.178
.099	.229
.113	.2545
.128	.309
.150	.347
.174	.393
.193	.447
.218	.491
.241	.5433
.276	.608
.314	.676
.362	.760
.406	.814
.448	.873
.507	.949

CH₂Cl₂ on Graphite, -25.29°C

mg/g	torr
.083	.161
.090	.161
.108	.190
.116	.209
.144	.255
.109	.196
.082	.149
.057	.107
.031	.051
.045	.080
.072	.129
.100	.181
.133	.232
.144	.2550
.186	.328
.224	.395
.266	.456
.318	.535
.376	.602
.430	.670
.495	.736
.544	.781
.589	.8143

CH_3Cl on Graphite, 0°C

mg/g	torr
.037	9.25
.081	13.92
.126	23.37
.295	32.81
.406	41.26
.428	43.15
.577	52.70
.760	63.54
.934	72.53
1.162	82.73
1.698	102.96
1.948	112.35
2.161	120.11
2.422	130.80
2.628	140.15
2.824	150.39
3.017	161.42
3.254	178.82
3.502	201.99
3.717	228.49
3.899	258.07
4.062	289.90
4.174	311.82
4.273	338.18
4.397	371.07
4.539	414.87
4.644	448.77
4.731	480.89

CH₃Cl on Graphite, -57.2°C

mg/g	torr
.087	.295
.105	.489
.125	.716
.14	.832
.155	.968
.128	.775
.099	.518
.083	.329
.066	.194
.052	0

CH₃Cl on Graphite, -56.6°C

mg/g	torr
.091	.378
.115	.658
.134	.813
.148	.968
.129	.794
.107	.581
.087	.387
.067	.213
.056	0

CH₃Cl on Graphite, -65.3°C

mg/g	torr
.028	.081
.052	.162
.070	.215
.079	.262
.087	.2616
.098	.262
.186	.544
.205	.544
.197	.544
.186	.5440
.197	.544
.290	.824
.314	.824
.295	.824
.273	.824
.284	.8241
.314	.924

CH₃Cl on Graphite, -83.2

mg/g	torr
.045	.054
.071	.095
.099	.129
.119	.161
.154	.203
.206	.257

CH₃Cl on Graphite, -81.4°C

mg/g	torr
.052	.072
.070	.111
.100	.154
.135	.201
.179	.257

CCl_4 on BN, 0°C

mg/g	torr
.096	.019
.114	.042
.140	.064
.165	.092
.186	.117
.205	.141
.223	.170
.246	.198
.264	.226
.292	.2656
.340	.348
.372	.403
.410	.472
.453	.541
.503	.610
.553	.692
.598	.761
.688	.871
.767	.9540
.914	1.073
1.154	1.188
1.496	1.267
1.857	1.317
2.077	1.360
2.241	1.404
2.403	1.470
2.564	1.5792
2.687	1.738
2.792	1.907
2.866	2.089
2.962	2.335
3.043	2.5419
3.134	2.854
3.215	3.167
3.304	3.489
3.374	3.810
3.443	4.123
3.509	4.435
3.371	4.795

CCl₄ on BN, 0°C (Continued)

mg/g	torr
3.620	5.079
3.671	5.382
3.718	5.704
3.765	6.026
3.799	6.3285
3.858	6.83
3.913	7.24
3.955	7.69
4.007	8.1560
4.109	9.20
4.218	10.00
4.344	11.04
4.465	11.94
4.607	12.93
4.781	13.73
4.919	14.67
5.098	15.62
5.300	16.51
5.521	17.60
5.752	18.40
5.970	19.15
6.203	19.89
6.461	20.54
6.750	21.24
6.973	21.68
7.227	22.13
7.383	22.47
7.604	22.82
7.794	23.22
8.006	23.51
8.178	23.72
8.492	24.02
8.692	24.35
9.034	24.73
9.481	25.16
9.888	25.45
10.591	25.76
10.033	25.30
11.012	25.80
12.036	26.30
12.692	26.75

CCl_4 on BN, 0°C (Continued)

mg/g	torr
13.490	27.14
14.379	27.69
15.437	28.24
16.666	28.78
18.069	29.18
19.560	29.53
21.319	30.03
23.54	30.37
37.18	31.57

CCl₄ on BN, -3.73°C

mg/g	torr
.084	.037
.126	.067
.159	.097
.191	.128
.217	.152
.238	.179
.265	.208
.319	.2666
.402	.371
.499	.491
.628	.642
.767	.772
.954	.898
1.121	.955
1.408	1.018
1.512	1.028
1.463	1.049
1.684	1.049
2.252	1.132
2.462	1.205
2.617	1.3096
2.787	1.483
2.925	1.711
3.008	1.885
3.081	2.054
3.711	3.583
4.208	3.681
4.689	3.765
5.200	3.839
6.15	3.997
7.10	4.146
8.05	4.288
8.99	4.442
9.942	4.588
11.04	4.791
11.98	5.009
13.07	5.254
14.02	5.528

CCl_4 on BN, -3.73°C (Continued)

mg/g	torr
15.01	5.835
15.91	6.219
17.05	6.701
17.65	7.038
18.29	7.45
18.89	7.94
19.64	8.50
20.28	9.221
20.63	9.81
20.93	10.23
21.33	11.72

CCl_4 on BN, -8.42°C

mg/g	torr
.102	.044
.172	.094
.209	.131
.253	.165
.299	.207
.367	.262
.428	.316
.512	.398
.592	.469
.684	.541
.791	.609
.987	.690
1.170	.721
1.608	.7680
2.161	.806
2.378	.846
2.601	.9416
2.752	1.078
2.915	1.279
3.013	1.455
3.141	1.704
3.239	1.919
3.374	2.261
3.502	2.632
3.588	2.896
3.709	3.375
4.023	4.8512
4.202	5.84
4.404	6.82
4.618	7.806
4.867	8.75
5.107	9.60
5.412	10.34
5.756	11.14
6.182	12.13
6.445	12.56
6.789	13.03
7.136	13.53

CCl_4 on BN, -8.42°C (Continued)

mg/g	torr
7.566	14.02
7.829	14.29
8.197	14.61
8.623	14.92
8.741	14.92
8.90	15.17
9.25	15.47
9.72	15.81
10.92	16.06

CCl_4 on BN, -9.02°C

mg/g	torr
.088	.019
.121	.035
.149	.051
.171	.066
.195	.084
.228	.108
.269	.139
.117	.038
.151	.061
.190	.092
.228	.124
.289	.174
.312	.194
.344	.2230
.402	.2699
.504	.362
.643	.474
.788	.571
1.094	.678
1.657	.734
2.215	.780
2.427	.831
2.571	.903
2.797	1.097
2.897	1.199
2.955	1.2898, 1.2921
3.018	1.427
2.090	1.572
3.206	1.835
3.322	2.051
3.397	2.2289
3.495	2.556
3.590	2.869
3.683	3.192
3.781	3.678
3.899	4.154
4.055	4.6357

CCl_4 on BN, -11.80°C

mg/g	torr
.107	.025
.149	.050
.191	.076
.223	.099
.251	.120
.298	.155
.367	.206
.438	.2480
.521	.315
.647	.402
.788	.488
1.024	.549
1.231	.579
1.775	.602
2.282	.6387
2.292	.640
2.666	.745
2.566	.696
2.915	.944
3.060	1.130
3.171	1.2937
3.295	1.506
3.397	1.724
3.499	1.941
3.591	2.180
3.685	2.437
3.781	2.712
3.886	3.067
3.993	3.55
4.114	3.99
4.235	4.52
4.323	4.91
4.432	5.38
4.532	
4.691	6.26
4.839	6.76
5.135	7.68
5.510	8.610

CCl_4 on BN, -11.96°C

mg/g	torr
.027	.099
.050	.149
.079	.195
.111	.243
.142	.284
.169	.318
.215	.386
.2725	.474
.370	.613
.433	.712
.474	.800
.558	1.080
.628	2.194
.596	1.536
.676	2.503
.763	2.685
.844	2.792
.9689	2.927
1.200	3.094
1.486	3.257
3.384	1.722
3.485	1.935
3.618	2.254
3.732	2.592
3.823	2.9013

CCl₄ on BN, -36.66°C

mg/g	torr
.0980	.0005
.147	.0015
.274	.0076
.330	.0117
.377	.0152
.432	.0203
.494	.0264
.628	.0412
.705	.0498
.824	.0620
.824	.0620
.889	.0681
1.070	.0793
1.410	.0838
1.854	.0843
2.541	.0854
2.815	.0899
2.876	.0991
3.018	.122
3.171	.163
3.271	.188
3.555	.285
3.902	.437
4.020	.513
4.183	.635
4.300	.732
4.439	.818
4.679	.986

CCl_4 on BN, -38.39°C

mg/g	torr
.098	.0005
.211	.0035
.267	.0059
.320	.0089
.409	.0148
.465	.0187
.591	.0300
.693	.0394
.768	.0463
.833	.0518
.907	.0582
1.000	.0631
1.089	.0661
1.447	.0700
1.759	.0700
1.987	.0710
2.371	.0715
2.624	.0725
2.834	.0759
2.971	.0858
3.064	.0966
3.255	.133
3.339	.163
3.455	.192
3.769	.286
4.018	.394
4.174	.488
4.351	.597
4.528	.715
4.718	.823
4.990	.981

CCl₄ on BN, -37.65°C

mg/g	torr
.168	.0021
.205	.0036
.277	.0073
.331	.0194
.404	.0167
.481	.0229
.563	.0302
.666	.0417
.750	.050
.845	.0594
.949	.0677
1.070	.0734
1.342	.0776
1.671	.0786
1.768	.0786
1.992	.0792
2.359	.0797
2.797	.0826
2.932	.0896
3.067	.1073
3.309	.177
3.590	.271
3.881	.380
4.088	.500
4.283	.635
4.463	.781
4.742	.969
4.863	1.047

CCl₄ on BN, -38.60°C

mg/g	torr
.102	.0006
.173	.0024
.368	.0113
.445	.0174
.562	.0270
.732	.0420
.817	.0500
.949	.0587
1.024	.0622
1.175	.0658
1.415	.0674
1.577	.0678
1.729	.0682
2.334	.0686
2.545	.0690
2.918	.0753
3.071	.0952
3.160	.111
3.320	.143
3.448	.174
3.669	.238
3.906	.313
4.118	.416
4.281	.511
4.423	.603
4.560	.686
4.705	.777

CCl₄ on BN, -42.94°C

mg/g	torr
.00044	.152
.0026	.242
.0048	.300
.0083	.369
.0118	.449
.0171	.527
.0211	.613
.0281	.718
.0342	.824
.0443	.984
.0452	1.194
.0455	1.461
.0456	1.868
.0456	2.234
.0462	2.450
.0478	2.839
.0579	2.999
.0777	3.204
.110	3.357
.123	3.446
.162	3.623
.224	3.899
.338	4.214
.421	4.395
.531	4.632
.627	4.863
.698	5.093
.794	5.386
.878	5.775

CHCl₃ on BN, 0°C

mg/g	torr
.034	.028
.047	.043
.056	.059
.078	.096
.088	.115
.098	.131
.109	.154
.148	.238
.195	.393
.246	.598
.300	.836
.335	.999
.380	1.212
.420	1.434
.475	1.6384
.535	1.897
.600	2.035
.668	2.431
.744	2.698
.801	2.901
.935	3.2565
1.077	3.588
1.245	3.896
1.443	4.220
1.615	4.455
1.771	4.689
1.913	4.8757
2.136	5.360
2.234	5.659
2.310	5.974
2.366	6.200
2.434	6.490
2.527	6.991
2.611	7.508
2.692	8.105
2.806	8.99
2.899	9.81

CHCl_3 on BN, 0°C (Continued)

mg/g	torr
3.020	11.05
3.118	12.031
3.218	13.13
3.318	14.30
3.436	15.810
3.520	16.96
3.618	18.33
3.727	19.786
4.039	23.66
4.388	27.49
4.812	31.32
5.393	35.25
6.175	39.18
7.373	42.80
8.588	45.54
10.191	48.27
12.483	50.90
16.426	53.74

CH_2Cl_2 on BN, 0°C

mg/g	torr
.005	.260
.014	.325
.025	.455
.042	.626
.055	.789
.068	.976
.079	1.276
.100	1.390
.114	1.6398
.136	1.959
.154	2.276
.173	2.618
.188	2.927
.195	3.2354
.227	3.618
.248	3.902
.274	4.292
.284	4.650
.301	4.8687
.331	5.243
.350	5.634
.371	6.130
.390	6.5058
.406	6.861
.441	7.60
.465	8.1127, 8.0046
.545	9.60
.627	11.24
.724	12.83
.838	14.37
.998	16.21
1.205	17.75
1.375	18.84
1.540	19.79
1.668	20.68
1.799	21.58
1.924	22.57

CH_2Cl_2 on BN, 0°C

mg/g	torr
2.057	23.92
2.173	25.71
2.327	28.44
2.485	31.87
2.671	36.10
2.855	41.32
3.039	46.49
3.211	51.66
3.397	56.98
3.576	62.25
3.769	67.47
3.979	72.84
4.235	77.66
4.490	82.93
4.695	86.56
5.226	93.67
5.782	99.79
6.410	104.96
6.978	108.89
8.0316	113.36
9.214	118.83
11.919	125.84
14.255	129.47

BIBLIOGRAPHY

1. D. M. Young and A. D. Crowell, "Physical Adsorption of Gases," Butterworths and Co., London, 1962, p. 2.
2. G. D. Halsey, Jr. in H. Saltberg, J. N. Smith, Jr., and M. Rogers, Editors, "Fundamentals of Gas-Surface Interactions," Academic Press, New York, 1971, p. 93.
3. R. A. Pierotti and H. E. Thomas in E. Matijevic', Ed., "Surface and Colloid Science," Volume IV, Wiley-Interscience, New York, 1971, p. 93.
4. See Ref. 1, p. 1.
5. D. F. Eggers, Jr., N. W. Gregory, G. D. Halsey, Jr., and B. S. Rabinovitch, "Physical Chemistry," Wiley, New York, 1964, p. 729.
6. T. L. Hill, Journal of Chemical Physics, 14, 441 (1946).
7. R. H. Fowler, Proceedings of Cambridge Philosophical Society, 32 144 (1936).
8. See Ref. 1, p. 113.
9. A. V. Kiselev, Russian Journal of Physical Chemistry, 35, 111 (1961).
10. W. J. Dunning in E. A. Flood, Ed., "The Gas-Solid Interface," Volume I, Marcel Dekker, New York, 1967, p. 282.
11. See Ref. 3, p. 185.
12. S. Ross and J. P. Oliver, "On Physical Adsorption," Interscience, New York, 1964, p. 186, frontispiece.
13. D. Graham, Journal of Physical Chemistry, 61, 1310 (1957).
14. R. R. Ramsey, Ph.D. Dissertation, Georgia Institute of Technology, Atlanta, Georgia.
15. T. Moeller, "Inorganic Chemistry," Wiley, New York, 1952, p. 666.
16. L. Pauling, "The Nature of the Chemical Bond," Second Edition, Cornell University Press, Ithica, 1940, p. 172.

BIBLIOGRAPHY (Continued)

17. R. S. Pease, Nature, 165, 722 (1950).
18. See Ref. 15, p. 758.
19. "Handbook of Chemistry and Physics," The Chemical Rubber Co., Cleveland, Ohio, 44th Edition, 1962, pp. 547, 557.
20. See Ref. 1, p. 277.
21. C. Orr, J. M. Dalla Valle, "Fine Particle Measurement," Mac-Millan, New York, 1959, p. 175.
22. See Ref. 12, p. 6.
23. J. W. McBain and A. M. Bakr, Journal of American Chemical Society, 48, 690 (1926).
24. J. W. McBain and H. T. S. Britton, Journal of American Chemical Society, 52, 2198 (1930).
25. J. W. McBain and R. F. Sessions, Journal of Colloid Science, 3, 213 (1948).
26. J. R. Darcy, D. M. Young and H. J. McDougal, Canadian Journal of Chemistry, 35, 689 (1957).
27. T. N. Rhodin, J. Amer. Chem. Soc., 72, 4343 (1950).
28. W. Lemcke and U. Hofmann, Angewandte Chemie, Heidelberg, 47, 37 (1934).
29. Instruction Manual for the Cahn R G Automatic Electrobalance, Cahn Instrument C. 15505 Minnesota Ave., Paramount, California.
30. S. Ross and H. J. Clark, J. Amer. Chem. Soc., 76, 4291 (1954).
31. Y. Laher, Ph.D. Dissertation, University of Paris, Orsay, 1970.
32. W. D. Machin and S. Ross, Proceedings of the Royal Society of London, A 265, 455 (1962).
33. A. Thomy and X. Duval, Colloques Internationaux Du Center National de la Recherche Scientifique, No. 152 (1963).
34. G. D. Halsey, Jr., J. Chem. Phys., 16, 931 (1948).
35. B. B. Fisher and W. G. McMillan, J. Amer. Chem. Soc., 79,

BIBLIOGRAPHY (Continued)

- 2969 (1957).
36. T. L. Hill, "Introduction to Statistical Thermodynamics," Addison-Wesley, Reading, Mass., 1960, p. 287.
 37. See Ref. 36, p. 292.
 38. See Ref. 3, pp. 220, 224.
 39. See Ref. 36, p. 306.
 40. See Ref. 3, p. 228.
 41. See Ref. 1, p. 121.
 42. R. A. Beebe and D. M. Young, J. Phys. Chem., 58, 93 (1954).
 43. See Ref. 5, p. 718.
 44. J. H. Singleton and G. D. Halsey, Jr., Canadian Journal of Chemistry, 33, 184 (1954).
 45. O. Sinanoglu and K. S. Pitzer, J. Chem. Phys., 32, 1279 (1960).
 46. T. L. Hill, Advances in Catalysis, 4, 212 (1952).
 47. P. H. Emmett and S. Brunaur, J. Amer. Chem. Soc., 59, 1553 (1937).
 48. See Ref. 1, p. 190.
 49. G. D. Halsey, Jr., Discussions of the Faraday Society, 8, 54 (1937).
 50. G. Jura, "Physical Methods in Chemical Analysis," Vol. 2, Academic Press, New York, 1951, p. 2.
 51. S. Brunauer, L. E. Copeland, D. L. Kantro in Flood, "Gas-Solid Interface," p. 94.
 52. E. L. Pace and A. R. Siebert, J. Phys. Chem., 64, 961 (1960).
 53. See Ref. 1, p. 105.
 54. See Ref. 10, p. 481.
 55. J. P. Hobson, J. Chem. Phys., 34, 1850 (1961).

BIBLIOGRAPHY (Continued)

56. See Ref. 5, p. 172.
57. W. A. Steele and G. D. Halsey, Jr., J. Phys. Chem., 22, 979 (1954).
58. J. R. Sams, J. Chem. Phys., 43, 2243 (1965).
59. See Ref. 3, p. 164.
60. See Ref. 3, p. 114.
61. J. R. Sams, G. Constabaris and G. D. Halsey, Jr., J. Phys. Chem., 64, 1689 (1960).
62. R. S. Hansen, J. Phys. Chem., 63, 743 (1959).
63. T. L. Hill, J. Chem. Phys., 17, 590 (1949).
64. See Ref. 10, p. 360.
65. R. A. Pierotti and G. D. Halsey, Jr., J. Phys. Chem., 63, 680 (1959).
66. H. Eyring, T. Ree and N. Hirai, Proceedings of National Academy of Science, U. S., 44, 683 (1958).
67. J. Walter and H. Eyring, J. Chem. Phys., 9, 343 (1941).
68. J. J. McAlpin and R. A. Pierotti, J. Chem. Phys., 41, 68 (1964).
69. See Ref. 3, p. 230.
70. J. J. McAlpin, Ph.D. Dissertation, Georgia Institute of Technology, Atlanta, Georgia, p. 33, 34.
71. A. E. Eisenstein and N. S. Gingrich, Physical Review, 62, 261 (1942).
72. R. Smallwood, Research Notebook, Georgia Institute of Technology, Atlanta, Georgia, p. 109.
73. A. P. Masis and M. D. Pena, Anales de La Real Sociedad Espanola de Fisica y Quimica, 54 B, 661 (1958). (See Chemical Abstracts 53, 17612c (1959)).
74. R. Whytlaw-Gray, C. G. Reeves and G. A. Bottomly, Nature, 181, 1004 (1958).

BIBLIOGRAPHY (Continued)

75. P. G. Francis and M. L. McGlashan, Transactions of the Faraday Society, (London) 51, 593 (1955).
76. E. W. Washburn, Editor, "International Critical Tables," Vol. III, McGraw-Hill, New York, 1928.
77. "Handbook of Chemistry and Physics," 46th Edition, The Chemical Rubber Co., Cleveland, Ohio, 1971, p. d-146.
78. R. A. Pierotti and R. E. Smallwood, Journal of Colloid Science, 22, 469 (1966).
79. A. C. Levy, M. S. Thesis, Georgia Institute of Technology, Atlanta, Georgia.
80. N. N. Avgul, A. V. Kiselev and I. A. Lyginia, Transactions of the Faraday Society, 59, 2113 (1963).
81. B. W. Davis and C. Pierce, J. Phys. Chem., 70, 1051, (1966).
82. N. N. Avgul, G. I. Berezin, A. V. Kiselev and I. A. Lyginia, Izvestiya Akademii Nauk-SSSR, Otdelnie Nauk, 2, 204 (1950).
83. V. A. Crawford and F. C. Tompkins, Trans. Faraday Soc., 46, 504 (1950).
84. A. L. Myers and J. M. Prausnitz, Transactions of Faraday Society, 61, 755 (1965).
85. Isirkyan and A. V. Kiselev, J. Phys. Chem., 65, 601 (1961).
86. J. D. Johnson and M. L. Klein, Trans. Faraday Soc., 60, 1964 (1964).
87. R. A. Pierotti, Chemical Physics Letters, 2, 420 (1968).
88. D. H. Everett, Trans. Faraday Soc., 46 453, 942 (1950).
89. See Ref. 1, p. 4.
90. See Ref. 12, p. 245.
91. D. Newsome, Ph.D. Dissertation, Georgia Institute of Technology, Atlanta, Georgia, 1972.
92. See Ref. 1, p. 184.

BIBLIOGRAPHY (Concluded)

93. A. Weissberger, Editor, "Technique of Organic Chemistry," Vol. III, Second Edition, Interscience, New York, 1955.
94. J. O. Hirschfelder, C. F. Curtiss and R. B. Bird, "Molecular Theory of Gases and Liquids," Wiley, New York, 1954, p. lll.
95. J. H. de Boer, "The Dynamical Character of Adsorption," Oxford, 1953.
96. J. D. Johnson and M. L. Klein, Trans. Faraday Soc., 60, 1964 (1964).
97. A. E. Sherwood and J. M. Prausnitz, J. Chem. Phys., 41, 429 (1964).

VITA

Joe D. DeLay was born in Murfreesboro, Tennessee November 15, 1938, but grew up and attended school in Chattanooga, Tennessee. His mother, Erlene DeLay, is a housewife and his father, Sam DeLay, is a meteorologist. He also has a younger brother and sister. Upon graduation from Tyner High School he won a scholarship to the University of Chattanooga; however, he attended Middle Tennessee State University at Murfreesboro and graduated in 1960 with a B.S. degree in mathematics and chemistry. While at M.T.S.U. DeLay received the Freshman Chemistry Achievement Award. In 1960 he entered the University of Georgia and in 1962 received an M.S. degree in chemistry. His thesis concerned the reaction kinetics of the solvolysis of ethyl iodide in solutions of varying dielectric strength. In 1962 DeLay took a position as a textile chemist with the Tennessee Eastman Company. In 1963 he became a chemistry teacher at Abilene Christian College, where he met and married his wife Kay. In 1965 he entered Georgia Tech where he was the recipient of National Science Foundation Traineeships and the DuPont Award for Teaching. DeLay is a member of the American Chemical Society and the Sigma Xi. At the time of this writing Joe DeLay is employed by Dekalb College where he teaches Freshman Chemistry and Physical Science. His permanent address is 602 Watts Avenue, Chattanooga, Tennessee.